Vol. 273: 227–227, 2004 | MARINE ECOLOGY PROGRESS SERIES Mar Ecol Prog Ser | Published June 8

THEME SECTION

Emergent properties of complex marine systems: a macroecological perspective

Coordination: **Andrea Belgrano**

Contributors to Theme Section: **A. Belgrano, J. A. Dunne, Z. V. Finkel, D. Grünbaum, H. Hillebrand, D. Ø. Hjermann, A. J. Irwin, M. Lima, N. D. Martinez, G. Ottersen, J. K. Parrish, O. Schofield, N. C. Stenseth, S. V. Viscido, R. J. Williams**

Foreword

Andrea Belgrano*

NCGR (National Center for Genome Resources), 2935 Rodeo Park Drive East, Santa Fe, New Mexico 87505, USA

A macroecological view of the ecosystem offers the possibility to integrate information at large spatial and temporal scales over a variety of complex ecological systems. Marine macroecology can be regarded as a new research agenda aiming to develop new models which can explain the emergent structures and dynamics of complex ecological systems in terms of basic physical and biological principles (Brown 1999). Macroecology theory as a way to describe the emergent properties in terrestrial systems has received relatively little attention in marine ecology. This Theme Section is a collection of articles that will discuss the importance of macroecological and complexity theory, in a very broad context, to untangling patterns that underlie the relationships between species abundance and other biotic and abiotic factors linking organismal biology, population dynamics, community ecology, food web structure, biodiversity, and behavioral ecology, to ecosystem structure and function. This macroecological view of different processes underlying the dynamics of marine ecosystems extends the general theory of macroecology and allometric scaling, developed mainly for terrestrial systems (Brown 1995, West et al. 1997), to a marine context as recently proposed by Li (2002). Ultimately we need to understand by first principles, from organism organization to ecosystem organization (Reynolds 2001), the basic common ecological rules that generate the variability and patterns that we observe across scales.

LITERATURE CITED

Brown JH (1995) Macroecology. Chicago University Press, Chicago

Brown JH (1999) Macroecology: progress and prospect. Oikos 87:3–14

Li WKW (2002) Macroecological patterns of phytoplankton in the northwest Atlantic Ocean. Nature 419:154–157

Reynolds CS (2001) Emergence in pelagic communities. Sci Mar 65:5–30

West GB, Brown JH, Enquist BJ (1997) A general model for the origin of allometric scaling laws in biology. Science 276:122–126

*Email: ab@ncgr.org

Vol. 273: 229–238, 2004 | MARINE ECOLOGY PROGRESS SERIES Mar Ecol Prog Ser | Published June 8

Indirect climatic forcing of the Barents Sea capelin: a cohort effect

Dag Ø. Hjermann[1], Nils Chr. Stenseth[1,2,*], Geir Ottersen[3,4,5]

[1]Centre for Ecological and Evolutionary Synthesis (CEES), Department of Biology, University of Oslo, PO Box 1050 Blindern, 0316 Oslo, Norway

[2]Department of Coastal Zone Studies, Institute of Marine Research, Flødevigen Research Station, 4817 His, Norway

[3]Institute of Marine Research, PO Box 1870 Nordnes, 5024 Bergen, Norway

[4]Bjerknes Centre for Climate Research/GEOS, University of Bergen, Allégaten 55, 5007 Bergen, Norway

[5]*Present address:* Centre for Ecological and Evolutionary Synthesis (CEES), Department of Biology, University of Oslo, PO Box 1050 Blindern, 0316 Oslo, Norway

ABSTRACT: Planktivorous capelin is a key species in the Barents Sea, being of great importance in the exploitation of plankton production in this subarctic region. However, in years with a successful reproduction of the Norwegian spring-spawning herring, large amounts of herring larvae drift into the Barents Sea, where they stay for 2 to 3 yr. The 1 to 2 yr old herring has a pronounced impact on capelin, eating large amounts of capelin larvae. The main fish predator of the Barents Sea, the Arcto-Norwegian cod, also consumes large amounts of post-larval capelin. In this study, we show how temperature and the North Atlantic Oscillation (NAO) indirectly influence the population dynamics of capelin by influencing the reproduction of herring and cod. After 1980, when the herring spawning stock had recovered after its collapse in 1969, we found that temperature strongly negatively influences capelin cohorts 2 yr before spawning. Capelin cohorts which have spawned 2 yr after a warm year tend to experience high predation from both young herring as larvae and from 3 to 6 yr old cod during the rest of their life. Other analyses confirm that present sea temperatures or previous NAO conditions have strong positive effects on the abundance of 0-group cod and herring. Thus, the climatic regime of the region ultimately determines the balance between capelin and herring, which in turn has pronounced consequences for the species composition and energy flow of the entire ecosystem.

KEY WORDS: Temperature · North Atlantic Oscillation · Cod · Herring · Time-series analysis · Indirect effects · Lagged effects

INTRODUCTION

Climatic forcing in a macroecological context

Marine biologists have long appreciated the profound influence of climate on ecological processes and patterns (Hjort 1914, Cushing 1982). A modelling study by Lekve et al. (2003) explicitly incorporated climate forcing when modelling the community dynamics of coastal benthic communities along the Norwegian Skagerrak coast. This work of Lekve et al. (2003) falls within the field of macroecology (see e.g. Brown & Maurer 1989)—a field which until now has been primarily exercised within the field of terrestrial ecology, and only recently been adopted for marine systems (e.g. Stevens 1996, Attrill et al. 2001, Belgrano et al. 2002, Li 2002, Smith & Brown 2002). In this paper we provide by focusing on the Barents Sea, another example of a macroecological approach to a marine system.

Although climatic forcing certainly is appreciated as an important external process within terrestrial ecosystems (see e.g. Stenseth et al. 2002, Mysterud et al. 2003), terrestrial ecologists have focused less on ex-

*Corresponding author. Email: n.c.stenseth@bio.uio.no

ternal forcing and much more on internal ecosystem processes (such as competition and trophic interactions). A marine approach to macroecology may therefore provide valuable conceptual feedback to the field of terrestrial macroecology. Furthermore, although macroecology deals with how species dynamically share the available food and space (e.g. Kendall et al. 1998), macroecological studies have tended to consider ecosystems as quite static in ecological time. Marine systems are highly dynamic, most conspicuously demonstrated by the dramatic changes in the abundance of pelagic fish (e.g. Klyashtorin 1998, Chavez et al. 2003). Such changes may be observed at several trophic levels as documented by Anderson & Piatt (1999). Their findings were based on fish-scale records covering hundreds of years; hence, spanning a period long before fishing had any significant effect on the population dynamics of the species in question (see also Baumgartner et al. 1992, Alheit & Hagen 1997, Corten 1999). Such decadal-scale fluctuations may be synchronized over large areas (e.g. across the Pacific) and are often assumed to be caused by large-scale climatic phenomena (Rodionov 1995, Schwartzlose et al. 1999, Chavez et al. 2003, but see Fréon et al. 2003).

Here, we focus on the effects of climate on the relationship between the 3 fish populations dominating the Barents Sea ecosystem: the Barents Sea capelin *Mallotus villosus*, the Norwegian spring-spawning herring *Clupea harengus*, and the Arcto-Norwegian cod *Gadus morhua*. Focusing on capelin, we explore how climate variation affects the dynamics of this population, effects which in turn might have marked effects on the structure and functioning of the entire ecosystem (Hamre 1994). Our analysis demonstrates that the observed effects of climate on capelin are, to a large extent, mediated through the reproduction of the coexisting cod and herring. The strength of a cod or herring cohort is, primarily, determined by the climatic conditions in the year of spawning (Hjort 1914). As a result, the climatic condition in a given year will have a lasting effect on the ecosystem in subsequent years, an effect we document here for capelin in the Barents Sea. Within the field of terrestrial ecology, this phenomenon is typically referred to as 'the cohort effect' (Stenseth et al. 2002). For instance, Mysterud et al. (2002) reported that the population density at the time of birth influenced the subsequent average body weight of adult red deer.

We adopt a macroecological approach in this paper. The classic macroecological approach has been to regard each species in a biota as one data point (see e.g. Brown 1999, Gaston & Blackburn 1999). While this is applicable to some marine systems (e.g. benthic habitats, Lekve et al. 2003), it may not be a fruitful approach for pelagic fish biota, which usually are dominated by a few species. Therefore, we will adopt a slightly different approach and focus on how biotic and climatic processes affect capelin and the balance between capelin and herring. We do this by focusing on the analysis of a 29 yr time series of capelin.

Barents Sea ecological system: a capelin-focused synoptic account

The Barents Sea covers an extensive geographic area (1.4×10^6 km^2) north of Norway and northwestern Russia. The climate of this sub-polar shelf sea is closely linked to the influx of relatively warm Atlantic water. Fluctuations in this inflow drive large variation in temperature, as well as nutrients, both between years and on longer time-scales (Ottersen & Stenseth 2001). There is also a large, but varying, influx of the calanoid copepod *Calanus finmarchicus* each spring from its main overwintering area in the Norwegian Sea (Slagstad & Tande 1996, Sundby 2000). The fish community is dominated by a few very abundant species, resulting in strong interspecific interactions (Hamre 1994, Figs. 1 & 2). The capelin, the dominant planktivore in the Barents Sea over the last 30 yr (Gjøsæter et al. 2002), follows the productive ice-melt zone in spring and summer and migrates back south to winter (Fig. 1). In January, maturing 2 to 4 yr old capelin start to separate from the rest of the population and migrate to the coasts of Norway and Russia to spawn. Most of them spawn only once (Gjøsæter 1998). By biomass, the capelin is the most abundant fish of the Barents Sea (up to 6×10^6 tonnes) — of which as much as 2.9×10^6 tonnes has been harvested (in 1977) (Gjøsæter 1998, Ushakov & Prozorkevich 2002).

Another pelagic plankton-feeder, the Norwegian spring-spawning herring, lives primarily in the Norwegian Sea but uses the Barents Sea as a nursing area. After spawning on the western coast of Norway, their offspring drift to the Barents Sea, where they live until they migrate to the Norwegian Sea, typically at Age 3 (Hamre 1994). Herring eat capelin larvae (cf. Fig. 1), and the presence of substantial amounts of 1 to 2 yr old herring (more than 0.75×10^6 million tonnes) is associated with very low capelin reproduction in most years, close to zero reproduction during some years (Gjøsæter & Bogstad 1998, Huse & Toresen 2000). Herring was practically absent from the Barents Sea after the collapse of the herring stock in 1969, until a successful reproduction in 1983 (Fig. 3c). Since the recovery of the herring stock, the capelin stock has collapsed twice, being reduced by approximately 97 % each time (Gjøsæter 1998, Fig. 3a,b).

The other main predator of capelin is cod, mainly 3 to 6 yr of age, that may consume up to 4×10^6 tonnes of capelin (1 yr and up) annually (Dolgov 2002). Capelin

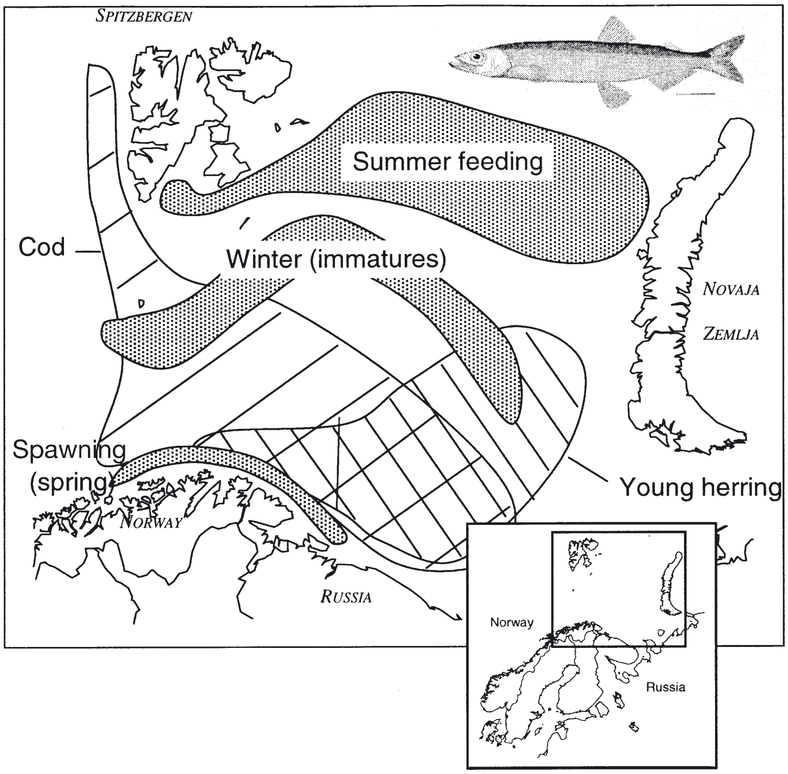

Fig. 1. *Mallotus villosus* and its predators. The study area, showing the summer, winter and spring spawning areas of capelin (grey), the winter area of immature cod *Gadus morhua* (hatching up to the left) and the areas of 1 to 2 yr old herring *Clupea harengus* (hatching up to the right). All areas are approximate and vary from year to year

are only weakly influenced directly by climate (the somatic growth is to some degree influenced by temperature, but is affected by density to a much stronger degree; Gjøsæter 1998). In contrast, the recruitment of both herring and cod (Fig. 3c) is strongly associated with warm years. Thus, in warm years, herring and cod tend to have good reproduction and produce strong year-classes (Ottersen et al. 1994, Ottersen & Loeng 2000, Toresen & Østvedt 2000, Ottersen & Stenseth 2001, Pope et al. 2001). One and 2 yr later, the strong herring year-class will exert a high predation pressure on capelin larvae, while 3 to 6 yr later, the strong cod year-classes will exert a high predation pressure on capelin of Ages 1 to 4.

Therefore, if climate mainly affects capelin indirectly through its predators, we expect that capelin spawned 1 and 2 yr after a warm year suffer most heavily from predation by both herring and cod (Fig. 4). If cod predation is important, the year-class 2 yr after a warm year will probably suffer most. The negative influence of temperature on capelin population growth rate with a 1 or 2 yr time lag forms the *a priori* hypothesis of this paper.

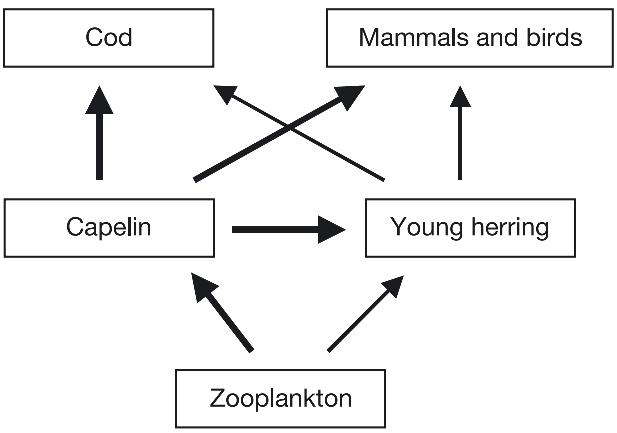

Fig. 2. Main components of the food web, showing the relationship between the focal species of this study: the capelin *Mallotus villosus*, the Arcto-Norwegian cod *Gadus morhua*, and the Norwegian spring-spawning herring *Clupea harengus*. Line thickness indicates roughly the importance of the pathways

MATERIALS AND METHODS

Climatic data. Annual mean sea temperatures from the Russian Kola meridian transect (33° 30′ E, 70° 30′ N to 72° 30′ N) were used (Bochkov 1982, Tereshchenko 1996); the most recent temperatures have been provided by the Polar Institute of Marine Fishery and Oceanography (PINRO, Murmansk). Monthly average values were calculated by averaging along the transect and from 0 to 200 m depth vertically (Fig. 3d). In addition, we used the winter index of the North Atlantic Oscillation (NAO), a measure of the distribution of atmospheric pressure in the North Atlantic (Hurrell et al. 2003, Stenseth et al. 2003). We have used the index based on the difference of normalized sea level pressure between Lisbon, Portugal and Stykkisholmur/Reykjavik, Iceland from December to March (available at www.cgd.ucar.edu/~jhurrell/ nao.html). Throughout the last decades, the NAO has been strongly correlated to Barents Sea temperature (Ottersen et al. 2001, Fig. 3d).

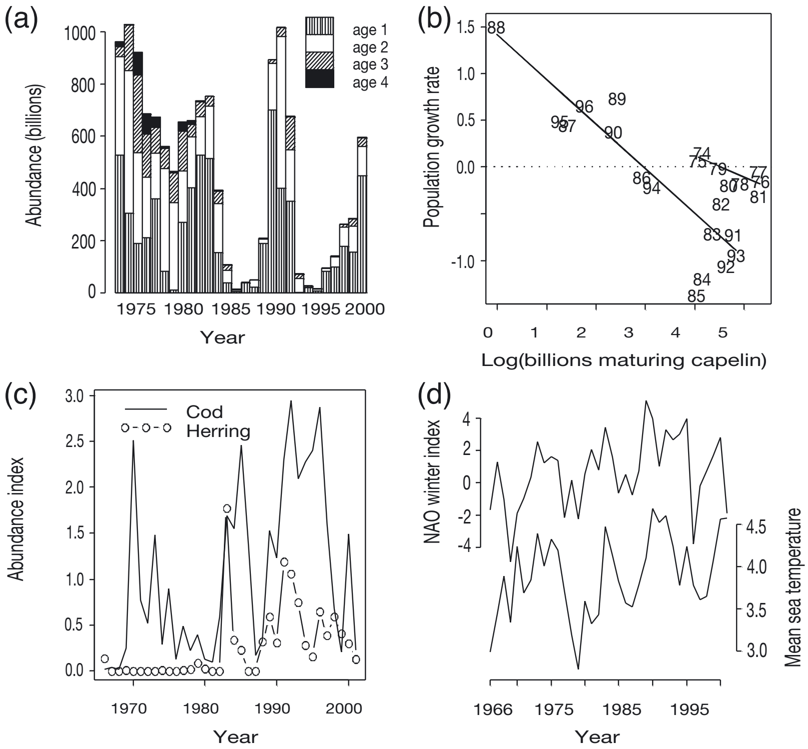

Fig. 3. (a,b) *Mallotus villosus*. (a) Abundance in the 28 yr period from 1973 to 2000, as estimated by the annual international acoustic survey of pelagic fish (September to October). (b) Population growth rate (r) for each cohort estimated from the data in (a), plotted against the spawning-stock size of the parental generation. Numbers refer to the year of spawning of the parental generation. (c) *Gadus morhua* and *Clupea harengus*. Abundance ('log-index') of zero-group, 1966 to 2001. (d) Winter North Atlantic Oscillation (NAO) index and annual mean sea temperature (0 to 200 m) in the Kola section, from 1966 to 2001

Capelin population growth. We estimated population growth based on estimates from the joint Russian/Norwegian acoustic survey of pelagic fish from 1973 to 2000. This survey is carried out annually in September to October as a joint effort between the Institute of Marine Research (IMR), Bergen and PINRO. We used the estimates of capelin abundance for each age, from 1 to 4 yr, as reported in the survey report (available at www.imr.no), and data of mean length obtained from IMR. We estimated the population growth rate based on the change in the number of maturing capelin (fish that will mature and attempt spawning the following spring; see below) over one generation. We defined the net population growth rate (r) as $\log(R_0)/T$, where R_0 is the mean number of maturing fish produced by each maturing fish in the previous generation and T is the average generation length (measured as the mean age at spawning):

$$R_0 = (M_{2,t+3} + M_{3,t+4} + M_{4,t+5})/(M_{2,t} + M_{3,t} + M_{4,t})$$
$$T = (3M_{2,t+3} + 4M_{3,t+4} + 5M_{4,t+5})/(M_{2,t} + M_{3,t} + M_{4,t})$$

where $M_{i,t}$ is the number of maturing capelin of age i in year t. The proportion of maturing capelin was estimated on the basis of average length, assuming a logistic relationship between individual length (L) and maturation, f: $f = 1/(1+e^{2.4(L_{50}-L)})$, where L_{50} was 13.9 cm for 3 and 4 yr olds and 14.2 cm for 2 yr olds (Gjøsæter 1998). Individual length was assumed to be normally distributed within each age group, with a standard deviation equal to that observed during the period covered by the time-series data (1.33, 1.24 and 1.01 for 2, 3 and 4 yr olds, respectively).

Since r is strongly dependent on spawner abundance (Fig. 3b), we controlled for spawner abundance in the analyses of r (i.e. we included [$M_{2,t}$ + $M_{3,t}$ + $M_{4,t}$] as a factor in the analyses).

Cod and herring 0-group abundance. We used abundance indices of pelagic 0-group (ca. 5 mo old) fish from 1966 to 1999, available from ICES (2002a,b) and originating from the International 0-group Survey in August and September each year (a cooperation between IMR and PINRO). The fish were sampled at several depths at a number of stations, using a small mesh midwater trawl (Randa 1982, 1984). We have used the so-called log-index, which is an index based on back-transformed logarithmic means (Randa 1982, 1984). In some of the reported analyses we also utilized the spawning stock biomass (SSB) of herring and cod, retrieved from ICES reports (ICES 2002a,b).

Statistical analyses. We analysed details of whether the per-generation growth rate (r) of capelin could be predicted from temperature 0 to 2 yr before spawning of the parental generation (hereafter denoted lag = 0 to 2), and NAO 0 to 4 yr before spawning. We also analyzed the relationship between capelin r and the 0-group abundance of cod and herring 0 to 3 yr before capelin spawning. Finally, we performed a similar analysis for the relationship between climate and the 0-group abundance of cod and herring. We used general additive models (GAM) with a loess smoother (span = 0.8) to allow for non-linear effects; the 'best' models were chosen on the basis of stepwise selection using, unless otherwise stated, Mallow's C_p (equivalent to the Akaike Information Criterium, AIC) as the optimization criterion.

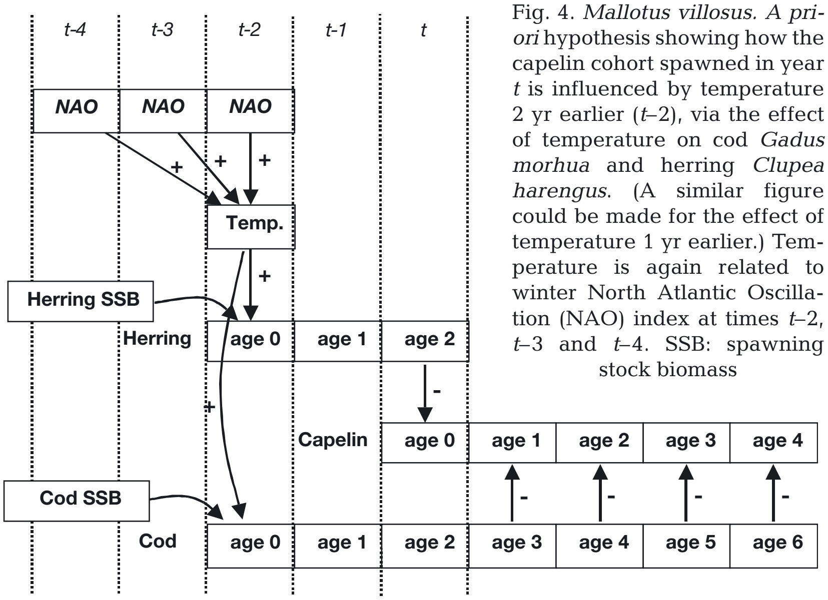

Fig. 4. *Mallotus villosus. A priori* hypothesis showing how the capelin cohort spawned in year t is influenced by temperature 2 yr earlier (t–2), via the effect of temperature on cod *Gadus morhua* and herring *Clupea harengus*. (A similar figure could be made for the effect of temperature 1 yr earlier.) Temperature is again related to winter North Atlantic Oscillation (NAO) index at times t–2, t–3 and t–4. SSB: spawning stock biomass

Table 1. Correlations (Pearson correlation coefficient) between the North Atlantic Oscillation (NAO) winter index and mean 0 to 200 m Kola temperature, during the period 1965 to 2001. Correlations were corrected for autocorrelation by adjusting the sample size by the factor $(1 - \alpha_1\alpha_2)(1 + \alpha_1\alpha_2)$, where α_1 and α_2 are each variable's lag-1 autocorrelation coefficient (Priestley 1981, Lekve et al. 1999). *$0.01 \leq p \leq 0.05$; **$0.001 \leq p \leq 0.01$; t: year

	NAO_t	$Temperature_t$
NAO_t	–	0.52**
NAO_{t-1}	0.34*	0.50**
NAO_{t-2}	0.13	0.42*
$Temperature_t$	0.52**	–
$Temperature_{t-1}$	0.07	0.48**
$Temperature_{t-2}$	0.09	0.18

RESULTS

Correlations between climate indicators

As shown in Table 1, the annual mean temperature at 0 to 200 m depth in the Kola section was both highly autocorrelated in time, and related to the NAO winter index of the last 3 yr. The NAO index is autocorrelated to a smaller degree, and is not related to previous temperatures.

Correlations between climate and capelin population growth (without herring and/or cod)

The relationship between cohort abundance and r is strong (Fig. 3b); hence, we do not report results from models not corrected for cohort abundance. We found a negative correlation with NAO 2 yr before capelin spawning (Table 2a). However, if we exclude the first 7 yr (1974 to 1980 spawners; i.e. the generations little affected by the return of herring in 1983), NAO with lag-2 loses some of its explanatory power ($F = 4.41$, $p = 0.056$). For this set of years, lag-2 temperature is seen to be a better explanatory factor (Table 2b). However, if we add the abundance of herring as an explanatory factor (using all years in the analysis), we found a strong and additive negative effect of the abundance of 0-group herring 1 and 2 yr before spawning (Table 2c). This model explained almost all variation in r (Fig. 5), but Mallow's C_p was even further improved by adding temperature and NAO (Table 2e). If herring was excluded as an explanatory factor, cod with a 1 yr time lag provided a quite high explanatory value as well (Table 2d).

Correlations between climate and the abundance of 0-group cod and herring

For cod, we found that if we did not control for cod SSB, the best model for 0-group abundance consisted of a linear, positive effect of current temperature as well as a non-linear effect of NAO 2 yr earlier (Table 3a). The amount of 0-group cod was lowest when the NAO index was intermediate 2 yr earlier (Fig. 6a). If we did control for SSB, however, the effect of NAO with a 2 yr lag was positive, and linearly related to cod abundance (Table 3b).

The best model for herring abundance (without herring SSB; Table 3c), was found to be a non-linear effect of NAO 2 yr earlier, similar to the model found for cod (Fig. 6c). In addition, we found a lagged non-linear effect of temperature 2 yr earlier (abundance declining for temperatures below ~3.4°C; Fig. 6b), and a linearly positive effect of the current NAO index. By controlling for herring SSB, we found a linearly positive effect of NAO 2 yr earlier, just as was found for cod (Table 3d). However, R^2 was low for this model.

DISCUSSION

Indirect effects of climate on capelin

Our analysis shows that reproduction and survival of capelin is indirectly, but strongly, linked to climate, as

Table 2. *Mallotus villosus.* Optimal statistical models explaining per-generation capelin population growth (r). Lags are relative to the spawning year of the parental stock. Analysis covers parental spawning years 1974 to 1996 (1981 to 1996 in b). Intercept estimates are not shown. NAO: North Atlantic Oscillation

	Estimate	F	p
(a) Best model without cod and herring 0-group abundance (R^2 = 0.63)			
log(capelin spawner abundance)	−0.33	27.88	<0.0001
NAO index (lag = 2)	−0.33	7.87	0.029
(b) As in (a), but using only 1981 to 1996 data (R^2 = 0.82)			
log(capelin spawner abundance)	−0.45	59.29	<0.0001
Sea temperature (lag = 2)	−0.43	6.18	0.027
(c) Best model without cod 0-group abundance and climate (R^2 = 0.84)			
log(capelin spawner abundance)	−0.33	61.94	<0.0001
Abundance herring 0-group (lag = 1)	−0.51	13.47	0.002
Abundance herring 0-group (lag = 2)	−0.49	12.18	0.002
(d) Best model without herring 0-group abundance and climate (R^2 = 0.70)			
log(capelin spawner abundance)	−0.37	−6.53	<0.0001
Abundance cod 0-group (lag = 1)	−0.32	−3.44	<0.003
(e) Best overall model (R^2 = 0.88)			
log(capelin spawner abundance)	−0.34	−8.72	<0.0001
Abundance herring 0-group (lag = 1)	−0.65	−4.37	<0.001
Abundance herring 0-group (lag = 2)	−0.44	−3.10	0.0065
NAO index (lag = 2)	−0.076	−1.85	0.082
Sea temperature (lag = 1)	0.35	2.10	0.051

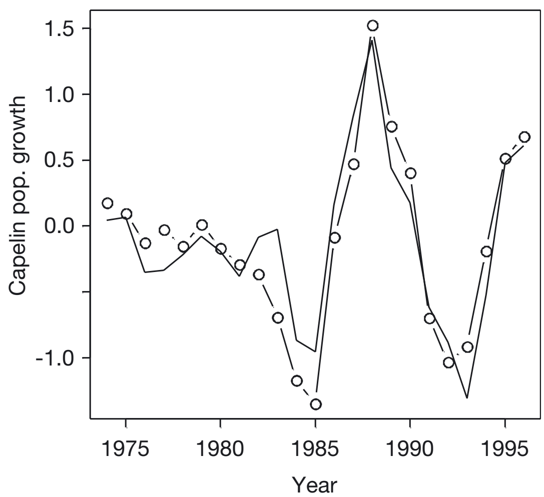

Fig. 5. *Mallotus villosus*. Predictions of population growth rate, in a linear model with abundance of capelin spawners as well as the abundances of 0-group herring 1 and 2 yr before spawning (–○– = observed; — = predicted)

hypothesized in Fig. 4. For the entire period from 1973 to 1996, capelin population dynamics were linked to the NAO 2 yr before spawning, hereafter denoted as NAO_{t-2} (Table 2a). Since NAO_{t-2} is related to temperature in Year t–2, t–1 and t ($Temp_{t-2}$, $Temp_{t-1}$ and $Temp_t$; Table 1), this finding links high capelin population growth to generally low temperatures (both in the year of spawning as well as in the 2 preceding years). However, the generally high level of capelin in the 1970s compared to the 1980s and 1990s influences this result. The late 1970s was a generally cold, low-NAO period, but also the SSB of herring was extremely low after the 1969 collapse. During 1981 to 1996, when the herring SSB became sufficiently large to produce rich year-classes of offspring, the best predictior for capelin population growth was $Temp_{t-2}$ (Table 2b), just as expected from Fig. 4. The hypothesized relationship of Fig. 4 is supported by 3 additional analyses: First, herring and cod 0-group abundance were each good predictors of capelin population growth (Table 2c,d). Second, including climate in addition to herring increases the explanation power by only 4% (R^2 = 0.84 and 0.88, respectively, Table 2c,e), indicating that direct effects of climate appear to be, at best, quite weak. Third, best models for cod and herring 0-group abundance confirm the strong effect of NAO with a 2 yr time lag (Table 3d). Also Hamre (2000), who explored a model with temperature, cod, capelin and herring, found that the temperature-herring-capelin link was the strongest dynamic element of his model.

The cod cohort spawned 2 yr before capelin would be 3 to 6 yr old when the capelin are 1 to 4 yr old (Fig. 4). Indeed, most capelin predated by cod are in fact eaten by these age groups (Dolgov 2002), which could be part of the explanation for the effect of $Temp_{t-2}$ (Table 2b). Excluding herring as an explanatory factor, we find the best explanatory factor to be cod 0-group abundance 1 yr, not 2 yr, before capelin spawning. Since they are highly correlated (R = 0.66, p < 0.001), it is, however, hard to discriminate between the effect of lag-1 and lag-2 cod abundance. According to the hypothesis outlined in Fig. 4, we would expect the best overall model for capelin growth to be a model with effects of herring and cod, and no effects of climate. This was not the case (Table 2e). Again, the effect of cod may be swamped by the effect of lag-1 and lag-2 herring abundance, since 54% of lag-1 cod abundance is explained by lag-1 and lag-2 herring abundance. In fact, herring abundance is much more closely correlated with the cod abundance (R = 0.60, p < 0.01) than with herring abundance (R = 0.32, p = 0.13) the year after. The 0-group survey has not been

Table 3. *Gadus morhua* and *Clupea harengus.* Optimal statistical models explaining influences on the abundance of 0-group cod (a,b) and herring (c,d). Years refer to the spawning year of the parental stock. Intercept estimates are not shown. SSB: spawning stock biomass

	Estimate	*F*	p	p (linearity)
(a) Cod 0-group abundance — without cod SSB ($R^2 = 0.53$)				
Sea temperature (lag = 0)	0.67	6.98	0.013	
NAO index (lag = 2)	Non-linear	7.87	<0.001	0.015
(b) Cod 0-group abundance — with cod SSB ($R^2 = 0.55$)				
log(cod SSB)	0.88	15.52	<0.001	
NAO index (lag = 2)	0.14	6.60	0.014	
(c) Herring 0-group abundance — without herring SSB ($R^2 = 0.51$)				
NAO index (lag = 0)	0.063	6.46	0.017	
Sea temperature (lag = 2)	Non-linear	3.10	0.042	0.078
NAO index (lag = 2)	Non-linear	7.06	0.002	0.007
(d) Herring 0-group abundance — with herring SSB ($R^2 = 0.36$)				
log(herring SSB)	0.078	8.07	0.007	
NAO index (lag = 2)	0.32	7.18	0.011	

found to give very good estimates for cod, since part of the 0-group cod already may have moved from a pelagic to a demersal habitat in this part of the year (Helle et al. 2000). However, the results were similar if we used Virtual Population Analysis (VPA) estimates of Age 3 cod. The good recruitment of capelin in the early 1970s during a high cod stock indicates that a high capelin stock is quite resilient to cod predation.

While climate clearly influences the spawning migrations and spawing locations of capelin (Ozhigin & Luka 1985, Tjelmeland 1987), this study shows no evidence for strong direct effects of climate on capelin dynamics. This confirms earlier findings that Barents Sea capelin is much more affected by predation (and harvest) than by direct climatic effects or climatic effects acting through plankton (Bogstad & Gjøsæter 1994, Gjøsæter 1998, Gjøsæter & Bogstad 1998). The same is true for the Icelandic stock (Vilhjalmsson 2002). In sharp contrast, year-class strength of the capelin stocks of the NW Atlantic is strongly linked with climate through direct effects (Leggett et al. 1984, Carscadden et al. 2000, 2001). For the beach-spawning stocks in this area, larval emergence is strongly linked to periods of onshore winds and warm, food-rich, predator-poor surface waters. Strong year-classes are associated with a high frequency of onshore winds during the critical period immediately after hatching. One could attribute the lack of effects in the Barents Sea and Icelandic stocks to the fact that they spawn on the bottom near the coast, in contrast to 4 of the 5 NW Atlantic stocks. However, the bottom-spawning stock in the NW Atlantic also appears to be positively affected by wind-forcing events, possibly linked to destratification at the time of emergence (Frank & Carscadden 1989). While researchers in the NW Atlantic have found capelin recruitment to be affected by wind conditions during a very short critical period (e.g. 10 d after median hatching; Leggett et al. 1984), we (and other researchers) have looked for possible effects only among much more broad-scaled environmental variables. Therefore, effects of wind or other environmental variables during a short critical period could be important in the Barents Sea capelin as well. However, not much residual variation in capelin success remains to be explained after taking predator abundance and broad-scaled climate into account (<20%; Table 2). Thus, our analyses indicate not merely that we have found no evidence of direct environmental effects, but also that there is not much room left for such effects. An interesting issue for future research is why direct environmental effects dominate the NW Atlantic capelin stocks, while predation dominates the Barents Sea stock.

In the analyses of climatic effects on the 0-group abundance of cod and herring, we found quite similar results regarding NAO_{t-2}. If we did not control for SSB (but did control for current temperature/NAO), NAO_{t-2} had a strongly non-linear effect in both cases, with intermediate NAO resulting in low 0-group abundance (Fig. 6a,c). Such non-linear responses to NAO have been reported in terrestrial systems (see Mysterud et al. 2003 for a review); however, we find it outside the scope of this study to pursue the background of this result. In the analyses where the effect of SSB is taken into account, it is interesting to note that NAO_{t-2} (being related to $Temp_{t-2}$, $Temp_{t-1}$ and $Temp_t$) in both cases had a more strongly positive effect than $Temp_t$. Thus, the present temperature condition does not appear to be the best predictor of cod and herring reproduction.

Significance of capelin in the Barents Sea system

When juvenile herring replaces capelin during capelin collapses, the entire ecosystem is changed. First, capelin is the only species able to effectively exploit the rich plankton bloom along the ice edge (Gjøsæter & Loeng 1987, Hassel et al. 1991, Gjøsæter et al. 2002). The herring does not go as far north as the capelin. The plankton-feeding polar cod *Boreogadus saida* tolerates cold waters, but forages further down in the water column and not as effectively as the capelin (Hamre 1994).

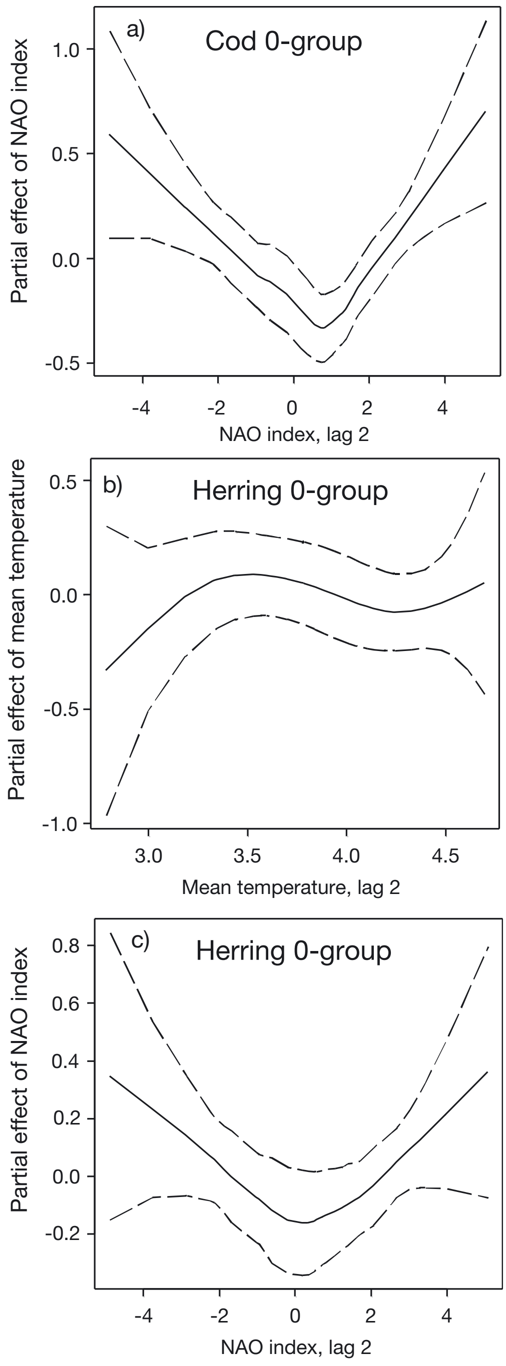

Fig. 6. Non-linear effects. (a) *Gadus morhua.* Partial effect of North Atlantic Oscillation (NAO) in the model of cod 0-group abundance without spawning stock biomass (SSB). (b),(c) *Clupea harengus.* Partial effect of temperature (b) and NAO (c) in the model of herring 0-group abundance without SSB

Second, the capelin effectively transports a substantial amount of energy from the remote central and northern Barents Sea to the coastal areas, where it becomes easily available for piscivorous fish, seabirds, mammals and fishery activities restricted to the southern parts of the Barents Sea. In contrast, much of the biomass accumulated by the herring is moved out of the Barents Sea when the 3 yr old herring returns to the Norwegian Sea. Third, several predatory species (e.g. cod) prefer capelin to herring, and other species (such as the common guillemot *Uria aalge*) appear to specialize on capelin. Finally, quite a low biomass of juvenile herring is able to block the reproduction of capelin, replacing a large capelin biomass with a small herring biomass. Altogether, the lagged effect of a warm period leads to large changes in the ecosystem at all levels, and a generally poorer transfer of energy from low to high trophic levels (von Quillfeldt et al. 2002).

CONCLUSION

The present analysis suggests that the survival of capelin in the Barents Sea depends on periods with poor recruitment of cod and herring (i.e. cold periods). In turn, this affects the whole ecosystem significantly. If the temperature of the Barents Sea varies in a periodic fashion, suggested by some authors (see discussion in Ottersen et al. 2000), this may lead to cycles in the ecosystem state. This was indeed found by Hamre (2000) when simulating the fish stocks with temperature cycles of 8 to 9 yr periods. In addition, he found the cyclic tendency to be exaggerated by a lagged negative effect on cod during capelin collapses.

The heat content of the Northern Atlantic has experienced an increasing trend over the last few decades (Barnett et al. 2001). According to available climate scenarios, this tendency is expected to continue (Vinnikov et al. 1999). Thus, the predation pressure on capelin from herring and cod may become permanently very high. Also, the southern ice limit will probably move northwards. One could imagine that the capelin simply would move its summer distribution northwards, too. However, that would lead to an increasing distance to the spawning grounds, if the spawning location is not radically changed. Also, the same 'ice edge effect' may not be seen when the ice moves further north, for instance, because of the larger bottom depths towards the northern Barents Sea. Altogether, in a global warming perspective, the capelin faces an uncertain future, at least its position as a major player in the Barents Sea ecosystem is uncertain.

In this investigation we have demonstrated that indirect climatic effects may have a profound impact on key species in the ecosystem. These effects act through what properly should be called a cohort effect, leading to a time lag between changes in climate and effects on the capelin. The changes in capelin abundance can in turn lead to new, lagged effects; for instance, the abundance of capelin affects the per capita egg production of cod (Marshall et al. 1999). Hence, climate change might lead to large changes in the ecosystem in 2 different ways. First, an increase in the average temperature resulting from global warming might lead to a quite dramatic decrease in the average capelin abundance, which undoubtedly leads to substantial changes in the energy flow, and species composition, of the ecosystem. Second, any change in the temporal pattern of temperature, e.g. how many years the warm periods typically last, may lead to a change in the dynamics of the ecosystem. The end product of such changed dynamics is much more difficult to predict. Therefore, as a result of the interplay between climate and the internal processes, modest changes in climate might ultimately lead to a very different ecosystem. In the light of the predicted future changes in climate, understanding this interplay is a challenge of great academic and practical importance.

Acknowledgements. We thank PINRO (Murmansk) for most kindly providing temperature data from the Kola transect as well as providing, together with the Institute of Marine Research, Bergen, the abundance and length data on the capelin. We also thank J. Hamre, H. Gjøsæter, K. Lekve and 2 anonymous reviewers for improving this paper through their input. This work was supported by the Research Council of Norway (D.Ø.H. through the *EcoClim*-project of the University of Oslo, and G.O. through the Strategic Institute Program 134278/130 between the University of Oslo and the Institute of Marine Research). The work was carried out within the framework of the international GLOBEC program.

LITERATURE CITED

Alheit J, Hagen E (1997) Long-term climate forcing of European herring and sardine populations. Fish Oceanogr 6: 130–139

Anderson PJ, Piatt JF (1999) Community reorganization in the Gulf of Alaska following ocean climate regime shift. Mar Ecol Prog Ser 189:117–123

Attrill MJ, Stafford R, Rowden AA (2001) Latitudinal diversity patterns in estuarine tidal flats: indications of a global cline. Ecography 24:318–324

Barnett TP, Pierce DW, Schnur R (2001) Detection of anthropogenic climate change in the world's oceans. Science 292:270–274

Baumgartner TR, Soutar A, Ferreirabartrina V (1992) Reconstruction of the history of Pacific sardine and northern anchovy populations over the past 2 millennia from sediments of the Santa-Barbara Basin, California. Calif Coop Ocean Fish Investig Rep 33:24–40

Belgrano A, Allen AP, Enquist BJ, Gillooly JF (2002) Allometric scaling of maximum population density: a common rule for marine phytoplankton and terrestrial plants. Ecol Lett 5:611–613

Bochkov YA (1982) Water temperature in the 0–200 m layer in the Kola-Meridian in the Barents Sea, 1900–1981. Sb Nauchn Tr Polar Inst Mar Fish Oceanogr Murmansk 46: 113–122

Bogstad B, Gjøsæter H (1994) A method for estimating the consumption of capelin by cod in the Barents Sea. ICES J Mar Sci 51:273–280

Brown JH (1999) Macroecology: progress and prospect. Oikos 87:3–14

Brown JH, Maurer BA (1989) Macroecology: the division of food and space among species on continents. Science 243: 1145–1150

Carscadden JE, Frank KT, Leggett WC (2000) Evaluation of an environment-recruitment model for capelin (*Mallotus villosus*). ICES J Mar Sci 57:412–418

Carscadden JE, Frank KT, Leggett WC (2001) Ecosystem changes and the effects on capelin (*Mallotus villosus*), a major forage species. Can J Fish Aquat Sci 58:73–85

Chavez FP, Ryan J, Lluch-Cota SE, Niquen M (2003) From anchovies to sardines and back: multidecadal change in the Pacific Ocean. Science 299:217–221

Corten A (1999) A proposed mechanism for the Bohuslan herring periods. ICES J Mar Sci 56:207–220

Cushing DH (1982) Climate and fisheries. Academic Press, London

Dolgov AV (2002) The role of capelin (*Mallotus villosus*) in the foodweb of the Barents Sea. ICES J Mar Sci 59:1034–1045

Frank KT, Carscadden JE (1989) Factors affecting recruitment variability of capelin (*Mallotus villosus*) in the Northwest Atlantic. J Conseil 45:146–164

Fréon P, Mullon C, Voisoin B (2003) Investigating remote synchronous patterns in fisheries. Fish Oceanogr 12:443–457

Gaston KJ, Blackburn TM (1999) A critique for macroecology. Oikos 84:353–368

Gjøsæter H (1998) The population biology and exploitation of capelin (*Mallotus villosus*) in the Barents Sea. Sarsia 83: 453–496

Gjøsæter H, Bogstad B (1998) Effects of the presence of herring (*Clupea harengus*) on the stock-recruitment relationship of Barents Sea capelin (*Mallotus villosus*). Fish Res 38:57–71

Gjøsæter H, Loeng H (1987) Growth of the Barents Sea capelin, *Mallotus villosus*, in relation to climate. Environ Biol Fish 20:293–300

Gjøsæter H, Dalpadado P, Hassel A (2002) Growth of Barents Sea capelin (*Mallotus villosus*) in relation to zooplankton abundance. ICES J Mar Sci 59:959–967

Hamre J (1994) Biodiversity and exploitation of the main fish stocks in the Norwegian–Barents Sea ecosystem. Biodivers Conserv 3:473–492

Hamre J (2000) Capelin and herring as key species for the yield of north-east Arctic cod. Results from multispecies model runs. Sci Mar 67(Suppl 1):315–323

Hassel A, Skjoldal HR, Gjøsæter H, Loeng H, Omli L (1991) Impact of grazing from capelin (*Mallotus villosus*) on zooplankton — a case-study in the northern Barents Sea in August 1985. Polar Res 10:371–388

Helle K, Bogstad J, Marshall CT, Michalsen K, Ottersen G, Pennington M (2000) An evaluation of recruitment indices for Arcto-Norwegian cod (*Gadus morhua* L.). Fish Res 48: 55–67

Hjort J (1914) Fluctuations in the great fisheries of northern Europe viewed in the light of biological research. Rapp P-V Réun Cons Perm Int Explor Mer 20:1–228

Hurrell JW, Kushnir Y, Ottersen G, Visbeck M (eds) (2003) The North Atlantic Oscillation: climatic significance and environmental impact. American Geophysical Union, Washington, DC

Huse G, Toresen R (2000) Juvenile herring prey on Barents Sea capelin larvae. Sarsia 85:385–391

ICES (2002a) Report of the Arctic Fisheries Working Group. ICES CM 2002/ACFM:18 International Council for the Exploration of the Sea, Copenhagen (also available at: www.ices.dk/committe/acfm/ wg/afwg/afwg.htm)

ICES (2002b) Report of the Northern Pelagic and Blue Whiting Fisheries Working Group. ICES CM 2002/ACFM:19 International Council for the Exploration of the Sea, Copenhagen (also available at: www.ices.dk/committe/acfm/wg/wgnpbw/wgnpbw.htm)

Kendall BE, Prendergast J, Bjornstad ON (1998) The macroecology of population dynamics: taxonomic and biogeographic patterns in population cycles. Ecol Lett 1:160–164

Klyashtorin LB (1998) Long-term climate change and main commercial fish production in the Atlantic and Pacific. Fish Res 37:115–125

Leggett WC, Frank KT, Carscadden JE (1984) Meteorological and hydrographic regulation of year-class strength in capelin (*Mallotus villosus*). Can J Fish Aquat Sci 41:1193–1201

Lekve K, Stenseth NC, Gjøsæter J, Fromentin JM, Gray JS (1999) Spatio-temporal patterns in diversity of a fish assemblage along the Norwegian Skagerrak coast. Mar Ecol Prog Ser 178:17–27

Lekve K, Stenseth NC, Johansen R, Lingjærde OC, Gjosaeter J (2003) Richness dependence and climatic forcing as regulating processes of coastal fish-species richness. Ecol Lett 6:1–12

Li WKW (2002) Macroecological patterns of phytoplankton in the northwestern North Atlantic Ocean. Nature 419:154–157

Marshall CT, Yaragina NA, Lambert Y, Kjesbu OS (1999) Total lipid energy as a proxy for total egg production by fish stocks. Nature 402:288–290

Mysterud A, Stenseth NC, Yoccoz NG, Ottersen G, Langvatn R (2003) The response of terrestrial ecosystems to climate variability associated with the North Atlantic Oscillation. In: Hurrell JW, Kushnir Y, Ottersen G, Visbeck M (eds) The North Atlantic Oscillation (NAO): climatic significance and environmental impact. American Geophysical Union, Washington, DC, p 235–262

Ottersen G, Loeng H (2000) Covariability in early growth and year-class strength of Barents Sea cod, haddock, and herring: the environmental link. ICES J Mar Sci 57:339–348

Ottersen G, Stenseth NC (2001) Atlantic climate governs oceanographic and ecological variability in the Barents Sea. Limnol Oceanogr 46:1774–1780

Ottersen G, Loeng H, Raknes A (1994) Influence of temperature variability on recruitment of cod in the Barents Sea. ICES Mar Sci Symp 198:471–481

Ottersen G, Adlandsvik B, Loeng H (2000) Predicting the temperature of the Barents Sea. Fish Oceanogr 9:121–135

Ottersen G, Planque B, Belgrano A, Post E, Reid PC, Stenseth NC (2001) Ecological effects of the North Atlantic Oscillation. Oecologia 128:1–14

Ozhigin VK, Luka GI (1985) Some peculiarities of capelin migrations depending on thermal conditions in the Barents Sea. In: Gjosaeter H (ed) The proceedings of the Soviet-Norwegian symposium on the Barents Sea capelin: Bergen, 14–19 August 1984. Institute of Marine Research, Bergen, p 135–147

Pope J, Large P, Jakobsen T (2001) Revisiting the influences of parent stock, temperature, and predation on the recruitment of the Northeast Arctic cod stock, 1930–1990. ICES J Mar Sci 58:967–972

Priestley MB (1981) Spectral analysis of time series. Univariate series. Academic Press, London

Randa K (1982) Recruitment indices for the Arcto-Norwegian Cod for the period 1965–1979 based on the international 0-group fish survey. ICES CM 1982/G:53. International Council for the Exploration of the Sea, Copenhagen

Randa K (1984) Abundance and distribution of 0-group Arcto-Norwegian cod and haddock 1965–1982. In: Godø OR, Tilseth S (eds) Proc Soviet-Norwegian Symp (Leningrad, 25–30 September 1983): Reproduction and recruitment of Arctic Cod. Institute of Marine Research, Bergen, p 192–212

Rodionov SN (1995) Atmospheric teleconnections and coherent fluctuations in recruitment to North Atlantic cod (*Gadus morhua*) stocks. Can Spec Publ Fish Aquat Sci 121: 45–55

Schwartzlose RA, Alheit J, Bakun A, Baumgartner TR and 17 others (1999) Worldwide large-scale fluctuations of sardine and anchovy populations. S Afr J Mar Sci 21:289–347

Slagstad D, Tande KS (1996) The importance of seasonal vertical migration in across shelf transport of *Calanus finmarchicus*. Ophelia 44:189–205

Smith KF, Brown JH (2002) Patterns of diversity, depth range and body size among pelagic fishes along a gradient of depth. Global Ecol Biogeogr 11:313–322

Stenseth NC, Mysterud A, Ottersen G, Hurrell JW, Chan KS, Lima M (2002) Ecological effects of climate fluctuations. Science 297:1292–1296

Stenseth NC, Ottersen G, Hurrell JW, Mysterud A, Lima M, Chan KS, Yoccoz NG, Ådlandsvik B (2003) Studying climate effects on ecology through the use of climate indices: the North Atlantic Oscillation, El Niño Southern Oscillation and beyond. Proc R Soc Lond B 270:2087–2096 (also available at: www.pubs.royalsoc.ac.uk/proc_bio/proc_bio.html)

Stevens GC (1996) Extending Rapoport's rule to Pacific marine fishes. J Biogeogr 23:149–154

Sundby S (2000) Recruitment of Atlantic cod stocks in relation to temperature and advection of copepod populations. Sarsia 85:277–298

Tereshchenko VV (1996) Seasonal and year-to-year variations of temperature and salinity along the Kola meridian transect. ICES CM (C:11):24

Tjelmeland S (1987) The effect of ambient temperature on the spawning migration of capelin. In: Loeng H (ed) The effect of oceanographic conditions on distribution and population dynamics of commercial fish stocks in the Barents Sea. Proc 3rd Soviet-Norwegian Symp Murmansk, 26 to 28 May 1986. Institute of Marine Research, Bergen, p 225–236

Toresen R, Østvedt OJ (2000) Variation in the abundance of Norwegian spring-spawning herring (*Clupea harengus*, Clupeidae) throughout the 20th century and the influence of climatic fluctuations. Fish Fish 1:231–251

Ushakov NG, Prozorkevich DV (2002) The Barents Sea capelin — a review of trophic interrelations and fisheries. ICES J Mar Sci 59:1046–1052

Vilhjalmsson H (2002) Capelin (*Mallotus villosus*) in the Iceland–East Greenland–Jan Mayen ecosystem. ICES CM 59:870–883

Vinnikov KY, Robock A, Stouffer RJ, Walsh JE and 5 others (1999) Global warming and Northern Hemisphere sea ice extent. Science 286:1934–1937

von Quillfeldt CH, Eliassen JE, Føyn L, Gulliksen B, Lydersen C, Marstrander L (2002) Marine verdier i havområdene rundt Svalbard (Marine values in the oceanic areas around Spitzbergen). Norwegian Polar Institute, Report No. 118, Tromsø

Editorial responsibility: Andrea Belgrano,
Santa Fe, New Mexico, USA

Submitted: April 16, 2003; Accepted: January 27, 2004
Proofs received from author(s): April 20, 2004

Vol. 273: 239–249, 2004 | MARINE ECOLOGY PROGRESS SERIES Mar Ecol Prog Ser | Published June 8

Individual behavior and emergent properties of fish schools: a comparison of observation and theory

Steven V. Viscido[1,2,*], Julia K. Parrish[1,2], Daniel Grünbaum[3]

[1]Department of Biology, [2]School of Aquatic and Fishery Sciences, and [3]School of Oceanography, Box 351800 Kincaid Hall, University of Washington, Seattle, Washington 98195, USA

ABSTRACT: Polarity, group velocity, and inter-individual spacing are characteristics of fish schools that strongly affect individual school members. However, these characteristics are group-level 'emergent properties': collective outcomes of behavioral interactions among members, not under direct control of any single member. The relationships between members' behaviors and the emergent group properties they produce are complex and poorly understood. In this study, we quantified 3D trajectories of all individual fish within 4- and 8-fish populations of *Danio aequipinnatus*, using stereo videography and a computerized tracking algorithm. We compared group polarity, group speed, and mean nearest-neighbor distances of schools within these populations to a simulation model that explored how fish responded to attraction/repulsion, alignment and random forces. Real fish exhibited a high degree of temporal variability in both polarity and group speed. Polarity and speed of simulated schools depended very strongly on the strength of the alignment force. Time-averaged polarity of real fish schools was most similar to simulated schools when alignment force was 1 to 5% of the attraction/repulsion force. For both real and simulated fish, a clear relationship existed between group speed and polarity: polarized groups were faster than non-polarized groups. We propose a multi-dimensional state space where several emergent property statistics are represented along the axes, and suggest certain 'preferred' ranges of state space within which animal groups tend to localize, and in which they can sustain distinct types of regular architecture.

KEY WORDS: Social aggregation · Schooling behavior · Emergent properties · Polarity · Group speed · Nearest-neighbor distance · *Danio aequipinnatus*

INTRODUCTION

Group formation is prevalent amongst almost all animal taxa (Wilson 1975). For example, more than 50% of fish species form schools (Shaw 1978), and 50% of bird species form feeding flocks (Lack 1968). Group-level characteristics — such as regular inter-individual spacing, a particular degree of polarization, or a characteristic group velocity — are generally believed to have important biological consequences (Parrish & Edelstein-Keshet 1999), potentially affecting member fitness by (1) determining foraging success (Cody 1971, Krebs et al. 1972), (2) providing defense against, or escape from, predation (Hamilton 1971, Vine 1971, Watt et al. 1997, Viscido & Wethey 2002), and (3) improving reproductive success (Lack 1968, Burger & Gochfeld 1991). However, because they result from collective interactions and are not under direct control of any group member, these characteristics are not under simple, direct selection. Instead, selection on schooling behaviors reflects the complex dynamics of social interactions within groups: the fitness of a novel schooling behavior is mediated partly through its effects on others in the group, as well as the changes in group characteristics that consequently result. Thus, traits with short-term benefits to individual members may fail to arise because of overriding negative long-term consequences at the group level. Conversely, traits that are beneficial at the group level may fail to persist because individuals who do not exhibit them

*Email: viscido@u.washington.edu

enjoy a relative advantage. Furthermore, some desirable group traits may be unattainable simply because no individual behaviors exist that could generate them.

Group characteristics that result from decentralized interactions are termed 'emergent properties' (Clark et al. 1997). Emergent properties of fish schools and bird flocks in particular have been frequently studied using simulation models. In most such models, each individual's behavioral choices are interpreted as a set of forces that affect the velocity or heading of an individual (e.g. Okubo 1986, Huth & Wissel 1990, Flierl et al. 1999). These forces include biomechanical and environmental forces such as drag (Flierl et al. 1999), attraction and repulsion forces between sets of neighbors (Warburton & Lazarus 1991, Romey 1996, Couzin et al. 2002), alignment or behavior-matching forces (Aoki 1982, Huth & Wissel 1992), and randomness (Reuter & Breckling 1994, Vabo & Nottestad 1997, Stocker 1999). Simulation models typically connect specific individual behaviors to emergent properties by following each individual's position over time and statistically quantifying group-level characteristics.

The strength of the modeling approach is the relative ease of exploring many behavioral variants; however, there are also weaknesses. Chief among these are (1) that it is unclear which statistical measures best reflect biologically important characteristics and (2) that few quantitative observations of fish movements inside schools are detailed and long enough to provide a basis for comparison with model assumptions (Partridge & Pitcher 1980, Aoki 1984, Parrish & Turchin 1997, Hiramatsu et al. 2000). The lack of observational data is primarily due to the difficulties of tracking relatively large, fast objects (e.g. fish, birds) in 3D space over an extended period of time (Parrish et al. 2002). These observational difficulties are an important limitation on our understanding of how social animal groups function and how the underlying social behaviors evolved.

In this study, we develop a quantitative database of individual movements within fish schools and compare it with a simplified individual-based model of fish schooling using a specific subset of emergent property statistics — mean nearest-neighbor distance (NND), group speed, and polarity — applied analogously to both real and model fish trajectories. We assess which parameter values most closely correspond to actual fish behaviors, and which of our group-level statistics appear most informative about the biological functions of fish schools. Specifically, because one of the more striking emergent properties of fish schools is their polarized arrangement (Couzin et al. 2002, Parrish et al. 2002), we focus our simulations on one behavioral force, the alignment force, and compare the emergent properties observed in simulations with those of real fish schools in laboratory populations by systematically varying that force.

We present here the observational methods we used to quantify fish movements, followed first by descriptions of our schooling simulations and then by summaries of the emergent property statistics. We show how these statistics differed between our observations and simulations, and discuss the implications of our results for the mechanisms of social group formation. Finally, we suggest future directions in the analysis of these mechanisms.

MATERIALS AND METHODS

Biological observations. We observed 4- and 8-fish groups of giant danios *Danio aequipinnatus*. This species was also the physical model for our simulated fish. The danios were 5.3 cm long on average (±0.6 SD, N = 14 fish measured) and had a mass of 1.7 g (±0.5 SD, N = 14 fish measured). Danios were held in two 600 l holding tanks on a fixed 14:10 h light:dark cycle and fed ad libitum. At 09:00 h on the day of an observation, 4 or 8 fish were haphazardly selected from holding tanks and placed into a 1 m^3 clear acrylic observation tank. The observation tank contained still water at the same temperature as the holding system, and was illuminated by nine 100 W floodlights equipped with fresnel diffusers and arranged to minimize both glare and shadows. Fish were filmed against a white background. Pilot trials showed no difference in behavior among acclimation times in the observation tank ranging from 6 to 24 h. Therefore, we acclimated animals for 6 h before recording their behavior.

We used Panasonic PVDV-401 mini-DV video cameras mounted directly over the tank (to record x–y movements) and at floor level (to record x–z movements) connected by firewire to 2 Sony DSR-20 digital tape decks. Tape decks and monitors were housed behind a screen such that an observer could operate the decks and observe fish behavior in real time without disturbing the animals. After filming for 30 minutes, the fish were removed from the observation tank, and a metal calibration frame was inserted. The frame consisted of a 7 × 7 square grid of small black beads located 14 cm apart. The frame was filmed in 4 different positions, facing toward and away from each camera to establish a coordinate system just inside the outer edges of the tank.

Preliminary trials indicated that fish in small groups occasionally spend time nudging against the sides of the tank, interacting with their own reflections rather than with other fish ('glass kissing'). Because glass kissing is clearly an artifact of the observational conditions and not a part of the animals' natural behavior, only video sequences with more than 10 consecutive minutes of 'natural' swimming within the central volume of the tank were retained. We then randomly selected a 5 min subset of the natural schooling behavior in each trial for analysis. Below, we present results from three 4-fish trials and three 8-fish trials.

Image capture and conversion: Digital recordings of fish observations were transferred via firewire to an Apple G4 Power PC computer at the standard NTSC frame rate (29.97 Hz) and converted to QuickTime movie format using Adobe Premier 5.1 for Macintosh. We divided each 5 min digital movie into smaller 30 s (900 frame) segments in Adobe Premier to facilitate analysis. Pixel coordinates of fish centroids in each camera view were obtained using automated NIH Image (v. 1.62 for Macintosh) macros. Analysis steps included background subtraction using the time-averaged image, thresholding, and recording of positions to an ASCII text file.

Trajectory reconstruction: The program we used for trajectory reconstruction, Tracker3D, was written in-house using MatLab (The Mathworks 2001, Release 12.1). This program used pixel coordinate data and calibration images to convert each fish position in each video frame to a ray through space in a real-world coordinate system, and then reconstructed fish trajectories within a camera view by associating the corresponding fish centroids in sequential frames using nearest-neighbor criteria. This simple criterion was adequate because data were oversampled.

Tracker3D then entered an 'editing' step in which the user could review the reconstructed paths and, if necessary, make corrections. Most often, because the 2D reconstruction step used very conservative path parameters, the user would simply join fragments of a trajectory into a single longer path. Whenever there was any doubt about whether to join fragments, we watched the original video on a 14″ TV monitor to help make our decision.

Tracker3D then entered the 3D reconstruction step, in which paths from both cameras were combined to triangulate trajectories in 3 dimensions. The criteria for associating paths between cameras were upper limits to distances of closest approach between the rays through physical space from paths in the 2 views, together with limits on plausible fish velocity between successive frames.

Details of the Tracker3D algorithms are available at www.ocean.Washington.edu/people/faculty/grunbaum/Tracker3D. The output from Tracker3D was a simple ASCII text file containing an identifier for each fish and its 3D (x-y-z) position. To reduce high-frequency noise due to frame-rate oversampling, the output file was then passed through a filtering program written in Perl that reduced the frame rate to 5 Hz. We used the filtered output to compute the polarity and speed of fish groups over time.

Computer simulation experiments. *Basic model:* We constructed a 3D model of fish schooling based loosely on preliminary measurements of danio movements taken from early film trials. Note that we did not attempt to perfectly emulate the real-world behavior of danios. Rather, we were interested in using computer simulations to inform us on general self-organization principles. Therefore, although our simulated fish are reasonably realistic, they are not perfectly so (e.g. gravity is not included). However, our simulations are a more physically realistic extension of existing sum-of-forces fish school models (e.g. Aoki 1982, Huth & Wissel 1990, Romey 1996, Couzin et al. 2002).

We set maximum speed at 12 body lengths (BL) s^{-1}, and the maximum force (F_{max}) was set to impart a 12 BL s^{-2} acceleration on the fish, reflecting limits we observed in a pilot study. Since real danios are ca. 5.3 cm long and have a mass of 1.7 g (see 'Biological observations' above), F_{max} = 102 dynes. Although real danios are laterally compressed, our model fish were cylindrical for simplicity, with 1 BL = 5.3 cm, and a body diameter 0.15 BL. Finally, because most fish have a rear blind area (Aoki 1982), we imposed a maximum (forward) viewing angle $\theta = \pm 150°$. Individuals outside the maximum viewing angle were ignored (Couzin et al. 2002).

Each simulation began at time $t = 0$ with a population of 4 or 8 fish scattered randomly within a spherical volume scaled to $12\pi BL^3$ per fish, centered at the origin. Thus, starting density was constant regardless of population size. All fish started with a random velocity, uniformly distributed between 0 and 6 BL s^{-1}. Individuals did not begin a simulation inside each other's body volume; however, during simulations such overlaps sometimes occurred. We considered these intrusions to be analogous to 'collisions' (i.e. mistakes in schooling behavior) and recorded when and where they occurred. Once the simulation began, the individuals were not constrained; the domain was empty and infinite. We used simulated population sizes of 4 and 8 fish so model results could be directly compared with the behavioral observations and ran each simulation for 1800 time steps (60 s at 30 Hz, so that each time step = 1/30 s). Each set of simulation conditions was replicated 15 times.

Behavioral movement rules: Many simulations use forces that accelerate the masses of individual fish to represent behavior (Aoki 1982, Niwa 1994, 1996, Romey 1996). The strength and direction of those forces are taken to implicitly reflect the consequences of complex sequences of events, including sensory perception, cognitive and reflexive processing, and swimming biomechanics. In this paper, we assumed all model fish were subject to only 2 force vectors: the 'social force' ($\mathbf{S}_i$) and the 'random force' ($\mathbf{R}_i$) on each fish i during time t. The social force likely depends on many parameters in real animals: (1) the number of influential neighbors (Warburton & Lazarus 1991), (2) the shape of the attraction/repulsion function (Romey 1996), (3) the strength of the 'alignment' force (Sannomiya & Duostari 1996), (4) the width of attraction, repulsion, and alignment regions (Couzin et al. 2002), and (5) the total population size (Flierl et al. 1999). In this paper, we explore the strength of the alignment force, and how it affects certain emergent properties of fish schools (e.g. polarity, group speed). We consider other factors elsewhere (Viscido et al. unpubl.).

To determine the behavioral decision of a fish, we first defined a total force vector ($\mathbf{F}_i$) on any individual i during time t as a sum of social and random forces (Inagaki et al. 1976, Matuda & Sannomiya 1980, Aoki 1982, Niwa 1994, Sannomiya & Duostari 1996):

$$\mathbf{F}_i = \mathbf{S}_i + \mathbf{R}_i \quad (1)$$

If the computed magnitude of $\mathbf{F}_i$ exceeded $F_{\max}$, the simulation program re-scaled $\mathbf{F}_i$ to have magnitude $F_{\max}$ (while preserving direction). Note that, in addition to random and social force, real fish will also experience an opposing force due to drag. For simplicity, we did not include drag in this model; the effects of drag are reported elsewhere (Viscido et al. unpubl.).

Social force: The total social force acting on fish i during time step t was the sum of social forces between fish i and each other member of the population:

$$\mathbf{S}_i = \sum_{j=1}^{\rho-1} \mathbf{S}_{ij} \quad (2)$$

where ρ is population size (ρ = 4 or 8), and $\mathbf{S}_{ij}$ represents the social force between fish i and each neighbor j. The social force, consisted of 2 distinct components: the attraction/repulsion force and the alignment force. Fish had a preferred distance to their neighbors (δ_p = 1.9 BL) based on observed preferred distances for *Chromis punctipinnis* (Parrish & Turchin 1997). We defined a neighbor fish j that was within ±0.5 BL of the preferred distance as being within the 'alignment zone' (Fig. 1a). Within the alignment zone, fish i experienced an alignment force due to j ($\mathbf{A}_{ij}$) in the swimming direction of fish j. We varied the magnitude of vector $\mathbf{A}_{ij}$ from 0.5 to 50% of $F_{\max}$ (i.e. always far less than the maximum possible attraction/repulsion force) in separate model runs. The magnitude of $\mathbf{A}_{ij}$ was constant throughout the alignment zone, and for all individuals in a given simulation experiment (Fig. 1b).

Outside the alignment zone, fish i was either attracted to, or repulsed from, fish j, depending on the distance between them. When fish j was closer than the repulsion distance δ_r, it was in the 'repulsion zone' (Fig. 1a), and the force acting on fish i due to fish j was directed along the vector from j to i. This 'repulsion force' increased linearly from $-F_{\max}$ at a distance of 0 from fish i, to 0 at exactly δ_r = 1.4 BL (Fig. 1b). When fish j was farther away than the attraction distance δ_a, fish j was in the 'attraction zone' (Fig. 1a), and the force acting on fish i due to fish j was directed along the vector from i to j. This 'attraction force' increased linearly from 0 at exactly δ_a = 2.4 BL to a maximum of $+F_{\max}$ at a distance of 5 BL (Fig. 1b). The social force remained at $+F_{\max}$ to a distance of 100 BL (except within the blind region), at which point fish j was assumed to be outside the visual range of fish i (and hence the social force was 0).

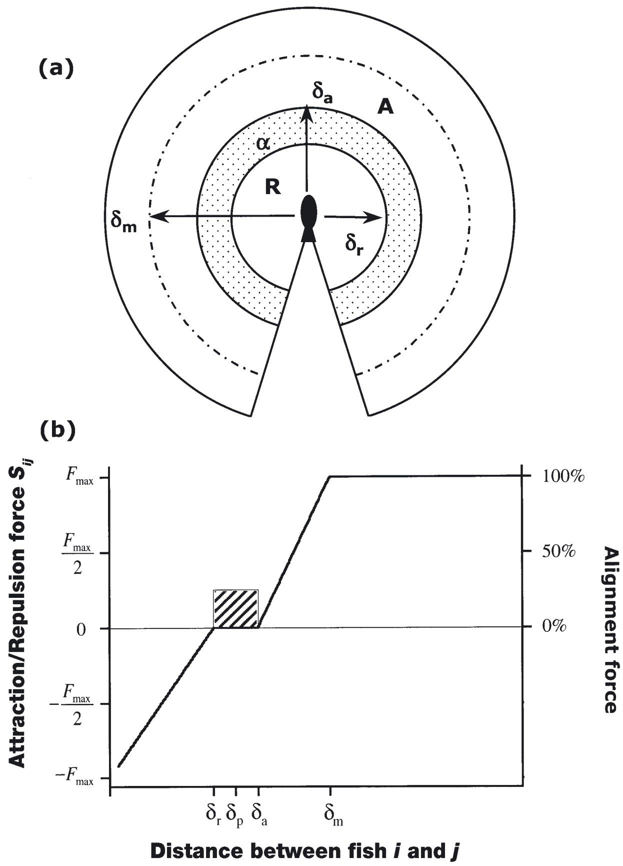

Fig. 1. Social attraction and alignment forces used in the simulation model. (a) The 3 regions over which social forces act: the repulsion zone (R), the alignment zone (α), and the attraction zone (A). Arrows point to the distance at which repulsion begins (δ_r), the distance at which attraction begins (δ_a), and the distance of maximum attraction (δ_m). The 60° arc behind the fish is the 'blind spot.' (b) The 2 forces over distance, with social (attraction/repulsion) force (thick line) in units of dynes, and alignment force (shaded area) as a percent of maximum force ($F_{\max}$). For simplicity only the 25% alignment force is shown. δ_p: preferred distance to neighbor

Random force: During each time step, a variable random force acted on each simulated fish, representing stochastic behavioral and environmental factors that were not explicitly modeled (Flierl et al. 1999). This random force was a vector with random direction and whose magnitude was a random normal variate, with a mean of 0 and a standard deviation of $F_{max}/6$ (i.e. 17 dynes). Because there was an upper limit to total force on an individual (F_{max}), this random force was a relatively smaller component of total force when social forces were large, such as when a fish was about to collide with a neighbor, or was separated from the school. Conversely, the random force was a relatively larger component of total force when social forces were small, such as when all neighbors were in the alignment zone (where forces were always 50% of attraction/repulsion or less), or when no neighbors were present within the maximum sensing distance (where social force was 0).

Statistical analysis. Because our observational experiments lasted a relatively long time (10 min), and therefore fish were likely to encounter the aquarium edge frequently during an observation, we tested whether our metrics might have been affected by the group's proximity to an edge surface. We compared the distance between the group center and the nearest tank edge, in each frame, to each of the 3 schooling metrics tested here, using a product-moment correlation. There was no relationship between edge proximity and any of the metrics used (4 fish: $r^2_{polarity} = 0.03$, $r^2_{speed} = 0.02$, $r^2_{NND} = 0.05$; 8 fish: $r^2_{polarity} = 0.01$, $r^2_{speed} = 0.01$, $r^2_{NND} = 0.03$; $p > 0.05$ in all cases).

We report statistical results for 3 emergent properties of both real and simulated fish schools: polarity, group speed, and mean NND. Polarity and group speed are characteristics of the group (not the individual), and we therefore computed a single value of each property for each group at each time step. Fish were defined as being in a group if they were within 5 BL of at least 1 other neighbor, and otherwise were considered stragglers (and, hence, not included in the group property analysis). When more than 1 group was present during a single time step (e.g. 2 groups of 4 fish in an 8 fish trial), we computed the average value across all groups, to obtain a single mean polarity and mean group speed for each time step. These group-based means were not 'weighted' in any way (e.g. by group size). NND is a property of individuals, and we therefore computed a single mean NND value for the entire population at each time step. Additional metrics at the individual, group, and population level, including path curvature, group size, and collision rate, are reported elsewhere (Viscido et al. unpubl.). We also display the polarity and group speed of a single group in several places (see Figs. 2 & 3). This second approach is merely a visual mechanism to demonstrate the observed group-level patterns (which would not be visible if 'averaged out'), and was not used for computing time-averaged statistics. In these cases only (see Figs. 2 & 3), we report the maximum value obtained by any group within the population for each time step.

Time averages of the 3 properties were computed for each single 30 s segment of a real fish trial. For simulations, we used the latter half (time steps 900 to 1800). This choice was designed to (1) make the simulation time period and the filmed time period comparable, and (2) eliminate the effects of initial conditions (i.e. reduce simulation artifacts). We also compared polarity and group speed using a correlation analysis.

Polarity: We estimated group polarity as the mean vector angle deviation between group and individual heading (Huth & Wissel 1992). Let $\mathbf{V}_i$ represent a unit velocity vector for fish i (scaled to preserve direction) and let $\mathbf{U}$ represent the unit velocity vector for the group's center. We compute the 3D angle deviation α_i between each fish's velocity vector and that of the group, by taking the inverse cosine of the dot product:

$$\alpha_i = \cos^{-1}(\mathrm{V}_i \cdot \mathrm{U}) \tag{3}$$

The group's polarity ϕ is then the mean of these angle deviations:

$$\phi = \frac{1}{G}\sum_{i=1}^{G}\alpha_i \tag{4}$$

where G represents the group size. Note that as ϕ approaches 0°, fish headings approach parallel, whereas when polarity approaches 90°, fish headings approach perpendicular. Because this metric is counter-intuitive (high numbers represent a low amount of polarity), we used a non-dimensionalized form of polarity (ϕ^*) defined as:

$$\phi^* = \frac{(90° - \phi)}{90°} \tag{5}$$

The non-dimensionalized polarity ϕ^* thus took on values ranging from 0 (completely non-polarized) to 1 (perfectly aligned). Note that this approach computes the polarity for a single group of fish; this measure was reported either as the maximum observed for all groups within the population (see Fig. 2), or as the mean across all groups within the population (see Figs. 4, 6 & 7).

Group speed: Group speed v_t in a single time step was computed as the magnitude of the group centroid's velocity vector from time t to $t + 1$. The speed was calculated in units of cm frame^{-1} for real fish and BL time step^{-1} for simulated fish and converted to cm s^{-1} and BL s^{-1}, respectively. For ease of comparison between real and simulated data, we used a non-dimensionalized form of group speed (v^*) computed as:

$$v^* = \frac{v_t}{v_{max}} \quad (6)$$

where v_{max} represents the maximum speed achieved across all replicates. For real fish, v_{max} represented the maximum for an entire trial (5 min); for simulated fish, v_{max} represented the maximum for all runs for each set of simulation conditions. The non-dimensionalized group speed v^* therefore ranged from 0 (stationary) to 1 (moving at the maximum velocity observed for that set of experimental conditions). Note that this approach computes the speed for a single group of fish; this measure was reported either as the maximum observed for all groups within the population at each time step (see Fig. 3), or as the mean across all groups within the population (see Figs. 6 & 7).

Nearest-neighbor distance: The NND for any fish i (NND_i) was the minimum distance $d_{i,j}$ between fish i to all neighbors j in the population ρ (Krebs 1989):

$$NND_i = \min(d_{i,1}, d_{i,2}, ..., d_\rho) \quad (7)$$

We report time-averaged NND values for each simulation run (N = 15 for each population size and alignment force strength) and each real fish trial (N = 3 for each population size). For real fish, we used 1 BL = 5.3 cm to obtain NND in units of BL. Note that computing NND in this fashion means that, in some cases, the same distance will be counted twice when there is a reflexive pair (e.g. A is the closest neighbor to B, and vice versa).

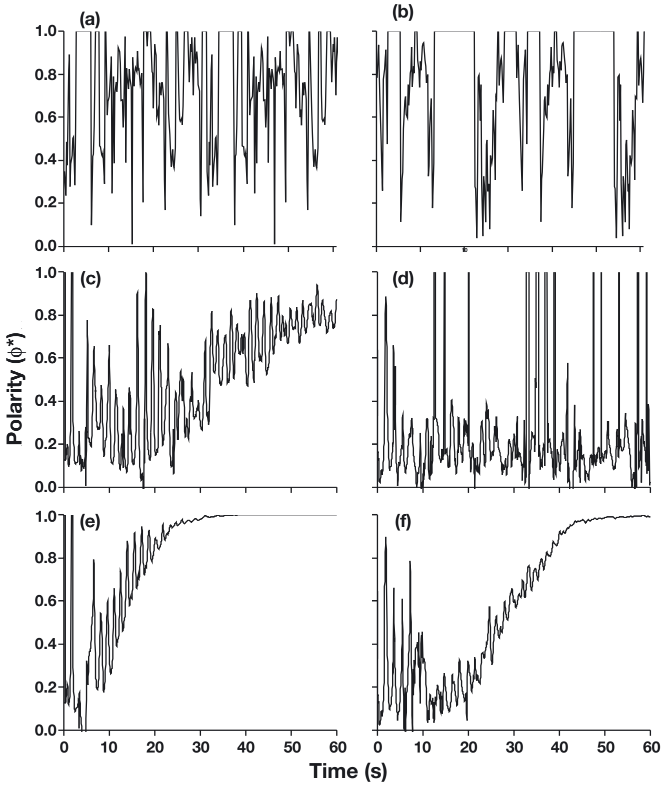

Fig. 2. Maximum observed polarity (ϕ*) across fish schools within a single trial over time for populations of (a) 4 real fish, (b) 8 real fish, (c) 4 simulated fish with an alignment force of 1% of F_{max}, (d) 8 simulated fish with an alignment force of 1% of F_{max}, (e) 4 simulated fish with an alignment force of 10% of F_{max}, and (f) 8 simulated fish with an alignment force of 10% of F_{max}

RESULTS

In our observations, the maximum observed polarity (ϕ*) of all giant danio schools within the population varied over the full possible range from 0 (non-polarized) to 1 (perfectly aligned) throughout each trial for both 4- and 8-fish populations (Fig. 2a,b). Fish schools in populations of 4 individuals had a mean polarity across all trials (N = 3) of 0.57 (±0.08 SD), whereas schools within 8-fish populations (N = 3) had a mean polarity of 0.41 (±0.11 SD). Group speeds (v_t) for schools within 4- and 8-fish populations were dynamic, ranging from 0 (stasis) to 11.6 cm s^{-1} (maximum) within 60 s (Fig. 3a, b). Mean speed was 7.35 cm s^{-1} (±1.79 S.D.) and 5.17 cm s^{-1} (±2.39 SD) for 4- and 8-fish populations, respectively. However, average relative (non-dimensionalized) speed was very similar for both 4 fish (v^* = 0.64 ± 0.15 SD) and 8 fish (v^* = 0.56 ± 0.26 SD) groups. NND was not affected by population size (2-sample t-test, t_s = 0.715, p > 0.25). Mean NND was 12.3 cm (±6.6 SD) (i.e. 2.3 ± 1.2 BL) for 4 fish and 16.8 cm (±19.6 SD) (i.e. 3.1 ± 1.8 BL) for 8 fish.

By comparison, ranges of polarity in simulated fish schools depended strongly on both the population size and the amount of alignment force (Fig. 2c–f). Even very small amounts of alignment force (e.g. 1% of F_{max}) caused schools within populations of 4 model fish to trend towards perfect alignment (Fig. 2c). Increasing population size, even to just 8 model fish, destroyed this alignment (Fig. 2d). For the stronger alignment forces used (e.g. 10% of F_{max}, Fig. 2e, f), schools always tended to near-perfect alignment, regardless of population size.

We quantified the relative effects of population size and alignment force strength on ϕ* using a 2-way ANOVA across all simulation runs. The 1-way comparisons were highly significant (df = 1, F = 247.20, p < 0.001 for population size; df = 6, F = 328.24, p < 0.001 for alignment force), indicating that both population size and alignment force affect alignment. Furthermore, the 2-way population size × alignment force interaction was also highly significant (df = 6, F = 32.65, p < 0.001), indicating that the population size affects how sensitive polarity is to alignment force.

To estimate the relative amount of alignment force real fish might experience to produce these observed

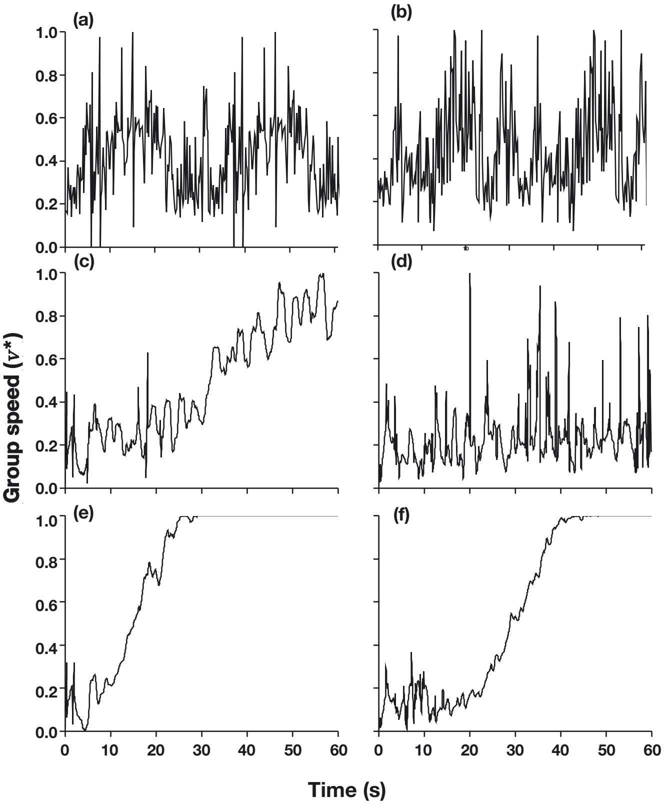

Fig. 3. Maximum observed group speed (v^*) across fish schools within a single trial over time for populations of (a) 4 real fish, (b) 8 real fish, (c) 4 simulated fish with an alignment force of 1% of F_{max}, (d) 8 simulated fish with an alignment force of 1% of F_{max}, (e) 4 simulated fish with an alignment force of 10% of F_{max}, and (f) 8 simulated fish with an alignment force of 10% of F_{max}

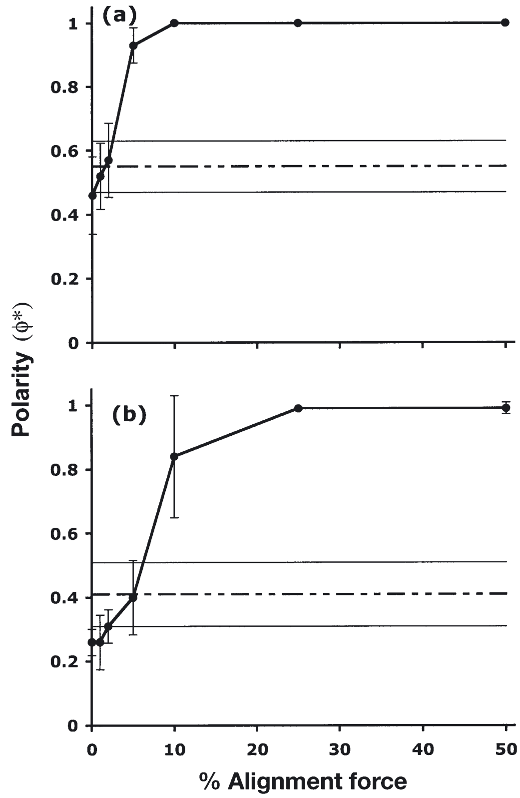

Fig. 4. Mean time-averaged polarity (ϕ^*) as a function of the alignment force strength, across all simulation experiments, for populations of (a) 4 and (b) 8 individuals. Alignment force strength is represented as a percentage of the maximum attraction/repulsion force F_{max}. For reference, the overall mean polarity for real fish is shown (dashed line) ± 1 SD (thin lines)

polarities, we plotted mean polarity for model fish across all replicates for each alignment force used, essentially creating a 'standard curve' (Fig. 4a). The mean polarity observed for schools in populations of 4 live fish was similar to simulations where the alignment force was 1 to 2% as strong as F_{max} (Fig. 4a), whereas the mean polarity observed for schools in populations of 8 live fish was most similar to simulations where the alignment force was just above 5% of F_{max} (Fig. 4b).

Schools in model populations of 4 fish quickly reached maximum speed (12 BL s^{-1}), with the time course of equilibrium exacerbated by increasing the alignment force strength (Fig. 3c,e). Increasing population size to 8 individuals damped this sensitivity, resulting in a relative group speed that was a fraction of the maximum observed ($v^* = 0.17 \pm 0.07$ SD at 1% alignment, Fig. 3d), a pattern visually similar to real fish (e.g. Fig. 3b). However, increasing the alignment force to 10% destroyed this similarity (Fig. 3f).

To quantify the relative effects of population size and alignment force strength on v^*, we performed a 2-way ANOVA across all simulation runs. As with polarity, 1-way comparisons were also highly significant (df = 1, $F = 193.34$, $p < 0.001$ for population size; df = 6, $F = 477.98$, $p < 0.001$ for alignment force), indicating that both population size and alignment force have strong effects on group speed. The 2-way population size × alignment force interaction for v^* was also highly significant (df = 6, $F = 40.66$, $p < 0.001$), indicating that population size affects how sensitive group velocity is to alignment force.

To deduce the relative amount of alignment force real fish might experience to produce observed NND values, we plotted mean NND for model fish across all replicates for each alignment force used, similar to the 'standard curve' created for polarity (Fig. 5). The mean NND observed in 4-fish populations, was similar to simulations where the alignment force was 1 to 2% as strong as F_{max} (Fig. 5a), whereas the mean NND observed in populations of 8 live fish was considerably higher in all cases than that observed in simulated schools (Fig. 5b). In general, however, the mean NND for simulated fish fell within ±1 SD of that observed for real fish, regardless of the alignment force used.

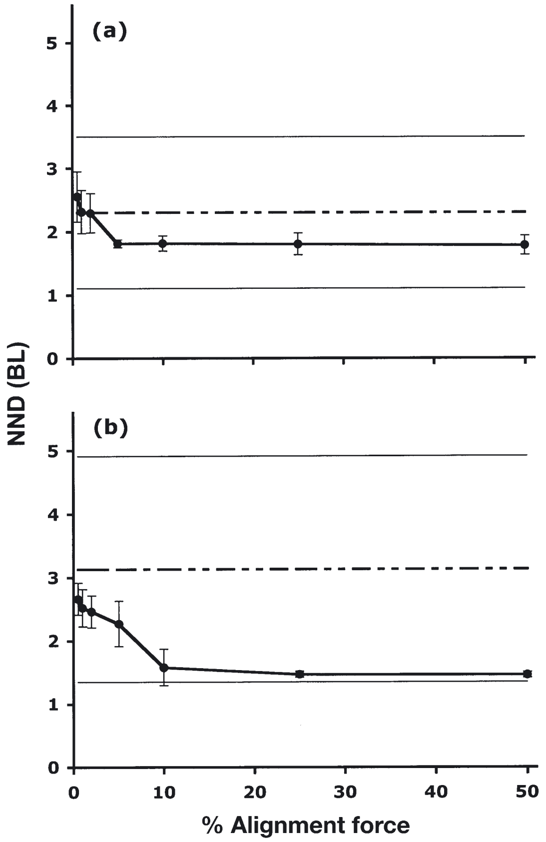

Fig. 5. Mean time-averaged nearest-neighbor distance (NND) as a function of the alignment force strength, across all simulation experiments, for populations of (a) 4 and (b) 8 individuals. Alignment force strength is represented as a percentage of the maximum attraction/repulsion force F_{max}. For reference, the overall mean NND for real fish is shown (dashed line) ±1 SD (thin lines)

To quantify the relative effects of population size and alignment force strength on NND, we performed a 2-way ANOVA across all simulation runs. As with the other metrics, the 2-way population size × alignment force interaction for NND was highly significant (df = 6, F = 13.42, $p < 0.001$), indicating that the value of each factor can change the NND that would otherwise be observed due to the other factor. However, when considering the 1-way effects, NND was significantly affected by alignment force alone (df = 6, F = 477.98, $p < 0.001$), but not by population size alone (df = 1, F = 0.0, $p > 0.95$). Thus, results with simulated fish reflected the results with real fish: population size, by itself, was not important in determining NND.

Correlation analysis showed a positive relationship between v^* and ϕ^*. For populations of 4 live fish, there was a moderate positive correlation between the 2 properties ($r^2 = 0.42$, $p < 0.01$, Fig. 6), while in populations of 8 live fish there was a stronger positive correlation ($r^2 = 0.67$, $p < 0.001$, Fig. 6). The relationship was even more dramatic ($r^2 = 0.98$ and 0.99, $p < 0.001$ in both cases) for simulated fish regardless of population size (Fig. 6). For real fish, the position of the time-averaged values along the v^*–ϕ^* axes depended partly on the individual fish in the school: each 8-fish trial had a 'characteristic' set of values (Fig. 6c), for example, suggesting that emergent properties depend very strongly on the quirks of the individual school members. For simulated fish (populations of which were always entirely identical), the position of the time-averaged values along the v^*–ϕ^* axes depended entirely upon the strength of the alignment force (Fig. 6b,d).

DISCUSSION

Our results quantify the relationship between the speed of motion and polarity of fish schools, and directly compare emergent properties displayed by real fish with those displayed in simulation. The similarity of simulated fish school behavior to that of real fish depended strongly on the alignment force strength of the former (Figs. 4 & 5).

Real fish schools showed a wide range of polarity values over time (Fig. 2), from completely non-polarized

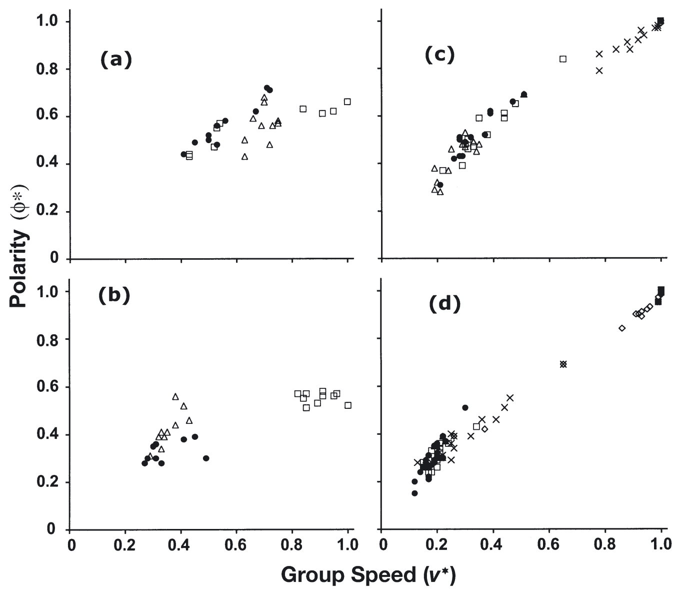

Fig. 6. Relationship between time-averaged group speed (v^*) and time-averaged polarity (ϕ^*) for simulation experiments with (a) 4 real fish, (b) 8 real fish, (c) 4 simulated fish, and (d) 8 simulated fish. Polarity ϕ^* is expressed as a function of group speed. For real fish (a,b), each point represents a 30 s time average, with triangles, squares, and circles representing the 3 different trials for that population size. For simulated fish (c,d), each point represents the 30 s time average for a single simulation run, with symbols representing percent of alignment force: 50% (■), 25% (▲), 10% (◇), 5% (×), 2% (●), 1% (□), and 0.5% (△)

(i.e. a 'swarm,' Shaw 1978) to perfectly aligned (i.e. a 'school,' Shaw 1978). Inspection of school polarity time series reveals that real fish schools were very strongly aligned most of the time, with irregular periods during which this orderly structure was destroyed and the school became a disorganized swarm (e.g. Fig. 2b). For real fish, therefore, an aligned school appears to be rather like a self-organized critical state, which is dynamically stable until something happens that destroys the self-organization (Bak et al. 1988, Wu & David 2002)—such as a single individual abruptly changing position, forcing other group members to re-shuffle. Schools within populations of 8 simulated fish with an alignment force of only 1% of F_{max} showed the opposite pattern, spending most of their time in a disorganized swarm, and then occasionally becoming a polarized school (e.g. Fig. 2d). However, if the alignment forced was substantially increased (to 10% or higher), continuous polarization resulted (Fig. 2f).

Theoretical studies have indicated that there may be a few dynamically stable group types, and that intermediate group types may be relatively unstable. For example, Couzin et al. (2002) found several dynamically stable collective behaviors—the swarm, the torus, and the parallel group—and predicted that animal groups should change rapidly between these 3 states, but spend little time in the intermediate states. Our findings agree with this prediction, for both real fish (where the stable state is a parallel group, Fig. 2a) and model fish (where the stable state is either a swarm or a school, Fig. 2e). In such dynamically stable configurations, transitions to another configuration are probably the result of changes in individual behavior (Couzin et al. 2002).

In model fish, polarity depended strongly on the population size as well as on the strength of the alignment force (Fig. 4). Even weak alignment strength (e.g. 1%) drove schools in 4-fish populations to perfect polarity, but it caused schools in 8-fish populations to enter a dynamically stable swarm configuration (Fig. 2). Couzin et al. (2002) showed convincingly that attraction and orientation zone widths are critical factors in determining group structure, and we hypothesize that the relative size of the zones we used played a key role in the differences observed between 4- and 8-fish populations. In a 4-fish population, all individuals could conceivably be in each other's alignment zone (Fig. 1), allowing rapid and unswerving alignment. In an 8-fish population, on the other hand, at least 1 neighbor will almost always lie outside each individual's alignment zone, leading to increasing disorganization as fish turn toward or away from those in the other zones. If our hypothesis is correct, then 4-fish model populations can reach a dynamically stable state, and 8-fish model populations can have their stable state changed from swarm to parallel school, by changing the size of 1 or more zones.

To date, most other zone-based models implicitly assume that the alignment force is equal in magnitude to the attraction/repulsion force (Aoki 1982, Huth & Wissel 1990, Hiramatsu et al. 2000, Inada & Kawachi 2002). As we have shown in this paper, alignment forces that are high relative to attraction/repulsion forces are likely to produce schools that have artificially high and invariable alignment (Figs. 2 & 4). Additionally, the little available experimental evidence indicates that such a high alignment force is unlikely in real fish. Using tank experiments to estimate the parameters of a zone-based model, Duostari & Sannomiya (1995) and Sannomiya & Duostari (1996) calculated the alignment force as being roughly $^1/_3$ to $^1/_2$ the strength of the attraction/repulsion force. Our own tank observations indicated that the time-averaged polarity of real fish schools is similar to that of simulated schools whose members experience an alignment force around 1 to 2% of the attraction/repulsion force's magnitude. However, with few exceptions (e.g. Hiramatsu et al. 2000) the polarity of real fish schools is rarely reported. Our results also indicate that time-averaged group statistics may be misleading, particularly when the group is rapidly transitioning between 2 very different states (Fig. 2).

Interestingly, while both group-level metrics examined here (polarity and group speed) varied depending on population size for simulated fish, the individual-level metric (NND) did not, either for real fish, or for simulated fish (Fig. 5). Indeed, simulated fish approached very nearly the preferred NND defined in the model, and they were increasingly good at maintaining that distance as alignment force increased. Simulated schools with higher alignment forces more perfectly approached the preferred NND because they were more perfectly polarized (Fig. 4), and members of polarized schools will be more likely to maintain a constant distance from one another. For real fish, NND may depend on fish body shape or sensory apparatus. For example, fish that have been blinded or had their lateral line damaged can still school, but their average NND is different from fish with all sensory systems intact (Pitcher et al. 1976).

For both real and simulated fish, group speed (v^*) and group polarity (ϕ^*) were positively correlated (Fig. 6). This implicitly makes sense: when the group is not aligned, individual members are facing in many different directions, and their velocity vectors will tend to cancel each other out, leading to little net movement for the group as a whole. It is also difficult, if not impossible, for non-aligned individuals to move very far without colliding with one another. On the other hand, when the group is highly aligned, individual members are facing in approximately the same direction, and this can lead to rapid group movement in that direction. To our knowledge, the relationship between group speed and velocity has not been investigated in previous models, although the experimental results of Hiramatsu et al. (2000) suggest a relationship.

Our results suggest certain ranges of state space over which animal populations can sustain a regular architecture. We imagine a 3D state space where each emergent property statistic measured in this study (NND, group speed, and polarity) is represented along an axis, and within which different group types can be placed (Fig. 7). The simple behavioral rules we used in this study (zone-based attraction, repulsion, and alignment, with only other group-mates as stimuli) lead to a certain subset of possible architectures. The relationship between polarity, group speed, and NND was extremely strong in our simulations (2-way regression, $r^2 = 0.98$, $p < 0.001$), and followed the functional form:

$$\phi^* = 0.25v^* - 0.61(\mathrm{NND}) + 1.84 \quad (8)$$

(indicated by the meshed plane, Fig. 7). Thus, if group types were observed in a different region of the state space, we would imagine other behavioral 'forces' were at work. For instance, in the Gulf of California, immense herring schools (hundreds of thousands) tend to hover in space, with group speed effectively zero, but are aligned almost perfectly (Parrish 1992). The herring school in this case is subject to a major force (predation risk) not considered in our simple attraction/repulsion/alignment scheme, the defense against which is to remain in polarized schools to facilitate escape (Parrish 1992). We hope to improve the realism of our model in the future by including factors such as internal state and predation risk, so that a greater diversity of group architecture types can be exhibited using a single set of simple rules.

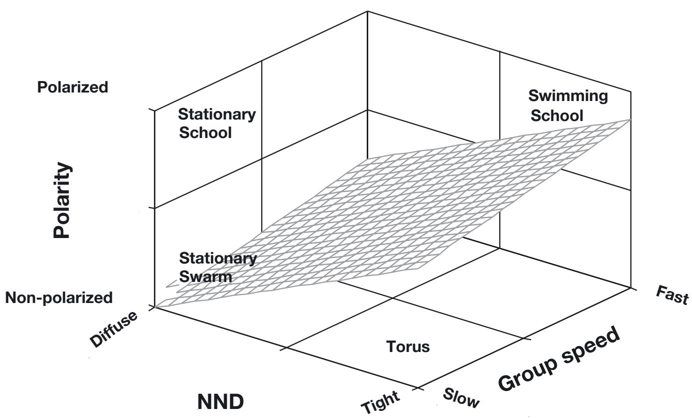

Fig. 7. Relationship between 3 different group properties: polarity, nearest-neighbor distance (NND), and group speed. The plane depicts a 2-way regression of polarity against NND and group speed for our model data shown in Eq. (8). Hypothetical positions within the 3D state space are shown for several common types of aggregations: stationary swarm (e.g. krill swarms, Ritz 1994), stationary school (e.g. polarized schools of 'hovering' herring, Parrish 1992), torus (e.g. Fig. 1 in Parrish et al. 2002, Couzin et al. 2002), fountain effect (e.g. Pitcher & Parrish 1993), and swimming school (e.g. swimming danio groups, Figs. 2 & 3)

The connection between different emergent properties such as group speed and polarity also suggests constraints on individual and group behavior: if the individual group members want the group to accelerate, for example, a viable strategy may be to increase their polarity or decrease their NND, such that the group moves to a different region of the 3D state space (Fig. 7). We also suspect that a few variable individuals can have a strong effect on group characteristics, and hence the position of the school in the 3D state space. For example, adding even a single individual whose movement rules differ from the other group members can change overall school structure and motion (Romey 1996). In the past, little attention has been given to how different emergent properties such as group speed and NND relate to one another. Instead, these properties are reported separately, and often only 1 or 2 properties are measured in a given study (reviewed in Parrish et al. 2002). Our research indicates that understanding the relationships between multiple emergent properties is an especially fruitful avenue for investigating group behavior. To further examine these questions, a more detailed version of the model is being implemented (Viscido et al. unpubl.). We are also conducting experiments with larger fish schools (16, 32), and in a larger experimental tank (4 m^3), as well as adding perturbations to the system (e.g. artificial predators) to make it less static.

The coupling of observational and modeling efforts can produce insights neither technique would provide by itself (Bumann et al. 1997). For example, our observations with real fish showed how polarity and group speed changed over time, providing a basis for comparison with the simulation results. That comparison indicated that a relatively simple simulation model, including only a large social force, a small alignment force, and a small random force, can produce results approaching those of real fish (Figs. 2 & 3). The model, in turn, suggested that the emergent properties observed in the live fish observations can only be achieved with a small alignment force. With too large an alignment force (above 5% of the total force), fish schools would be perfectly and invariably aligned, which they are not in real life (Fig. 2a,b), whereas with too small an alignment force, groups would be completely non-polarized (Fig. 4). Thus, our model indicates that, in the absence of other environmental factors (e.g. foraging behavior, predation avoidance), these schooling fish may primarily be concerned with maintaining the proper distance to their neighbors, and only secondarily concerned with alignment. How those other environmental factors would affect both model and real fish behavior is an important avenue of future investigation.

Acknowledgments. This paper benefited from the assistance of many helpful individuals. J. Weitzman, B. Cheney, T. Mongillo, and I. MacFarland assisted with observations, fish care, and motion analysis. S. Menden-Druer helped produce the Tracker3D algorithms. T. Daniel, M. Kot, C. Bergstrom, T. Reluga, and the rest of the University of Washington's Mathematical Biology group provided several useful discussions on the analysis of both modeling and observational results. We also thank the participants of the Conference on Swarming Behavior at UCLA for useful feedback. Two anonymous reviewers gave insightful criticism that greatly improved the paper. Funding was provided by NSF grant CCR-9980058 to J.K.P. and D.G.

LITERATURE CITED

Aoki I (1982) A simulation study on the schoolng mechanism in fish. Bull Jpn Soc Sci Fish 48:1081–1088

Aoki I (1984) Internal dynamics of fish schools in relation to inter-fish distance. Bull Jpn Soc Sci Fish 50:751–758

Bak P, Tang C, Wiesenfeld K (1988) Self-organized criticality. Physiol Rev A 38:364–374

Bumann D, Krause J, Rubenstein D (1997) Mortality risk of spatial positions in animal groups: the danger of being in the front. Behaviour 134:1063–1076

Burger J, Gochfeld M (1991) The common tern: its breeding biology and social behavior, 1st edn. Columbia University Press, New York

Clark M, Irwig K, Wobke W (1997) Emergent properties of teams of agents in the Tileworld. Lect Notes Art Int 1209: 164–176

Cody ML (1971) Finch flocks in the Mohave desert. Theor Popul Biol 2:142–158

Couzin ID, Krause J, James R, Ruxton GD, Franks NR (2002) Collective memory and spatial sorting in animal groups. J Theor Biol 218:1–11

Duostari MA, Sannomiya N (1995) A simulation study on schooling behaviour of fish in a water tank. Int J Syst Sci 26:2295–2306

Flierl G, Grunbaum D, Levin S, Olson D (1999) From individuals to aggregations: the interplay between behavior and physics. J Theor Biol 196:397–454

Hamilton WD (1971) Geometry for the selfish herd. J Theor Biol 31:295–311

Hiramatsu K, Shikasho S, Mori K (2000) Mathematical modeling of fish schooling of Japanese medaka using basic behavioral patterns. J Fac Agric Kyushu Univ 45:237–253

Huth A, Wissel C (1990) The movement of fish schools: a simulation model. In: Alt W, Hoffman G (eds) Biological motion. Springer-Verlag, Berlin, p 578–590

Huth A, Wissel C (1992) The simulation of the movement of fish schools. J Theor Biol 156:365–385

Inada Y, Kawachi K (2002) Order and flexibility in the motion of fish schools. J Theor Biol 214:371–387

Inagaki T, Sakamota W, Kuroki T (1976) Studies on the schooling behavior of fish. II. Mathematical modeling of schooling form depending on the intensity of mutual force between indivdiuals. Bull Jpn Soc Sci Fish 42:265–270

Krebs CJ (1989) Ecological methodology, 1st edn. Harper Collins, New York

Krebs JR, MacRoberts MH, Cullen JM (1972) Flocking and feeding in the great tit *Parus major*—and experimental study. Ibis 114:507–534

Lack D (1968) Ecological adaptations for breeding in birds, 1st edn. Chapman & Hall, London

Matuda K, Sannomiya N (1980) Computer simulation of fish behavior in relation to fishing gear. I. Mathematical model of fish behavior. Bull Jpn Soc Sci Fish 46:689–697

Niwa H (1994) Self-organizing dynamic model of fish schooling. J Theor Biol 171:123–136

Niwa H (1996) Newtonian dynamical approach to fish schooling. J Theor Biol 181:47–63

Okubo A (1986) Dynamical aspects of animal grouping: swarms, schools, flocks and herds. Adv Biophys 22:1–94

Parrish JK (1992) Levels of diurnal predation on a school of flat-iron herring, *Harengula thrissina*. Environ Biol Fishes 24:257–263

Parrish JK, Edelstein-Keshet L (1999) Complexity, pattern, and evolutionary trade-offs in animal aggregation. Science 284:99–101

Parrish JK, Turchin P (1997) Individual decisions, traffic rules, and emergent pattern in schooling fish. In: Parrish JK, Hamner WM (eds) Animal groups in three dimensions, 1st edn. Cambridge University Press, Cambridge, p126–141

Parrish JK, Viscido SV, Grunbaum D (2002) Self-organized fish schools: an examination of emergent properties. Biol Bull 202:296–305

Partridge BL, Pitcher TJ (1980) The sensory basis of fish schools: relative roles of lateral line and vision. J Comp Physiol 135A:315–325

Pitcher TJ, Parrish JK (1993) Functions of shoaling behaviour in teleosts. In: Pitcher TJ (ed) Behaviour of teleost fishes, 2nd edn. Chapman & Hall, New York, p 363–439

Pitcher TJ, Partridge BL, Wardle CS (1976) A blind fish can school. Science 194:963–965

Reuter H, Breckling B (1994) Self-organization of fish schools: an object-oriented model. Ecol Model 75:147–159

Ritz DA (1994) Social aggregation in pelagic invertebrates. Adv Mar Biol 30:156–216

Romey WL (1996) Individual diferences make a difference in the trajectories of simulated schools of fish. Ecol Model 92: 65–77

Sannomiya N, Duostari MA (1996) A simulation study on autonomous decentralized mechanism in fish behaviour model. Int J Syst Sci 27:1001–1007

Shaw E (1978) Schooling fishes. Am Sci 66:166–175

Stocker S (1999) Models for tuna school formation. Math Biosci 156:167–190

Vabo R, Nottestad L (1997) An individual-based model of fish school reactions: predicting antipredator behaviour as observed in nature. Fish Oceanogr 6:155–171

Vine I (1971) Risk of visual detection and pursuit by a predator and the selective advantage of flocking behavior. J Theor Biol 30:405–422

Viscido SV, Wethey DS (2002) Quantitative analysis of fiddler crab flock movement: evidence for 'selfish herd' behaviour. Anim Behav 63:735–741

Warburton K, Lazarus J (1991) Tendency-distance models of social cohesion in animal groups. J Theor Biol 150:473–488

Watt PJ, Nottingham SF, Young S (1997) Toad tadpole aggregation behaviour: evidence for a predator avoidance function. Anim Behav 54:865–872

Wilson EO (1975) Sociobiology: the new synthesis, 1st edn. Harvard University Press, Cambridge, MA

Wu J, David JL (2002) A spatially explicit hierarchical approach to modeling complex ecological systems: theory and applications. Ecol Model 153:7–26

Editorial responsibility: Andrea Belgrano, Santa Fe, New Mexico, USA

Submitted: April 16, 2003; Accepted: March 30, 2004
Proofs received from author(s): April 22, 2004

Vol. 273: 251–267, 2004 | MARINE ECOLOGY PROGRESS SERIES Mar Ecol Prog Ser | Published June 8

Strength, slope and variability of marine latitudinal gradients

Helmut Hillebrand[1,2,*]

[1]Institute for Marine Research, University of Kiel, Section for Marine Ecology, Düsternbrooker Weg 20, 24105 Kiel, Germany

[2]*Present address:* Institute for Botany, University of Cologne, Gyrhofstrasse 15, 50931 Cologne, Germany

ABSTRACT: Latitudinal declines of species richness from the tropics to the poles represent a general spatial pattern of diversity on land. For the marine realm, the generality of this pattern has frequently been questioned. Here, I use a database with nearly 600 published gradients (198 of which were marine) to assess whether there is a marine latitudinal diversity gradient of similar average strength and slope as that for terrestrial organisms. Using meta-analysis techniques, I also tested which characteristics of organisms or habitats affected gradient strength and slope. The overall strength and slope of the gradient for marine organisms was significantly negative and of similar magnitude compared to gradients for terrestrial organisms. Marine gradients were on average stronger as well as steeper than freshwater gradients. Latitudinal gradients were clearly a regional phenomenon, with stronger gradients and steeper slopes for diversity assessed on regional than on local scales. The gradient parameters differed also between oceans and between different habitats, with steeper gradients related to the pelagial rather than the benthos. There were on the other hand no significant differences between hemispheres and between different gradient ranges, although such differences have often been presumed. The most important organismal characteristic related to gradient structure was body mass, with significant gradients related to large organisms. A significant increase in gradient strength with increasing trophic level was observed. The meta-analysis also revealed strongest gradients for nekton and mobile epifauna, whereas the gradients were weak for sessile epifauna and for infauna. In conclusion, marine biota reveal a similar overall decline in diversity with latitude to that observed in terrestrial realms, but the strength and slope of the gradient are clearly subject to regional, habitat and organismal features.

KEY WORDS: Diversity · Latitude · Evolution · Dispersal · Meta-analyses · Macroecology · Habitat type

INTRODUCTION

The latitudinal decline of species richness is the most general and most robust spatial pattern of biological diversity. The increase in species richness towards the tropics was early recognised by naturalists (Humboldt 1828, Hawkins 2001) and has been described for a large number of organisms (Fischer 1960, Pianka 1966, Huston 1994, Hillebrand & Azovsky 2001). A few notable exceptions have been reported, such as aquatic macrophytes (Bolton 1994), ichneumonid insects (Owen & Owen 1974), sediment infauna (Thorson 1952) and unicellular eukaryotes (Hillebrand & Azovsky 2001). Despite the long and intensive research effort, there is still an astonishing lack of consensus about the mechanisms leading to this gradient (Pianka 1966, Rohde 1992).

Much of the discussion on latitudinal gradients is confined to terrestrial biota, whereas several of the exceptional taxa—showing no or reversed gradients—dwell in marine habitats. A decade ago, Clarke (1992) asked whether there is a general latitudinal decline of diversity in the sea. Although some groups showed strong longitudinal gradients, Clarke (1992) showed several examples where gradients were lacking. Discussing high polar diversity in the southern hemi-

*Email: helmut.hillebrand@uni-koeln.de

sphere (see also Brey et al. 1994) and several methodological issues, Clarke (1992) concluded that there was no convincing evidence for a general latitudinal diversity trend for marine biota. Moreover, he stated that there was no consensus on which scale the diversity gradient should be assessed. In the decade following that publication, a large number of marine organisms were investigated and significant latitudinal gradients were found (Rex et al. 1993, 2000, Roy et al. 1998, 2000b, Gray 2002 [for the northern hemisphere], Macpherson 2002) or not found (Wilson 1998, Barnes & Arnold 2001, Ellingsen & Gray 2002, Gray 2002 [for the southern hemisphere]). It is thus still open to question whether marine latitudinal gradients are as consistent as terrestrial ones and which factors would explain the differences between marine and terrestrial realms. In addition to comparing the average gradient strength and slope between marine and other realms, it is important to identify factors affecting gradient strength and slope in the marine realm. These factors may be regional differences in ecosystems (between oceans or hemispheres), differences between habitats (coastal vs deep-sea benthos) or between organisms (from large mobile consumers to small planktonic producers). The generality (average strength and slope) and the variation in latitudinal gradients are the 2 main subjects of this paper.

The lack of an overall picture on how important the latitudinal pattern is in the sea is connected to the fact that latitudinal gradients are often investigated for single groups of organisms and underlying causes are often corroborated by simple covariation between diversity, latitude and a 3rd variable proposed to explain the gradient (Currie et al. 1999). Meta-analysis can be used to analyse the latitudinal diversity gradient generally (Gurevitch & Hedges 1993, Rosenberg et al. 2000, Hillebrand & Azovsky 2001), and allows one to test how the latitudinal gradient differs for different subsets of the earth's biota and regions. In addition to testing average gradient strength and slope for different realms (marine vs terrestrial), the analysis allows identification of variables (organismal traits, habitat types, regions) that significantly affect gradient structure. As for any reviewing and summarising technique, the increase in generality is connected to a decrease in resolution. Without doubt, marine diversity patterns are more complex than simple trends with latitude: (1) regional hotspots and coldspots of diversity exist for different groups of marine organisms (Hughes et al. 2002, Price 2002, Worm et al. 2003); (2) there are strong regional aspects of diversity (Gray 2001a, Ellingsen & Gray 2002); (3) diversity does not necessarily peak at the equator (Rutherford et al. 1999); and (4) diversity is obviously not similar north and south of the equator (Gray 2001b, 2002). However, the overarching question remains: does the marine realm harbour more of such regional diversity patterns modifying the latitudinal gradient than the terrestrial realm?

For an overall assessment of the generality of the latitudinal gradient, I assembled data from nearly 600 gradients of diversity with latitude described in the literature. In a previous contribution (Hillebrand 2004) I analysed large-scale trends for all kinds of biota and habitats across marine, terrestrial and freshwater systems. Here, I focus on questions pertaining to the marine realm, which was represented by 198 gradients. I tested the following hypotheses on marine habitats and organisms: (1) there is a significant overall decline of marine diversity with latitude, i.e. average gradient strength and slope are significantly negative; (2) the average strength and slope of the marine gradients are of similar magnitude to those for terrestrial and freshwater organisms; (3) the gradient strength and slope differ between different marine regions, organisms and habitat types.

MATERIALS AND METHODS

Data. Information on latitudinal gradients was obtained from the literature; for a detailed account see Hillebrand (2004). I used 4 abstracting services and databases to assemble the information: Cambridge Biological Abstracts, ISI Web of Science, JSTOR, and the Aquatic Science and Fisheries Abstracts. Identical search strings ('latitudinal gradient', 'latitude AND diversity' or 'latitude AND species richness') were used in these databases. Additionally, recent reviews were searched (Rohde 1992, 1999, Huston 1994, Rosenzweig 1995, Currie et al. 1999) as well as the bibliography of the papers detected. From a total of more than 1000 studies checked, 232 studies conformed to the following selection criteria: (1) the number of observations had to be 3 or more; (2) the range of latitudes covered had to be at least 10 degrees; (3) if only 3 or less sites were investigated, they had to be placed in the same continent or ocean (thus avoiding comparisons between, for example, tropical diversity in Asia and temperate diversity in North America). The general approach was rather inclusive than exclusive, since arbitrary deletion of studies may strongly bias the outcome of the analysis (Englund et al. 1999). Therefore, the studies included here will obviously differ in quality and in resolution. A major advantage of meta-analysis is, however, that studies are weighted by a measure of uncertainty. For example, a study on 3 sites in the less well known Pacific has considerably less impact on the overall results than a study on 300 well investigated sites in the Atlantic.

Meta-analyses (and other reviewing techniques) can suffer from a publication bias, resulting in data material which mainly contains significant results (Gurevitch & Hedges 1999, Blenckner & Hillebrand 2002, Kotiaho & Tomkins 2002). Moreover, meta-analyses may be influenced by unrepresentative selection of organisms in the primary studies (Hillebrand & Blenckner 2002) and the use of arbitrary selection criteria in assembling the database (Englund et al. 1999). The latter was avoided by using very unrestrictive selection criteria (see above). To broaden the basis of this analysis and to avoid the impact of publication bias, I also included studies that were not originally designed to test for latitudinal gradients, but which reported diversity measures for local habitats or regions across different latitudes.

The 232 studies included in this analysis reported 581 gradients of diversity with latitude. Each of these gradients represents the assessment of diversity of a particular group of organisms, which were either taxonomically or functionally defined, at different latitudes. A complete electronic appendix containing all details on the gradients and studies is published together with a more general analysis of these data (Hillebrand 2004).

For each gradient, I obtained the correlation coefficient (r) between latitude and diversity, as well as the slope (b), its standard error (SE_b) and the intercept (a) of the linear regression of diversity on latitude. These values were used to calculate the strength and the slope of each gradient. The gradient strength was defined as Fisher's z-transform of r (r_Z), which was calculated as:

$$r_z = \frac{1}{2} \times \ln\left(\frac{1+r}{1-r}\right) \quad (1)$$

For each value of r_Z, sampling variance was calculated from the number of observations (N) included in the gradient as:

$$\mathrm{var}_{r_z} = \frac{1}{N-3} \quad (2)$$

The slope (b) was also used in a weighted meta-analysis with the square of the standard error as the variance estimate (Hillebrand et al. 2001). The slope and the correlation coefficients are not entirely independent parameters of a linear relationship, but separate analysis is warranted by the different aspects measured by the 2 effect sizes (Hillebrand 2004).

Classifications. The gradients were classified with respect to variables characterising the organismal group, the habitat type, the geography, the scale and analytical details of each study (see Hillebrand 2004 for additional details). These classifications were chosen to allow objective assignment of levels to the different studies. Therefore, bold categories were favoured over more detailed, but also more speculative, units. Organismal groups were characterised in a 'functional' and a taxonomic category. The 'functional' differentiation comprised microalgae, macrophytes, protozoa, crustacean zooplankton, other zooplankton, meiofauna, arthropod zoobenthos, colonial zoobenthos, molluscan zoobenthos, other zoobenthos, fish, other vertebrates, parasites. These functional groups are obviously not homogeneous, but describe organisms sharing some of their characteristics (body size, trophic role, habitat use). These groups are used to test for broad differences in the strength or slope of the gradients, but not to infer any common evolutionary history. The taxonomic differentiation was at phylum level (Bacillariophyta, Spermatophyta, Arthropoda, Chordata, Cnidaria, Porifera, Tentaculata, Mollusca, Nemathelminthes, Annelida, Echinodermata, Plathelminthes, Protozoa, Chaetognatha). For each type of organism, the mode of dispersal (flying, own mobility, pelagic larvae, pelagic adults, seeds/spores, and parasitic transfer) and the most prominent life form (nekton, mobile epifauna, sessile epifauna, infauna, plankton, flying, parasite) were noted. When organisms had different dispersal or life forms, the assignment of a level followed the majority of species. Moreover, the trophic position was characterised in broad categories (such as carnivores, herbivores, autotrophs or omnivores). All groups containing different trophic levels, such as annelids, were assigned omnivores, which therefore represents a very broad category. Mean organism body mass was noted (log g wet weight) from estimates published in the literature (Hillebrand 2004). Many estimates were available as ranges for a certain organismal group (Peters 1983). To acknowledge the higher number of smaller organisms in any size range, I used the mean of the log-transformed range.

Besides categorising the realm (marine, freshwater, terrestrial), the type of habitat was characterised in broad categories as either pelagic (subdivided into coastal or open ocean), benthic (subdivided into coastal or deep sea), estuaries or host biota (for parasites). The geographic position of the gradient was characterised by (1) hemisphere (either northern, southern or both, the latter for analyses not differentiating between northern or southern position) and (2) the longitude (Atlantic, Pacific, Indian Ocean, world-wide).

Spatially, I characterised the study as either regional or local due to its sampling grain: all studies reporting diversity for certain sites or sampling points were defined as local, which corresponds to the measurement of α-diversity within samples or habitats (Whittaker 1960); all studies using regional scales by using provinces or latitudinal grids were designated as regional (γ-diversity) (Hillebrand 2004). To analyse whether the inclusion of polar seas would affect the latitudinal gradients due to the proposed high polar diversity (Clarke 1992, Brey et al. 1994), I characterised the spatial extent of the gradient in 3 variables: minimum latitude, maximum latitude and latitude range (max-min). The minimum latitude is that nearest the equator in the original study, and the maximum is the most poleward.

Statistics. Weighted meta-analysis on r_Z and b was used to calculate average magnitudes for gradient strength or slope and to detect significant differences between data obtained from different studies (Gurevitch & Hedges 1993, 1999, Rosenberg et al. 2000, Hillebrand et al. 2001). Grand mean effect sizes (E^{++}) and their 95% confidence intervals (CI) were obtained using the bootstrapping procedure in MetaWin 2.0 (Rosenberg et al. 2000). Difference of the CI from zero indicated significant average gradient strengths and slopes.

For all classification variables, meta-analyses were used to calculate group-wise effect sizes (E^{+}) and their CIs. An analysis of heterogeneity divided the total heterogeneity in the effect sizes into heterogeneity explained by the categorical variables (Q_b) and residual heterogeneity (Q_w). A mixed effect model was used throughout (Gurevitch & Hedges 1993, 1999, Rosenberg et al. 2000, Hillebrand et al. 2001), which avoids the assumption that there is 1 true effect size for the entire data set or a category within a grouping variable. Significance levels for the analysis of heterogeneity were obtained from 25 000 randomisations. Significantly different variable categories were assigned from non-overlapping CIs. For the continuous variables, a weighted regression was used (Rosenberg et al. 2000), where slope and intercept were calculated and the significance was tested by the heterogeneity explained by the regression model.

Multiple use of data requires adjustment of significance levels, which was done using a Bonferroni adjustment of p (Sokal & Rohlf 1995), with $p_{adj} = p \times k$ and k = the number of variables used = 14. Bonferroni adjustments are known to be highly conservative; therefore, I not only discuss significant differences ($p_{adj} < 0.05$), but also trends with $p_{adj} < 0.15$ (corresponding to $p < 0.01$ prior to adjustment).

For r_Z, the actual measure of diversity did not significantly affect the effect size (meta-analysis, $p_{adj} = 0.269$). For b, however, the difference between the measures was significant ($p_{adj} = 0.001$), with species richness resulting in steeper slopes than any other measure. Therefore, I restricted all forthcoming analyses involving b to those employing species richness as the diversity measure.

RESULTS

The overall strength of marine latitudinal gradients

E^{++} for both response variables (r_Z, b) were negative and differed significantly from zero (Table 1). Over the wide range of organisms and habitats covered, marine organisms showed a significant latitudinal decline of diversity towards the poles. Moreover, marine gradients had average magnitudes of strength and slope similar to those of terrestrial ones, and both marine and terrestrial gradients were significantly stronger and steeper than freshwater gradients (Table 1). For gradient strength, the highest E^{++} was found in the marine realm, although the difference to the terrestrial realm was not significant (overlapping CI). The average decline of marine diversity with latitude was significant even though 66 of the 198 original reported gradients were not significant. Thus, there is a clear gradient generalised over all marine taxa, even when many non-significant data are included.

A clear separation between regional and local scales was found for both slopes and strengths (Fig. 1). Latitudinal gradients were on average both

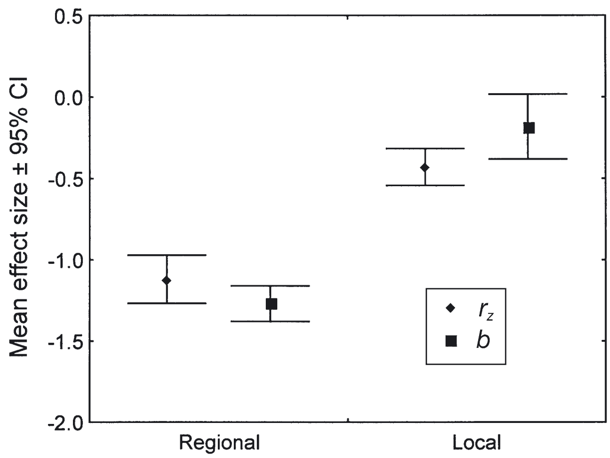

Fig. 1. Mean effect sizes (±95% confidence intervals, CI) for slope (b) and strength (r_Z) of the latitudinal gradient of diversity separated for local and regional data sets

Table 1. Grand mean effect sizes (E^{++}) and their 95% confidence intervals (CI) for gradient strength (r_Z) and slope (b) for marine, freshwater and terrestrial gradients of diversity with latitude (k = number of gradients)

Realm	k	r_Z		k	b	
		E^{++}	CI		E^{++}	CI
Marine	198	−0.82	−0.93 to −0.71	129	−1.10	−1.40 to −0.84
Freshwater	68	−0.26	−0.40 to −0.12	42	−0.21	−0.38 to −0.06
Terrestrial	286	−0.79	−0.87 to −0.71	199	−1.25	−1.49 to −1.04

stronger and steeper for regional data sets (γ-diversity) than for local ones (α-diversity). This difference was significant for both r_Z and b (Table 2). However, even the local effect size remained significantly different from zero. To avoid biasing results in the analyses, I separated all forthcoming analyses into regional and local data sets.

Table 2. Analysis of heterogeneity for gradient scale (regional or local) on gradient strength (r_Z) and slope (b) for marine latitudinal patterns. The table gives the response variable, the degrees of freedom (df) and the heterogeneity (Q) between (bet.) and within (with.) categories and the adjusted significance level (p_{adj})

Variable	$df_{bet.}$	$Q_{bet.}$	$df_{with.}$	$Q_{with.}$	p_{adj}
r_Z	1	62.32	188	243.56	<0.001
b	1	94.19	127	1448.32	<0.001

Geographical position of the study

Regional gradient strength was significantly different between oceans (Table 3); the difference pertained to significantly stronger gradients in the Atlantic than in any other ocean (Fig. 2a). Local gradient strength also differed significantly between oceans, but without such clear differences. A non-significant contrast was observed in regional slopes (Table 3), where steep but variable declines of diversity were observed in the Indian Ocean, whereas the Atlantic and Pacific Oceans had similar and flatter average slopes (Fig. 2d). On a regional scale, the average slope and strength was significantly negative for all oceans, except for the Pacific Ocean (Fig. 2a,d).

The strength and slope of the gradient did not differ between the northern and southern hemispheres (Table 3), and E^+ were almost identical for both parameters (Fig. 2b,e). Studies comprising data from both hemispheres showed slightly weaker gradients on regional scales (Fig. 2b) compared to those restricted to either northern or southern hemispheres. Again, all E^+ on regional scales were significantly negative (Fig. 2b,e).

The spatial extension of the gradient was analysed by 3 continuous variables: the minimum latitude, the maximum latitude and the range of latitudes observed. The minimum latitude did not affect slope or strength on any scale (Table 3). The maximum latitude affected only local slopes, where gradients

Table 3. Analysis of heterogeneity on gradient strength (r_Z) and slope (b) for regional and local marine latitudinal diversity patterns. The table gives the category and response variable, the degrees of freedom (df), the heterogeneity (Q) between (bet.) and within (with.) categories and the adjusted significance level (p_{adj})

Category	Variable	Regional					Local				
		$df_{bet.}$	$Q_{bet.}$	$df_{with.}$	$Q_{with.}$	p_{adj}	$df_{bet.}$	$Q_{bet.}$	$df_{with.}$	$Q_{with.}$	p_{adj}
Longitude	r_Z	3	73.21	104	116.91	<0.001	3	15.88	78	94.07	0.043
	b	3	25.33	93	1171.82	1	3	7.10	28	62.32	1
Hemisphere	r_Z	2	11.25	104	121.07	0.115	2	3.73	79	71.32	1
	b	2	15.50	93	1170.10	1	2	5.08	29	56.70	1
Range	r_Z	1	8.34	102	123.39	0.054	1	37.03	80	84.12	<0.001
	b	1	0.01	95	1205.09	1	1	19.29	30	67.29	<0.001
Minimum	r_Z	1	2.63	102	118.48	1	1	6.31	78	79.74	0.168
	b	1	0.41	95	1207.89	1	1	5.91	30	61.80	0.210
Maximum	r_Z	1	6.70	102	124.18	0.126	1	18.65	78	65.92	0.833
	b	1	0.15	95	1205.77	1	1	11.71	30	70.41	0.009
Habitats	r_Z	4	18.76	103	112.49	0.065	5	19.05	76	93.41	0.047
	b	4	86.90	92	1046.96	0.644	4	10.60	27	69.69	1
Body weight	r_Z	1	8.84	99	118.18	0.041	1	2.83	80	80.71	1
	b	1	55.46	95	1144.78	<0.001	1	0.51	30	63.85	1
Trophic position	r_Z	6	21.24	101	121.80	0.117	6	11.73	75	84.48	1
	b	6	106.43	90	1036.17	1	5	13.51	25	48.83	1
Life form	r_Z	6	41.19	100	111.94	0.002	5	19.78	66	85.76	0.061
	b	5	80.73	90	1090.61	1	4	14.83	21	47.85	1
Dispersal mode	r_Z	5	16.25	102	113.69	0.295	4	6.73	77	88.96	1
	b	5	69.30	91	1095.40	1	2	4.71	29	71.49	1
Organismal group	r_Z	11	94.91	94	94.91	<0.001	10	43.44	71	99.42	0.006
	b	9	102.69	85	1027.47	1	6	20.10	22	44.90	1
Phylum	r_Z	9	32.30	89	11.23	0.091	9	27.16	59	79.19	0.083
	b	5	46.82	80	1051.43	1	6	16.74	15	29.85	1

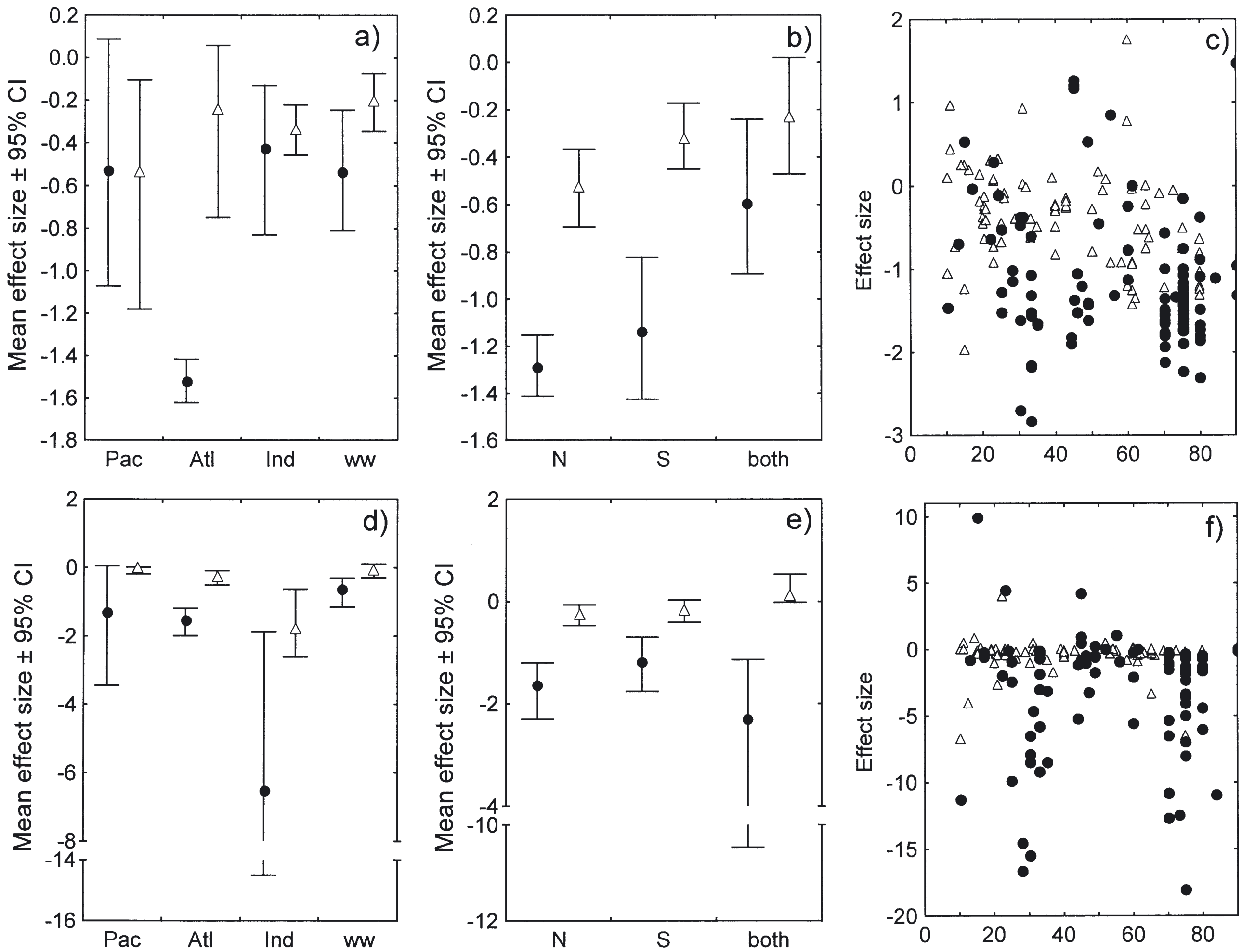

Fig. 2. Mean effect sizes (±95 % confidence intervals, CI) for (a–c) strength (r_Z) and (d–f) slope (b) of the latitudinal gradient of diversity separated for local (△) and regional (●) data sets. Effect sizes are given for (a,d) different oceans (Pac: Pacific; Atl: Atlantic; Ind: Indian; ww: worldwide studies), (b,e) different hemispheres (N = northern and S = southern hemisphere), and (c,f) different latitudinal ranges. For the latter, range is the difference between maximum and minimum latitude observed

advancing more towards the poles had steeper slopes. Since the high polar diversity of the southern hemisphere was explicitly proposed as changing the structure of latitudinal gradients in the marine realm, I redid the analysis for each hemisphere separately, but this did not change the outcome: the maximum latitude investigated affected only the slope of the gradient and only at local scales, and it did so similarly at northern and southern latitudes. In contrast to minimum and maximum latitudes, the latitudinal range affected the slope significantly at both local and regional scales, and tended to affect regional gradient strength as well (Table 3). In all 3 cases, the relationship was negative (Table 4), i.e. data covering a wider range of latitudes revealed stronger and steeper latitudinal gradients (Fig. 2c,f).

Habitats

Regional and local gradient strength differed significantly or nearly significantly with different habitat types (Table 3). Significantly stronger regional gradients were found for the open ocean pelagial than for the coastal benthos (Fig. 3a). Generally, pelagic gradients tended to be stronger than benthic gradients. Weakest gradients were found for local host-specific organisms, whereas this pattern was not found for the equivalent regional data. The habitat-wise local gradient strength differed significantly between coastal and deep-sea benthos, the latter revealing stronger gradients. Regarding slopes, no significant effect of habitat types was found (Table 3). However, an interesting contrast to the results on gradient strength was that

Table 4. Regression parameters for weighted meta-analysis with a continuous model. Independent variables were latitudinal range and body size, dependent variables were the weighted effect sizes strength (r_Z) and slope (b). The slope and intercept of the regression are given with standard errors for regional and local diversity estimates

Variable	Effect size	Scale	Slope	SE	Intercept	SE
Range	r_Z	Regional	−0.009	0.003	−0.584	0.207
		Local	−0.013	0.002	0.154	0.107
	b	Regional	0.0003	0.004	−1.434	0.240
		Local	−0.007	0.002	0.182	0.081
Body size	r_Z	Regional	−0.085	0.029	−1.199	0.071
		Local	−0.041	0.096	−0.561	0.096
	b	Regional	−0.211	0.028	−1.544	0.069
		Local	−0.018	0.025	−0.228	0.115

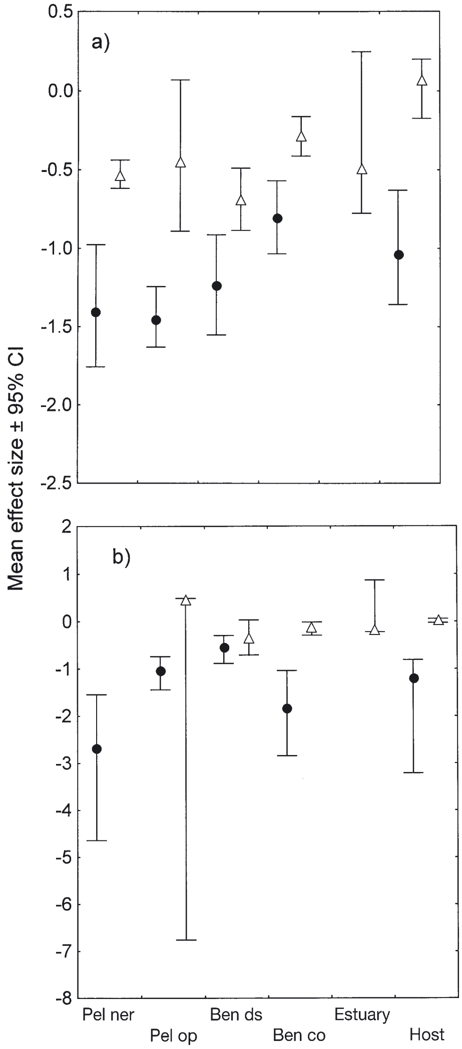

Fig. 3. Mean effect sizes (±95% confidence intervals, CI) for (a) strength (r_Z) and (b) slope (b) of the latitudinal gradient of diversity separated for local (△) and regional (●) data sets. Effect sizes are given for different habitats (Pel ner: pelagic neritic; Pel op: pelagic open ocean; Ben ds: benthic deep sea; Benthic co: benthic coastal; Estuary; and Host)

steepest gradients pertained to the neritic pelagial (compared to oceanic) and coastal benthos (compared to deep sea) (Fig. 3b). Slope and strength of the gradient were significantly negative in the regional data set irrespective of the habitat type (Fig. 3a,b).

Organisms

The organismal characteristic most strongly affecting gradient strength or slope was body mass (Table 3, Fig. 4). For regional scales, there was a consistent negative relationship between body mass and the effect size for both r_Z and b (Tables 3 & 4). Strongest and steepest gradients were confined to large organisms whereas small organisms showed weak and flat gradients (Fig. 4). The impact of body mass was significant for regional gradient strength and regional slope (Table 3). The slopes of the continuous meta-analysis model were consistently negative, even for the non-significant regression on local effect sizes (Table 4).

Only gradient strength significantly varied with other broad organismal traits. The trophic position affected regional gradient strength. Although the effect was marginally non-significant (Table 3), there was a conspicuous trend of increasing gradient strength with increasing trophic level: autotrophs showed weak gradients not significantly different from zero, whereas there was a tendency towards stronger gradients with increasing trophic position, and strongest gradients pertained to omnivores and carnivores (Fig. 5a). At the local scale, gradients were also weakest for autotrophs, and strongest for carnivores. Parasites had weak local gradients but strong regional gradients, which remained a consistent pattern for other organismal traits (Fig. 5b,c). The life form also affected gradient strength at both spatial scales (Table 3). Except for weak regional gradients in the few studies on pelagic seabirds (flying, Fig. 5b), the difference between life forms was mainly due to weak gradients in sessile organisms and infauna. These groups showed the weakest relationship to latitude at both spatial scales, whereas nekton, plankton and mobile epifauna showed steeper gradients (Fig. 5b).

Dispersal types did not affect gradient strength significantly (Table 3), but the group-wise average effects reflect some of the patterns seen before: weak gradients were related to flying organisms and to autotrophic organisms dispersing via seeds. For the other dispersal models (mobile adults, passively transported adults, pelagic larvae), the regional gradient strengths were very similar and always significantly

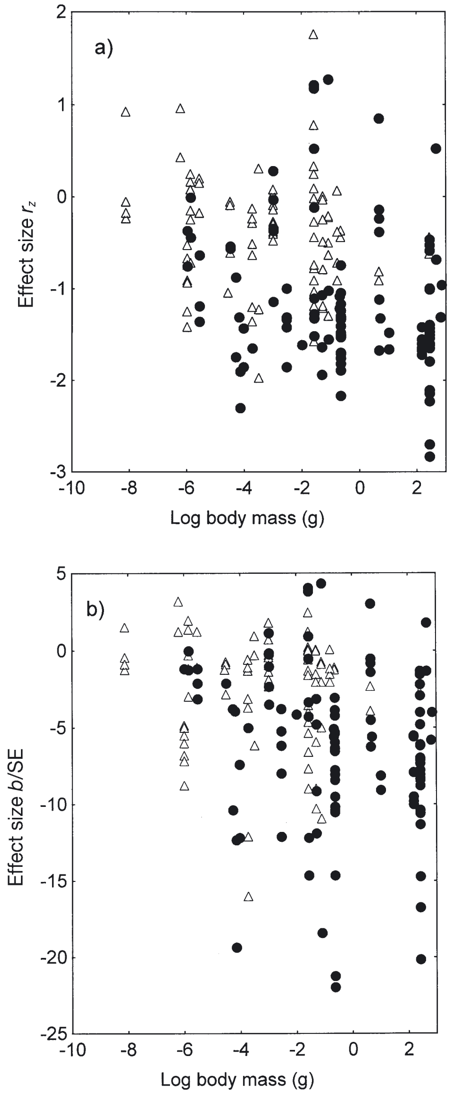

Fig. 4. Effect sizes for (a) strength (r_Z) and (b) slope (b) of the latitudinal gradient of diversity related to organismal body mass and separated for local (△) and regional (●) data sets

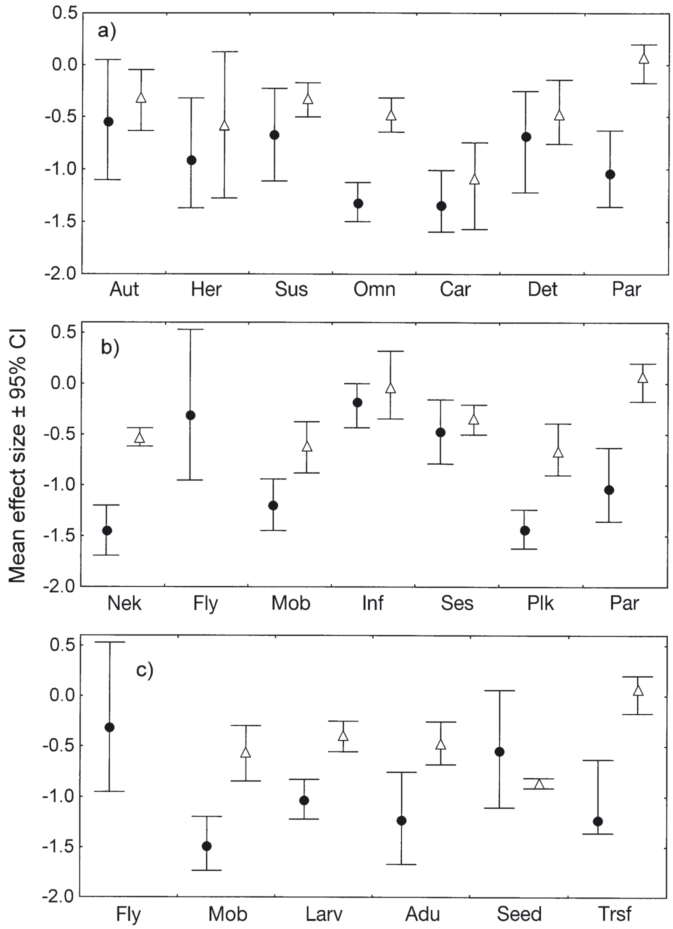

Fig. 5. Mean effect sizes (±95% confidence intervals, CI) for strength (r_Z) of the latitudinal gradient of diversity separated local (△) and regional (●) data sets. Effect sizes are given for (a) different trophic levels (Aut: autotrophic; Her: herbivores; Sus: suspension feeder; Omn: omnivores; Car: carnivores; Det: detritivores and microbivores; Par: parasites), (b) different living modes (Nek: nekton; Fly: flying seabirds; Mob: mobile epifauna; Inf: infauna; Ses: sessile epifauna; Plk: plankton; Par: parasites), and (c) different dispersal modes (Fly: flying; Mob: mobile adults; Larv: pelagic passive larvae; Adu: passively transported adults; Seed: seeds or spores; Trsf: transfer)

different from zero (Fig. 5c). None of the 3 classification variables (dispersal type, living mode and trophic position) had significant impacts on the slope of the gradient (Table 3).

The 'functional' group (organismal group) of organisms significantly affected regional and local gradient strength (Table 3). Putting the 'functional' types in size order from microalgae to fish (Fig. 6a) reveals that the increase in regional gradient strength with body mass is reflected by weak gradients for microalgae, protists, meiofauna and colonial zoobenthos (such as bryozoa) and strong gradients for arthropod and molluscan zoobenthos as well as fish. In between, there is a strong deviation from the body mass trends for marine macrophytes and zooplankton. The non-significance of marine macrophyte gradients reflects the data on trophic position (cf. autotrophs, Fig. 5a). Zooplankton exhibited very strong gradients, which may drive the pattern of strong pelagic gradients observed previously. Phlyogenetic differentiation is also represented by different gradient strengths (Table 3). Strongest gradients were revealed for Arthropoda and Chordata (which contain the largest individuals) and for predatory Chaetognatha. Weak regional gradients were observed for Nemathelminthes and Porifera. On a very coarse level, there was an increase in gradient strength with more recent phylogeny (Fig. 6b). Despite the significant variation in gradient strength with organismal group, it

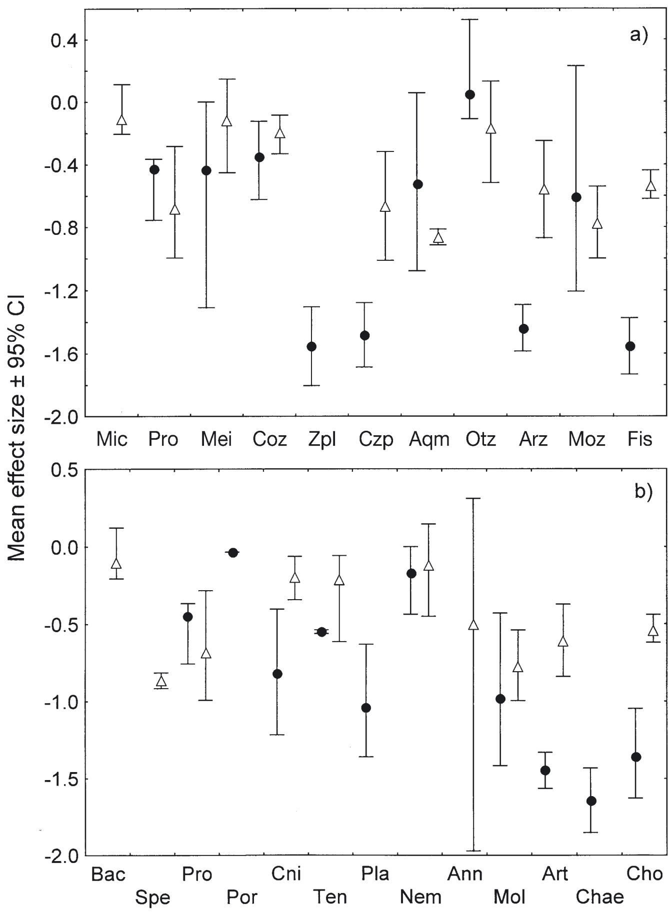

Fig. 6. Mean effect sizes (±95% confidence intervals, CI) for strength (r_Z) of the latitudinal gradient of diversity separated for local (△) and regional (●) data sets. Effect sizes are given for (a) different functional organismal types (Mic: microalgae; Pro: protists; Mei: meiofauna; Coz: colonial zoobenthos; Zpl: other zooplankton; Czp: crustacean zooplankton; Aqm: aquatic macrophytes; Otz: other zoobenthos; Arz: arthropod zoobenthos; Moz: molluscan zoobenthos; Fis: fish), and (b) different phyla (Bac: Bacillariophyta; Spe: Spermatophyta; Pro: Protozoa; Por: Porifera; Cni: Cnidaria; Ten: Tentatulata; Pla: Plathelminthes; Nem: Nemathelminthes; Ann: Annelida; Mol: Mollusca; Art: Arthropods; Chae: Chaetognatha; Cho: Chordata)

should be noted that almost all types of organisms revealed average latitudinal gradients which were significantly negative at the regional scale. The only consistent exceptions were aquatic macrophytes and the group of other zoobenthos. The slope of the gradient was not affected by either functional or phylogenetic classification of organisms.

DISCUSSION

Using meta-analysis to analyse the strength and slope of the latitudinal gradient in diversity revealed that marine biota on average show a significant latitudinal gradient (corroborating hypothesis 1). The strength and slope of the marine gradients were of similar magnitude to those of gradients for terrestrial biota (partly supporting hypothesis 2), and both these groups had stronger and steeper gradients than freshwater organisms (partly refuting hypothesis 2). Latitudinal gradients differed significantly in different marine regions, habitat types and for different organisms (supporting hypothesis 3). Here, I discuss these results by (1) addressing the generality of marine diversity gradients, (2) comparing the pattern found in the meta-analysis to previous single studies, and (3) outlining the consequences of these findings for different underlying causes of the latitudinal gradient.

The generality of marine latitudinal gradients

In contrast to freshwater, marine gradients were as strong as or even stronger than terrestrial gradients. Moreover, marine latitudinal diversity declines were significant at both regional (γ-diversity) and local scales (α-diversity). Only a decade ago, Clarke (1992) asked whether latitudinal gradients are less common in the sea than elsewhere. Several marine organisms are characterised by weak gradients due to low body mass (diatoms, protozoa), organism type (macrophytes) and life form (infauna). Despite the lack of significant gradients in these and other marine organisms and habitats, the first main conclusion from this analysis is that there is a significant average trend of decreasing marine diversity with increasing latitude. This conclusion is based on a large database, covering all world oceans, many kinds of habitats and organisms spanning almost 10 orders of magnitude in body mass. Although meta-analyses generally can be biased by selective publication of significant results (Blenckner & Hillebrand 2002, Kotiaho & Tomkins 2002), the present database contains more than one-third of nonsignificant gradients, which indicates that such bias has been avoided in this case. The original data (Hillebrand 2004) reflect strong differences in sampling effort, taxonomic resolution and definition of target organism groups. However, this does not affect the general conclusion of a significant average latitudinal decline in marine diversity. Meta-analysis techniques take sampling effort into account (see 'Materials and methods'). The gradient was moreover significantly negative for most pre-defined groups, at least for regional diversity (Figs. 2–6), which indicates that the gradient is not restricted to certain organismal groups, geographic regions or habitats.

The gradient of decreasing diversity with increasing latitude is thus without doubt one of the most general patterns of species distribution. It can be found for all kinds of organisms and habitats (Rohde 1978, 1992, this study), and even for other biological attributes such as human languages (Mace & Pagel 1995, Moore et al. 2002). Besides, it is also a very old spatial pattern and already present in fossil diversity varying with paleolatitude (Stehli et al. 1969, Raymond et al. 1989).

The overall significant trend does not mean that gradients are invariant. In contrast, the high proportion of non-significant gradients and the significant effect of several variables on the gradient parameter strength and slope showed that latitudinal gradients are variable across scales, habitats and organisms. Moreover, latitudinal gradients are crude abstractions in one dimension, since they do not reflect longitudinal or bathymetrical variation in diversity. The presence of strong latitudinal gradients in the marine realm does not preclude the existence of more complex patterns of diversity in 3D space (see 'Introduction'). Still, the decline of marine diversity with latitude is obviously a consistent aspect of marine diversity and requires investigation of (1) the factors influencing the shape of the gradient and (2) the primary causes of the gradient.

The shape of marine latitudinal gradients

The differences in gradient strength and slope between regional and local data sets were the most obvious patterns found for both slope and strength. Similar results were obtained in a general analysis of gradients in all realms (Hillebrand 2004), with stronger and steeper gradients found on regional scales. This difference between scales of diversity assessment was not due to systematic errors such as higher autocorrelation of diversity estimates on regional scales (Hillebrand 2004). Latitudinal gradients are thus clearly a regional phenomenon, although the gradients are still significant at local scales. The latitudinal gradients mainly reflect the fact that the maximum number of species (regional richness) declines with latitude, and to a lesser extent the number of locally coexisting species. This also indicates that species turnover (β-diversity) increases towards the tropics (Stevens & Willig 2002).

In addition to scale, body mass was a second important factor influencing the strength and slope of the latitudinal gradient. The importance of body mass had previously been shown with a much smaller database (Hillebrand & Azovsky 2001) and is also present over the entire data set (Hillebrand 2004). In addition to the direct impact of body mass on both slope and strength, differences found with other variables (organismal group, dispersal mode) were also partly related to body mass.

Despite the consistent impact of body mass, it is unlikely that body mass per se affects the latitudinal gradient. None of the proposed hypotheses for the latitudinal gradient (see below) predicts a consistently different relationship between the underlying factor and organismal groups of different mass. Before discussing the probable effect of body mass on gradient structure, 2 points have to be noted with respect to body mass. First, substantial variation is evident in the relationship between body mass and gradient strength and slope, respectively. Evidently, the body mass impact on the gradient is important only over a wide range of sizes. Some variation in the body mass gradient can be explained by the impact of organismal groups with extraordinarily weak (macrophytes) or strong gradients (Chaetognatha) (see below for more details). Second, the impact of body mass on the latitudinal gradient is not equivalent to studies relating latitude and body mass (Gillooly & Dodson 2000, Roy et al. 2000a). Whereas the latter studies investigated changes in body mass with latitude *within* a certain organismal group, the present analysis analysed the variation in the shape of the gradient *between* organismal groups of different size.

The effect of body mass may be related to dispersal chance, energetic constraints and/or population size (Hillebrand 2004). Dispersal chance depends on passive transport and active mobility. The chance of passive transport depends on large-scale currents and is proposed to increase with decreasing body mass due to high individual number (= high number of propagules), short generation times and high transportability (Fenchel 1993, Fenchel et al. 1997, Finlay et al. 1997). The notion of ubiquitous dispersal of eukaryotic microbes has been proposed by ecologists (Fenchel 1993, Finlay et al. 1996), but criticised by taxonomists (Mann & Droop 1996, Foissner 1999, Sabbe et al. 2001). Recent tests of the proposed ubiquity using the distribution of protists (Finlay et al. 2001, Hillebrand et al. 2001) revealed that microbial organisms are—if not ubiquitous—at least widely dispersed. For meiofauna, equivocal results on latitudinal gradients have been obtained (Boucher 1990, Lambshead et al. 2000, 2001, 2002, Mokievsky & Azovsky 2002), whereas the weakness of large-scale diversity patterns for smallest organisms has repeatedly been shown (Finlay et al. 1999, 2001, Hillebrand & Azovsky 2001). This weakness does not necessarily imply a complete lack of biogeography (Smith 1982, Dolan 2000, Wilkinson 2001), but it implies a less important role of restricted distribution for unicellular eukaryotes compared to larger organisms. The weak biogeography is also not simply due to biased taxonomic knowledge, since restricting data to a single taxonomic source still resulted in weak regional patterns of species distribution (Hillebrand et al. 2001). Some studies even suggested a boundary size delimiting ubiquitous and restricted distribution, either 2 mm (Finlay 2002) or 100 µm (Wilkinson 2001), but the results discussed above render it rather improbable that such a threshold size exists on a general level. Moreover, the overall dispersal chance may be related to body mass in a non-linear fashion. The passive component of dispersal is overall negatively correlated to body size (larger organisms with less dispersal chance), but large organisms may be more able to migrate actively.

The regional increase in gradient strength with trophic level corresponds well to the overall picture from marine, terrestrial and freshwater habitats (Hillebrand 2004). That marine data show the same overall trend is not due to a simple body mass effect, since autotrophs include microalgae as well as macroalgae and aquatic vascular plants, and carnivores include chaetognaths as well as many fish. Single studies on macrophytes found either no significant gradient at all (Bolton 1994), or significant gradients in the Atlantic, whereas macroalgal diversity in the Pacific did not decline (Gaines & Lubchenco 1981) and even increased (Santelices & Marquet 1998) towards the poles. A possible reason for rather low tropical macrophyte diversity might be the competition for space with corals (Bolton 1994).

Parasites exhibited weak local gradients, whereas regional parasitic gradients were strong (Fig. 5a) and comparable to their host organisms. The reason for the weak local gradients is not entirely clear, but local parasite surveys may have a high risk of undersampling rare species.

Among life forms, the strength of the gradient varied significantly in the meta-analysis, and except for parasites, weak local as well as regional gradients were confined to sessile epifaunal and infaunal organisms. The absence of a latitudinal gradient for endobenthic marine fauna was postulated quite early (Thorson 1952, 1957), and later named 'Thorson's rule'. Later studies found significant gradients also for sediment-dwelling macrozoobenthos (Roy et al. 2000b, Gray 2002 for the northern hemisphere), but my analysis shows that infaunal gradients tend to be generally weak. The possible reasons for the weakness of endobenthos and sessile epibenthos are not straightforward. Thorson's (1952, 1957) original argument was that infauna are protected from temporal environmental fluctuations and experience a spatially rather homogeneous habitat, but heterogeneity is no longer proposed as a major reason for gradients (Roy et al. 2000b, see also below).

Species richness varies not only across latitude but also across longitude. The pattern is less regular, but has been known for as long as the latitudinal gradient (Humboldt 1828). The implications of longitudinal differences became evident in the variation of gradient strength in different oceans found in the meta-analysis. The different geological background of different oceans (Poore & Wilson 1993) has been evoked to explain their different species richness. Although the Pacific Ocean is older than the Atlantic, the present analysis revealed weaker gradients for the Pacific at regional scales. The Indian Ocean was represented in the least studies and its latitudinal extent is smallest. An interesting pattern, however, emerged: the slope of the gradient was very steep in the Indian Ocean, whereas the strength was weak. This pattern corresponds to the notion that biodiversity hotspots dominate the spatial pattern of diversity in the Indian Ocean, from which diversity radially decreases (Hughes et al. 2002). High overall richness and radial rather than latitudinal gradients correspond well to the steep slope and the weak strength of the latitudinal gradient.

Several authors suggested that latitudinal patterns should be different between hemispheres, both for land-living organisms (Blackburn & Gaston 1996, Gaston & Williams 1996) and in the sea (Culver & Buzas 2000, Gray 2001a,b, 2002). Proposed reasons comprise different land-to-sea ratios in area between the hemispheres and the high marine diversity in the Antarctic compared to the Arctic (Brey et al. 1994, Gray 2001a). Although hemispheric differences in diversity patterns were described for some groups, this difference was clearly not general. Northern and southern hemispheres harbour latitudinal gradients of similar average strength and slope in the marine realm. To accommodate concerns on the poor quality of older polar diversity assessments in the literature, I re-analysed the difference between hemispheres with data published during the last decade (1993 to 2003). This restriction did not change the outcome: slope and strength of the gradient were not significantly different between northern and southern hemispheres. Moreover, the proposed high Antarctic diversity did not change the strength of the gradients in studies including polar seas: increasing maximum latitude included in the original study did not reduce gradient strength and slope as would be expected from high diversity near the Antarctic. Clearly, these results do not negate the existence of higher diversity of certain organismal groups at southern rather than northern polar latitudes, which has been documented widely (Brey et al. 1994, Gray 2001a,b, 2002). Even though these differences between the poles exist, they do not result in an overall changed structure of the latitudinal gradient across all groups. This pattern may change with more detailed knowledge on polar diversity. More data are necessary to address the questions for which groups polar diversity in the southern hemisphere is high and how this affects the global diversity trend.

In contrast to the maximum and minimum values of latitude, the latitudinal range over which diversity was assessed strongly affected the slope and also gradient strength. A more complete coverage of the latitudinal range obviously decreased slope and correlation coefficients, i.e. resulted in steeper and stronger gradients. Whereas this pattern was significant in the marine data set, it did not emerge in the general analysis including terrestrial and freshwater data (Hillebrand 2004). Thus, extending the analysis poleward or close to the equator is highly recommended for future assessments of latitudinal gradients.

Different large marine habitats differed rather weakly in their gradient strength and slope and, at a regional scale, all habitats revealed significant diversity clines with latitude. Again, the similarity of the gradient strength is more surprising than the significant differences. However, some distinctions in gradient strength were observed. In particular, the gradients in the pelagic environment were as strong as or even stronger than in benthic habitats, although large-scale currents are possibly able to blur biogeographic patterns in the pelagial. However, the openness may be less than expected, since large-scale current systems can confine marine fauna to certain regions (Williams et al. 2001, see also below). The importance of regional oceanography for the connection and separation of marine organisms is a highly underdeveloped area of research on marine biodiversity. The unexpectedly strong pelagic gradients may be based on the organismal subsets (weak macrophyte gradients always being benthic, strong fish gradients rather being pelagic).

Although the slope of the latitudinal diversity cline was less steep in deep seas compared to coastal benthos (cf. Fig. 3b), the gradient strength was stronger in the deep sea than in the coastal benthos. Bearing the speciality of the different habitats in mind, the similarity is more stunning than the difference. Much research has been devoted to exploring the diversity of the deep sea, which clearly is extraordinary in many aspects (Hessler & Sanders 1967, Sanders 1968, Haedrich 1985, Grassle & Maciolek 1992, Rex et al. 1993, Wilson 1998, Lambshead et al. 2000, Richer De Forges et al. 2000, Gray 2002). However, with respect to the latitudinal gradient structure, deep-sea benthos is not special compared to other marine habitats. Rex et al. (2000) also found strong similarity between deep-sea and shallow-water latitudinal gradients for gastropod species richness. This observation does not preclude the existence of trends in latitudinal gradients with bathymetry, which however could not be resolved in this analysis.

Underlying causes of the latitudinal gradient

The generality of any possible explanation for the latitudinal gradient has been a long-standing debate. The search for a primary cause of the latitudinal gradient has led to a rather unsubstantiated discussion on whether there is one central cause (Rohde 1992, Pianka 2000) or if many causes covary (Kaufman 1995, Gaston 2000, Macpherson 2002) to produce the pattern observed. In contrast to the discussion on the generality of the explanations for the gradient, it has been well accepted that the exceptional reversed gradients (such as macroalgae) are based on non-general local interactions or group characteristics (Clarke 1992, Bolton 1994). The generality of a meta-analysis can provide information on the suitability of different models often used to explain the latitudinal gradient.

Mid-domain models predict the highest species richness in the middle of a range defined by hard boundaries without involving ecological or evolutionary forces. Defining earth as a domain with the poles as hard boundaries, mid-domain models predict higher tropical diversity simply from a higher chance of species ranges overlapping in the centre of the domain (Colwell & Hurtt 1994). Subsequent evidence was found for global gradients (Colwell & Hurtt 1994, Lyons & Willig 1997, Willig & Lyons 1998, Jetz & Rahbek 2001, Koleff & Gaston 2001), regional gradients (Lees et al. 1999), and even altitudinal gradients (Rahbek 1997). The consistency of the latitudinal gradient across all habitats and biota actually sustained the impression of a general, non-biological trend. The mid-domain model is a null model, and ecological and evolutionary forces may result in deviations, which are reflected by the structure in the slopes and strengths of latitudinal gradients observed here. Random placement of geographic boundaries according to mid-domain models may set a general tendency towards higher tropical species richness, but the strength and slope of the gradient are affected by the type of organism, life form, trophic position, body weight, habitat type, and geographic position.

Gradients in energy (or a surrogate for energy) and area covary with latitude and have been proposed as ultimate causes of the latitudinal gradient. A long-standing debate has been fuelled about whether energy or area gradients are fundamental for the latitudinal diversity gradient. Following suggestions on the large area of the tropics (Terborgh 1973), the area hypothesis was mainly proposed by Rosenzweig (1992, 1995), and defended (Rosenzweig & Sandlin 1997) against notions that area per se cannot explain species richness patterns due to low species richness in large biomes such as some oceanic habitats (Rohde 1997, 1998). Some studies revealed positive correlations between regional area and species richness (Blackburn & Gaston 1997, Ruggiero 1999). However, other studies falsified this pattern, stating that neither were tropical biomes larger nor was richness related to area at biome scales (Hawkins & Porter 2001). A common notion in several contributions on the area hypothesis, however, is that productivity may influence the importance of area as a factor determining latitudinal gradients (Rohde 1997, 1998, Rosenzweig & Sandlin 1997, Chown & Gaston 2000). At the same time, favouring productivity (energy) as a primary cause, the impact of scale on the species-energy hypothesis is acknowledged (Currie 1991). The scale dependence of the energy hypothesis is also clearly related to the scale dependence of the productivity– diversity relationship (Waide et al. 1999, Mittelbach et al. 2001, Rajaniemi 2003), suggesting a rather unimodal response of diversity to productivity at local scales and linear at regional scales (Chase & Leibold 2002). Thus, area and energy may be interconnected variables with respect to diversity gradients (Gaston & Blackburn 2000).

The species energy hypothesis was proposed by Wright (1983) and has received much supporting evidence (Currie 1991, Fraser & Currie 1996), especially in marine environments (Roy et al. 1998, Rutherford et al. 1999). However, the high evidential support may also be based on the high number of surrogate parameters used for energy, which comprise air temperature, sea temperature (Rutherford et al. 1999, Roy et al. 2000b), irradiance (Roy et al. 1998), biomass (Fraser & Currie 1996), productivity (Woodd-Walker et al. 2002), actual evapotranspiration (Currie 1991) and potential evapotranspiration (Currie 1991). The major drawback of the energy hypothesis, however, is that it does not present the mechanistic link transferring higher energy into higher diversity (Huston 1999). Energy input may explain how much biomass can be built up, but not how this is distributed over several species (Gaston & Blackburn 2000, Hurlbert & Haskell 2003). A recent model based on the energy equivalence rule related temperature effects on biochemical kinetics to species richness (Allen et al. 2002). This proposal is still under discussion (Allen et al. 2003, Storch 2003), but points at a possible mechanism whereby increasing process rates with temperature result in increasing net diversification. Such a relationship between climate and speciation has long been postulated, stating that energy in general, and temperature in particular, have consistent consequences for generation times and mutation rates (Rensch 1954). The proposition has recently been tested, finding indeed increased diversification rates for butterflies and birds at low latitudes (Cardillo 1999).

The effective evolutionary time model invokes speciation as a major process regulating the latitudinal gradient of diversity (Rohde 1992, Stephens & Wiens 2003), but relates the higher speciation in the tropics to gradients similar to those used in the environmental gradient model (area, energy, variability). The differentiation between the 2 models (environmental gradient vs effective evolutionary time) is difficult due to the scarce information from fossil data. However, those studies allowing a comparison of fossil and recent diversity gradients indicate higher net diversification in the tropics than in temperate areas (Buzas et al. 2002). Moreover, there is increasing evidence that the tropics are major centres of evolutionary novelty (Crane & Lidgard 1989, Jablonski 1993). Also in marine habitats, faunas in the tropics evolved faster than in temperate areas (Stehli et al. 1969). In bivalves, the latitudinal gradients decrease with age of the clades, showing that species evolving in the tropics slowly radiate into neighbouring biomes (Crame 2000). Similarly, foraminiferan species richness in tropical waters was based on rare species without fossil records, i.e. species from recent diversification and with endemic distribution (Buzas & Culver 1999).

Higher speciation rates in the tropics can only be a cause of the marine latitudinal gradient if large-scale dispersal or migration does not lead to fast spreading of organisms across latitudes. The importance of dispersal limitation has been stressed in recent years in order to explain community assembly and species composition in terrestrial habitats (Zobel 1997, Hubbell et al. 1999, Zobel et al. 2000, Hubbell 2001). Marine systems have traditionally been viewed as rather open systems with high dispersal rates. Nonetheless, there is increasing evidence (at least in some marine systems) that large-scale dispersal is less common than previously hypothesised (Jones et al. 1999, Swearer et al. 1999, Cowen et al. 2000, Marsh et al. 2001). Cowen et al. (2000) found strong evidence for the prevalence of short distance dispersal in marine systems. Jones et al. (1999) showed high importance of self-recruitment in coral reef fish populations, although this may not be directly related to confinement or ranges: Victor & Wellington (2000) showed that pelagic larval duration was not consistently related to distribution range in reef fishes. However, the main hypothesis emerging from these studies is that a continuum from very open to almost enclosed marine locations can be found, determined by oceanographic factors, life history, and propagule features. Therefore, even on large evolutionary time scales, most organisms do not extend their distribution easily (Rohde 1998).

Least general of all explanatory models are those involving ecological interactions (Jeanne 1979). Ecological interactions are clearly able to structure local diversity, especially the interaction of consumption and resource competition (Huston 1979, Worm et al. 2002). However, in order to contribute to the latitudinal gradient, the interactions have to vary systematically with latitude. Such consistent change in ecological interactions with latitude has received some support (Möller 1998, Pennings et al. 2001). Also in marine habitats, evidence was found for latitudinal gradients in ecological interactions, but the changes in the sign of the ecological interactions were not consistent. Different harshness of conditions may shift interactions between macrophytes from being competitive in benign northern climates towards being mutualistic in harsh (heat-stressed, tropic) climates (Bertness & Ewanchuk 2002). Competitive interactions may increase at higher latitudes of the northeastern Pacific due to higher larval supply (Connolly & Roughgarden 1998). A latitudinal trend towards higher plant palatability was found for salt-marsh plants offered to herbivores (Pennings et al. 2001). Except for the inconsistencies of stronger or weaker interactions at higher latitudes, many studies falsified the proposition of interactions being more specific (Beaver 1979, Ollerton & Cranmer 2002), more intense (Hubbell 1980), or more density-dependent (Lambers et al. 2002) in the tropics. In my analysis, the model is additionally falsified by the higher generality of the gradient at regional scales. Thus, while latitudinal differences in ecological interactions exist, they are unlikely to be the ultimate cause of the gradient. However, the existing difference between regional and local gradients of diversity indicates the importance of ecological interactions in modifying the gradient at small scales.

Acknowledgements. I thank Andrea Belgrano for organising the stimulating session on 'Emergent properties' at the ASLO conference in Salt Lake City, Utah. The manuscript profited from comments by Stefanie Moorthi, Andrea Belgrano and 4 anonymous reviewers. Financial support was provided by the Swedish National Research Council (Vetenskapsrådet, 621-2002-215) and the Institute for Marine Research Kiel.

LITERATURE CITED

Allen AP, Brown JH, Gillooly JF (2002) Global biodiversity, biochemical kinetics, and the energy-equivalence rule. Science 297:1545–1548
Allen AP, Brown JH, Gillooly JF (2003) Reply to comment on 'Global biodiversity, biochemical kinetics, and the energy-equivalence rule'. Science 299:346
Barnes DKA, Arnold R (2001) A growth cline in encrusting benthos along a latitudinal gradient within Antarctic waters. Mar Ecol Prog Ser 210:85–91
Beaver RA (1979) Host specifity of temperate and tropical animals. Nature 281:139–141
Bertness MD, Ewanchuk PJ (2002) Latitudinal and climate-driven variation in the strength and nature of biological interactions in New England salt marshes. Oecologia 132: 392–401
Blackburn TM, Gaston KJ (1996) Spatial patterns in the species richness of birds in the New World. Ecography 19: 369–376
Blackburn TM, Gaston KJ (1997) The relationship between geographic area and the latitudinal gradient in species richness in New World birds. Evol Ecol 11:195–204
Blenckner T, Hillebrand H (2002) North Atlantic Oscillation signatures in aquatic and terrestrial ecosystems — a meta-analysis. Global Change Biol 8:203–212
Bolton JJ (1994) Global seaweed diversity: patterns and anomalies. Bot Mar 37:241–245
Boucher G (1990) Patterns of nematode species diversity in temperate and tropical subtidal sediments. PSZN I: Mar Ecol 11:133–146
Brey T, Klages M, Dahm C, Gorny M and 6 others (1994) Antarctic benthic diversity. Nature 368:297
Buzas MA, Culver SJ (1999) Understanding regional species diversity through the log series distribution of occurrences. Divers Distrib 8:187–195
Buzas MA, Collins LS, Culver SJ (2002) Latitudinal difference in biodiversity caused by higher tropical rate of increase. Proc Natl Acad Sci USA 99:7841–7843
Cardillo M (1999) Latitude and rates of diversification in birds and butterflies. Proc R Soc Lond B Biol Sci 266:1221–1225
Chase JM, Leibold MA (2002) Spatial scale dictates the productivity-biodiversity relationship. Nature 416:427–430
Chown SL, Gaston KJ (2000) Areas, cradles and museums: the latitudinal gradient in species richness. Trends Ecol Evol 15:311–315
Clarke A (1992) Is there a latitudinal diversity cline in the sea? Trends Ecol Evol 7:286–287
Colwell RK, Hurtt GC (1994) Nonbiological gradients in species richness and a spurious Rapoport effect. Am Nat 144: 570–595
Connolly SR, Roughgarden J (1998) A latitudinal gradient in northeast Pacific intertidal community structure: evidence for an oceanographically based synthesis of marine community theory. Am Nat 151:311–326
Cowen RK, Lwiza KMM, Sponaugle S, Paris CB, Olson DB (2000) Connectivity of marine populations: open or closed. Science 287:857–859
Crame JA (2000) Evolution of taxonomic diversity gradients in the marine realm: evidence from the composition of recent bivalve faunas. Paleobiology 26:188–214
Crane PR, Lidgard S (1989) Angiosperm diversification and paleolatitudinal gradients in cretaceous floristic diversity. Science 246:675–678
Culver SJ, Buzas MA (2000) Global latitudinal species diversity gradient in deep-sea benthic foraminifera. Deep-Sea Res I 47:259–275
Currie DJ (1991) Energy and large-scale patterns of animal- and plant-species richness. Am Nat 137:27–49
Currie DJ, Francis AP, Kerr JT (1999) Some general propositions about the study of spatial patterns of species richness. Ecoscience 6:392–399
Dolan JR (2000) Tintinnid ciliate diversity in the Mediterranean Sea: longitudinal patterns related to water column structure in late spring. Aquat Microb Ecol 22:69–78
Ellingsen KE, Gray JS (2002) Spatial patterns of benthic diversity: is there a latitudinal gradient along the Norwegian continental shelf? J Anim Ecol 71:373–389
Englund G, Sarnelle O, Cooper SD (1999) The importance of data-selection criteria: meta-analyses of stream predation experiments. Ecology 80:1132–1141
Fenchel T (1993) There are more small than large species? Oikos 68:375–378
Fenchel T, Esteban GF, Finlay BJ (1997) Local versus global diversity of microorganisms: cryptic diversity of ciliated

protozoa. Oikos 80:220–225
Finlay BJ (2002) Global dispersal of free-living microbial eukaryote species. Science 296:1061–1063
Finlay BJ, Esteban GF, Fenchel T (1996) Global diversity and body size. Nature 383:132–133
Finlay BJ, Maberly SC, Cooper JI (1997) Microbial diversity and ecosystem function. Oikos 80:209–213
Finlay BJ, Esteban GF, Olmo JL, Tyler PA (1999) Global distribution of free-living microbial species. Ecography 22: 138–144
Finlay BJ, Esteban GF, Clarke KJ, Olmo JL (2001) Biodiversity of terrestrial protozoa appears homogeneous across local and global spatial scales. Protist 152:355–366
Fischer AG (1960) Latitudinal variation in organic diversity. Evolution 14:64–81
Foissner W (1999) Protist diversity: estimates of the near-imponderable. Protist 150:363–368
Fraser RH, Currie DJ (1996) The species richness-energy hypothesis in a system where historical factors are thought to prevail: coral reefs. Am Nat 148:138–159
Gaines SD, Lubchenco J (1981) A unified approach to marine plant-herbivore interactions. II. Biogeography. Annu Rev Ecol Syst 13:111–138
Gaston KJ (2000) Global patterns in biodiversity. Nature 405: 220–227
Gaston KJ, Blackburn TM (2000) Pattern and process in macroecology. Blackwell Scientific Publications, Oxford
Gaston KJ, Williams PH (1996) Spatial patterns in taxonomic diversity. In: Gaston K (ed) Biodiversity. Blackwell Scientific Publications, Oxford, p 202–229
Gillooly JF, Dodson SI (2000) Latitudinal patterns in the size distribution and seasonal dynamics of new world, freshwater cladocerans. Limnol Oceanogr 45:22–30
Grassle JF, Maciolek NJ (1992) Deep-sea species richness: regional and local diversity estimates from quantitative bottom samples. Am Nat 139:313–341
Gray JS (2001a) Antarctic marine benthic biodiversity in a world-wide latitudinal context. Polar Biol 24:633–641
Gray JS (2001b) Marine diversity: the paradigms in patterns of species richness. Sci Mar 65:41–56
Gray JS (2002) Species richness of marine soft sediments. Mar Ecol Prog Ser 244:285–297
Gurevitch J, Hedges LV (1993) Meta-analysis: combining the results of independent experiments. In: Scheiner SM, Gurevitch J (eds) Design and analysis of ecological experiments. Chapman & Hall, New York, p 378–398
Gurevitch J, Hedges LV (1999) Statistical issues in ecological meta-analyses. Ecology 80:1142–1149
Haedrich RL (1985) Species number-area relationship in the deep sea. Mar Ecol Prog Ser 24:303–306
Hawkins BA (2001) Ecology's oldest pattern? Trends Ecol Evol 16:470
Hawkins BA, Porter EE (2001) Area and the latitudinal diversity gradient for terrestrial birds. Ecol Lett 4:595–601
Hessler RR, Sanders HL (1967) Faunal diversity in the deep-sea. Deep-Sea Res 14:65–78
Hillebrand H (2004) On the generality of the latitudinal gradient of diversity. Am Nat 163:192–211
Hillebrand H, Azovsky AI (2001) Body size determines the strength of the latitudinal diversity gradient. Ecography 24:251–256
Hillebrand H, Blenckner T (2002) Regional and local impact on species diversity—from pattern to processes. Oecologia 132:479–491
Hillebrand H, Watermann F, Karez R, Berninger UG (2001) Differences in species richness patterns between unicellular and multicellular organisms. Oecologia 126:114–124
Hubbell SP (1980) Seed predation and the coexistence of tree species in tropical forests. Oikos 35:214–229
Hubbell SP (2001) The unified neutral theory of biodiversity and biogeography. Princeton University Press, Princeton, NJ
Hubbell SP, Foster RB, O'Brien ST, Harms KE, Condit R, Wechsler B, Wright SJ, Loo de Lao S (1999) Light-gap disturbances, recruitment limitation, and tree diversity in a neotropical forest. Science 283:554–557
Hughes TP, Bellwood DR, Connolly SR (2002) Biodiversity hotspots, centres of endemicity, and the conservation of coral reefs. Ecol Lett 5:775–784
Humboldt Av (1828) Über das Universum—die Kosmosvorträge 1827/28 in der Berliner Singakademie. Edited from listener's notes, printed 1993 by Insel Verlag, Frankfurt
Hurlbert AH, Haskell JP (2003) The effect of energy and seasonality on Avian species richness. Am Nat 161:83–97
Huston M (1979) A general hypothesis of species diversity. Am Nat 113:81–101
Huston MA (1994) Biological diversity: the coexistence of species in changing landscapes. Cambridge University Press, Cambridge
Huston MA (1999) Local processes and regional patterns: appropriate scales for understanding variation in the diversity of plants and animals. Oikos 86:393–401
Jablonski D (1993) The tropics as a source of evolutionary novelty through geological time. Nature 364:142–144
Jeanne RL (1979) A latitudinal gradient in rates of ant predation. Ecology 60:1211–1224
Jetz W, Rahbek C (2001) Geometric constraints explain much of the species richness pattern in African birds. Proc Natl Acad Sci USA 98:5661–5666
Jones GP, Milicich MJ, Emslie MJ, Lunow C (1999) Self-recruitment in a coral reef fish population. Nature 402: 802–804
Kaufman DM (1995) Diversity of new world mammals: universality of the latitudinal gradients of species and bauplans. J Mammal 76:322–334
Koleff P, Gaston KJ (2001) Latitudinal gradients in diversity: real patterns and random models. Ecography 24:341–351
Kotiaho JS, Tomkins JL (2002) Meta-analysis, can it ever fail? Oikos 96:551–553
Lambers JHR, Clark JS, Beckage B (2002) Density-dependent mortality and the latitudinal gradient in species diversity. Nature 417:732–735
Lambshead PJD, Tietjen J, Ferrero T, Jensen P (2000) Latitudinal diversity gradients in the deep sea with special reference to North Atlantic nematodes. Mar Ecol Prog Ser 194:159–167
Lambshead PJD, Tietjen J, Moncrieff CB, Ferrero TJ (2001) North Atlantic latitudinal diversity patterns in deep-sea marine nematode data: a reply to Rex et al. Mar Ecol Prog Ser 210:299–301
Lambshead PJD, Brown CJ, Ferrero TJ, Mitchell NJ, Smith CR, Hawkins LE, Tietjen J (2002) Latitudinal diversity patterns of deep-sea marine nematodes and organic fluxes: a test from the central equatorial Pacific. Mar Ecol Prog Ser 236:129–135
Lees DC, Kremen C, Andriamampianina L (1999) A null model for species richness gradients: bounded range overlap of butterflies and other rainforest endemics in Madagascar. Biol J Linn Soc 67:529–584
Lyons SK, Willig MR (1997) Latitudinal patterns of range size: methodological concerns and empirical evaluations for New World bats and marsupials. Oikos 79:568–580
Mace R, Pagel M (1995) A latitudinal gradient in the density

of human languages in North-America. Proc R Soc London B Biol Sci 261:117–121
Macpherson E (2002) Large-scale species-richness gradients in the Atlantic Ocean. Proc R Soc Lond B Biol Sci 269: 1715–1720
Mann DG, Droop SJM (1996) Biodiversity, biogeography and conservation of diatoms. Hydrobiologia 336:19–32
Marsh AG, Mullineaux LS, Young CM, Manahan DT (2001) Larval dispersal potential of the tubeworm *Riftia pachyptila* at deep-sea hydrothermal vents. Nature 411:77–80
Mittelbach GG, Steiner CF, Scheiner SM, Gross KL and 5 others (2001) What is the observed relationship between species richness and productivity? Ecology 82:2381–2396
Mokievsky V, Azovsky A (2002) Re-evaluation of species diversity patterns of free-living marine nematodes. Mar Ecol Prog Ser 238:101–108
Möller AP (1998) Evidence of larger impact of parasites on hosts in the tropics: investment in immune function within and outside the tropics. Oikos 82:265–270
Moore JL, Manne L, Brooks T, Burgess ND, Davies R, Rahbek C, Williams P, Balmford A (2002) The distribution of cultural and biological diversity in Africa. Proc R Soc Lond B Biol Sci 269:1645–1653
Ollerton J, Cranmer L (2002) Latitudinal trends in plant-pollinator interactions: are tropical plants more specialised? Oikos 98:340–350
Owen DF, Owen J (1974) Species diversity in temperate and tropical Ichneumonidae. Nature 249:583–584
Pennings SC, Siska EL, Bertness MD (2001) Latitudinal differences in plant palatability in Atlantic coast salt marshes. Ecology 82:1344–1359
Peters RH (1983) The ecological implications of body size. Cambridge University Press, Cambridge
Pianka ER (1966) Latitudinal gradients in species diversity: a review of concepts. Am Nat 100:33–46
Pianka ER (2000) Evolutionary ecology, 6th edn. Benjamin Cummings, San Francisco, CA
Poore GCB, Wilson GDF (1993) Marine species richness. Nature 361:597–598
Price ARG (2002) Simultaneous 'hotspots' and 'coldspots' of marine biodiversity and implications for global conservation. Mar Ecol Prog Ser 241:23–27
Rahbek C (1997) The relationship among area, elevation, and regional species richness in neotropical birds. Am Nat 149: 875–902
Rajaniemi TK (2003) Explaining productivity-diversity relationships in plants. Oikos 101:449–457
Raymond A, Kelley PH, Lutken CB (1989) Polar glaciers and life at the equator: the history of Dinantian and Namurian (Carboniferous) climate. Geology 17:408–411
Rensch B (1954) Neue Probleme der Abstammungslehre, 2nd edn. Ferdinand Enke Verlag, Stuttgart
Rex MA, Stuart CT, Hessler RR, Allen JA, Sanders HL, Wilson GDF (1993) Global-scale latitudinal patterns of species diversity in the deep-sea benthos. Nature 365:636–639
Rex MA, Stuart CT, Coyne G (2000) Latitudinal gradients of species richness in the deep-sea benthos of the North Atlantic. Proc Natl Acad Sci USA 97:4082–4085
Richer De Forges B, Koslow JA, Poore CGB (2000) Diversity and endemism of the benthic seamount fauna in the southwest Pacific. Nature 405:944–947
Rohde K (1978) Latitudinal gradients in species diversity and their causes. I. A review of the hypotheses explaining the gradients. Biol Zentrbl 97:393–403
Rohde K (1992) Latitudinal gradients in species diversity: the search for the primary cause. Oikos 65:514–527
Rohde K (1997) The larger area of the tropics does not explain latitudinal gradients in species diversity. Oikos 79: 169–172
Rohde K (1998) Latitudinal gradients in species diversity. Area matters, but how much? Oikos 82:184–190
Rohde K (1999) Latitudinal gradients in species diversity and Rapoport's rule revisited: a review of recent work and what can parasites teach us about the causes of the gradients? Ecography 22:593–613
Rosenberg MS, Adams DC, Gurevitch J (2000) MetaWin, Version 2.0. Statistical Software for Meta-Analysis. Sinauer Associates, Sunderland, MA
Rosenzweig ML (1992) Species diversity gradients: we know more and less than we thought. J Mammal 73:715–730
Rosenzweig ML (1995) Species diversity in space and time. Cambridge University Press, Cambridge
Rosenzweig ML, Sandlin EA (1997) Species diversity and latitudes: listening to area's signal. Oikos 80:172–176
Roy K, Jablonski D, Valentine JW, Rosenberg G (1998) Marine latitudinal diversity gradients: tests of causal hypotheses. Proc Natl Acad Sci USA 95:3699–3702
Roy K, Jablonski D, Martien KK (2000a) Invariant size-frequency distributions along a latitudinal gradient in marine bivalves. Proc Natl Acad Sci USA 97:13150–13155
Roy K, Jablonski D, Valentine JW (2000b) Dissecting latitudinal diversity gradients: functional groups and clades of marine bivalves. Proc R Soc Lond B Biol Sci 267:293–299
Ruggiero A (1999) Spatial patterns in the diversity of mammal species: a test of the geographic area hypothesis in South America. Ecoscience 6:338–354
Rutherford S, D'Hondt S, Prell S (1999) Environmental controls on the geographic distribution of zooplankton diversity. Nature 400:749–753
Sabbe K, Vanhoutte K, Lowe RL, Bergey EA, Biggs BJF, Francoeur S, Hodgson D, Vyverman W (2001) Six new *Actinella* (Bacillariophyta) species from Papua New Guinea, Australia and New Zealand: further evidence for widespread diatom endemism, in the Australasian region. Eur J Phycol 36:321–340
Sanders HL (1968) Marine benthic diversity: a comparative study. Am Nat 102:253–282
Santelices B, Marquet PA (1998) Seaweeds, latitudinal diversity patterns, and Rapoport's rule. Div Distr 4:71–75
Smith HG (1982) The terrestrial protozoan fauna of South Georgia. Polar Biol 1:173–179
Sokal RR, Rohlf FJ (1995) Biometry, 3rd edn. WH Freeman, New York
Stehli FG, Douglas RG, Newell ND (1969) Generation and maintenance of gradients in taxonomic diversity. Science 164:947–949
Stephens PR, Wiens JJ (2003) Explaining species richness from continents to communities: the time for speciation effect in emydid turtles. Am Nat 161:112–128
Stevens RD, Willig MR (2002) Geographical ecology at the community level: perspectives on the diversity of new world bats. Ecology 83:545–560
Storch D (2003) Comment on 'Global biodiversity, biochemical kinetics, and the energy-equivalence rule'. Science 299:346
Swearer SE, Caselle JE, Lea DW, Warner RR (1999) Larval retention and recruitment in an island population of a coral-reef fish. Nature 402:799–802
Terborgh J (1973) On the notion of favorableness in plant ecology. Am Nat 107:481–501
Thorson G (1952) Zur jetzigen Lage der marinen Bodentier-Ökologie. Zool Anz Suppl 16:276–327
Thorson G (1957) Bottom communities (sublittoral or shallow shelf). Geol Soc Am Mem 67:461–534

Victor BC, Wellington GM (2000) Endemism and the pelagic larval duration of reef fishes in the eastern Pacific Ocean. Mar Ecol Prog Ser 205:241–248

Waide RB, Willig MR, Steiner CF, Mittelbach G, Gough L, Dodson SI, Juday JP, Parmenter R (1999) The relationship between productivity and species richness. Annu Rev Ecol Syst 30:257–300

Whittaker RH (1960) Vegetation of the Siskiyou Mountains, Oregon and California. Ecol Monogr 30:279–338

Wilkinson DM (2001) What is the upper size limit for cosmopolitan disribution in free-living microorganisms? J Biogeogr 28:285–291

Williams A, Koslow JA, Last PR (2001) Diversity, density and community structure of the demersal fish fauna of the continental slope off western Australia (20 to 35° S). Mar Ecol Prog Ser 212:247–263

Willig MR, Lyons SK (1998) An analytical model of latitudinal gradients of species richness with an empirical test for marsupials and bats in the new world. Oikos 81:93–98

Wilson GDF (1998) Historical influences on deep-sea isopod diversity in the Atlantic Ocean. Deep-Sea Res II 45: 279–301

Woodd-Walker RS, Ward P, Clarke A (2002) Large-scale patterns in diversity and community structure of surface water copepods from the Atlantic Ocean. Mar Ecol Prog Ser 236:189–203

Worm B, Lotze HK, Hillebrand H, Sommer U (2002) Consumer versus resource control of species diversity and ecosystem functioning. Nature 417:848–851

Worm B, Lotze HK, Myers RA (2003) Predator diversity hotspots in the blue ocean. Proc Natl Acad Sci USA 100: 9884–9888

Wright DH (1983) Species-energy theory: an extension of species-area theory. Oikos 41:496–506

Zobel M (1997) The relative role of species pools in determining plant species richness: an alternative explanation of species coexistence? Trends Ecol Evol 12:266–269

Zobel M, Otsus M, Liira J, Moora M, Möls T (2000) Is small-scale species richness limited by seed availability or microsite availability? Ecology 81:3274–3282

Editorial responsibility: Andrea Belgrano, Santa Fe, New Mexico, USA

Submitted: April 16, 2003; Accepted: January 27, 2004
Proofs received from author(s): May 17, 2004

Vol. 273: 269–279, 2004 | MARINE ECOLOGY PROGRESS SERIES Mar Ecol Prog Ser | Published June 8

Resource limitation alters the ¾ size scaling of metabolic rates in phytoplankton

Zoe V. Finkel[1,*], Andrew J. Irwin[1,2], Oscar Schofield[1]

[1]Institute of Marine & Coastal Sciences, Coastal Ocean Observation Laboratory, Rutgers University, New Brunswick, New Jersey 08901, USA

[2]Biology Department, College of Staten Island, City University of New York, 2800 Victory Blvd, Staten Island, New York 10314, USA

ABSTRACT: Under optimal growth conditions, many metabolic rates scale to the ¾ power of mass. We show that resource limitation can alter this size scaling of metabolic rates if resource acquisition depends on organism size. A prime example of size-dependent resource acquisition is light harvesting by phytoplankton. The size-dependence of light acquisition causes a deviation in the ¾ size scaling of growth and photosynthetic rates under growth-limiting irradiance. The degree of deviation from the ¾ size-scaling exponent depends on the size-dependence of physiological acclimation in response to resource limitation. Phytoplankton acclimate to light limitation by changes in pigment concentration. We calculate the pigment concentration required to maximize photosynthetic rate, and predict that the light-limited photosynthetic rate must scale to the ⅔ power of cell volume. These theoretical results are consistent with the size scaling of pigment concentration and photosynthetic rate of phytoplankton cultures. Our results suggest that deviation from the ¾ size-scaling exponent for metabolic rate under resource-limiting conditions is the consequence of the size-dependence of both resource acquisition and physiological acclimation to resource availability.

KEY WORDS: ¾ rule · Allometry · Light absorption · Macroecology · Nutrient uptake · Phytoplankton · Resource limitation · Size scaling

INTRODUCTION

Macroecology is the study of the emergent statistical properties of complex ecological systems (Brown 1995). Many fundamental macroecological patterns, such as abundance and diversity, have been related to organism size (Gould 1966, Peters 1983, Bonner 1988, Brown 1995, Kerr & Dickie 2001, Trammer 2002). These patterns, in part, reflect the relationship between an organism's size and its metabolic rate (Peters 1983, Brown 1995). From bacteria to large mammals, body size (V) can be used to predict metabolic rate (M):

$$M = k\left(\frac{V}{V_0}\right)^b \quad (1)$$

where k is metabolic rate at reference size, and b is the size-scaling exponent of the power-law dependence of M on V/V_0. Metabolic rate most commonly refers to growth or respiratory rate but can include any anabolic or catabolic rate. Organism size can be quantified as total body mass, as estimated by total carbon or dry weight, or as cell volume for microbes (Montagnes et al. 1994). Regardless of the proxy used for body size, normalizing organism size to a reference size, V_0, is necessary to keep the dimensions consistent with metabolic rate as defined in Eq. (1). Related organisms often have similar values of k but it can be quite variable between taxonomically distinct groups (Chisholm 1992). In contrast, under optimal growth conditions, b for the organism's metabolic rate is so frequently ¾ that it is referred to as the ¾ rule (Kleiber 1947, Peters 1983, West et al. 1997).

Recent work suggests that this ¾ rule for metabolic rates is a consequence of the geometric scaling proper-

*Email: finkel@imcs.rutgers.edu

ties of transport networks (West et al. 1997, Banavar et al. 2002). West et al. (1997) argued that fractal transport networks regulate metabolic rates with a maximum possible size-scaling exponent of $\frac{3}{4}$. They observed that many biological surfaces are effectively fractal and thus have non-Euclidean scaling. They modify a surface-rule argument to obtain a scaling exponent of $\frac{3}{4}$ instead of $\frac{2}{3}$. Banavar et al. (2002) show that an efficient Euclidean resource delivery network which allows metabolic rate to be independent of organism size must itself scale as $V^{\frac{4}{3}}$. In many organisms, the transport network is an approximately constant proportion of body mass, and thus the metabolic rate scales to the $\frac{3}{4}$ power of body volume or mass (Banavar et al. 2002).

However, every rule has exceptions. Deviations in the size-scaling exponent have been associated with sub-optimal environmental conditions, such as extremes in temperature and irradiance (Schlesinger et al. 1981, Peters 1983, Sommer 1989, Finkel 2001, Gillooly et al. 2001). Theoretical models based on geometric scaling properties of transport networks suggest that imbalances in supply and demand could cause deviations from the $\frac{3}{4}$ rule (Banavar et al. 2002). Under resource limitation, the supply of energy and nutrients does not match the demands of growth rate. There is at present no theoretical description of how resource limitation will alter the size scaling of metabolic rates.

Under optimal environmental conditions, the energy required to acquire resources is at a minimum, and organisms can maximize the conversion of resources into growth and reproduction. Under these optimal growth conditions, the maximum intrinsic growth rate is obtained, and the $\frac{3}{4}$ size scaling of metabolism is often achieved (Kleiber 1961, Peters 1983). As the environmental conditions depart from optimal conditions, resources become more difficult to obtain, resulting in a decreased growth rate. In order to maximize the efficiency of resource acquisition in a variable environment, cellular physiology adjusts through a suite of acclimation processes (Morris & Glover 1974, Jones 1978, Berry & Bjorkman 1980, Falkowski & LaRoche 1991, Evans & Poorter 2001). The cost of acclimation combined with the degree to which resources are limiting is dependent on body size (Raven 1984, Agustí 1991, Hudson & Morel 1993). This, in turn, alters the size-scaling exponent associated with metabolic rate. A quantitative understanding of how resource limitation will alter the size scaling of metabolic rates increases the general applicability of the $\frac{3}{4}$ rule by reconciling some of the discrepancies between experimental and field data and theoretical models.

We use light-limited phytoplankton as a model system to assess resource driven deviations from the $\frac{3}{4}$ rule. Phytoplankton are ideal experimental organisms for allometric studies due to their extremely large size range: ~1 µm to several millimeters in diameter (Round et al. 1990, Raven & Kubler 2002). Phytoplankton metabolic rates are central to the global biogeochemical cycles of carbon, nitrogen, oxygen, silicon, phosphorus and iron, and account for 40% of global primary production (Falkowski 1994). We focus on light limitation as the limiting resource for 3 reasons: (1) there is a mature physical theory that describes light acquisition in cells (Kirk 1976, Morel & Bricaud 1981); (2) there are well-tested, mechanistic, quantitative models of light harvesting and growth as a function of irradiance; and (3) the growth rate of a majority of the phytoplankton cells in the oceans is limited by light (Cullen et al. 1982). Nutrients such as nitrate, phosphate and iron are also known to limit primary production in the ocean. We chose not to explicitly model the effect of nutrient limitation on the size scaling of metabolic rate because there is much less data on how the different nutrient uptake systems respond to changes in nutrient concentration and how this influences the size-dependence of nutrient uptake.

Here, we develop a physiologically based mechanistic model to explain how disequilibria between supply and demand for light can alter the $\frac{3}{4}$ size scaling of metabolic rates. Our objectives are to calculate how physiological acclimation to light limitation leads to altered cellular composition and the anomalous size scaling of photosynthesis in unicellular phytoplankton. We use a biophysical model of light absorption to determine the cellular chlorophyll concentration that maximizes photosynthesis for cells of different sizes. This permits us to calculate the size-dependence of photosynthesis as a function of irradiance. Model results are compared with experimental data, testing our hypothesis that resource limitation can alter the $\frac{3}{4}$ size scaling of metabolic rates.

METHODS

We assume that natural selection acts to maximize the cell division rate of the individual cell. Over large size-ranges and within taxonomically similar groups, under optimal experimental growth conditions, evidence suggests that growth rate is a function of the internal transport network and is described by the $\frac{3}{4}$ rule (Eq. 1; Hemmingsen 1960, Kleiber 1961, Peters 1983, West et al. 1997, Banavar et al. 2002). Under light limitation, growth rate is limited by the acquisition of photons. Below, we describe the photosynthetic response to varying irradiance as a function of cell size and show how an optimal light-harvesting strategy can be used to predict the change in size scaling of photosynthetic rate with resource supply.

Table 1. List of symbols

Symbol	Definition and examples	Input variables, and typical range of values	Units	Source
a	Cellular optical absorption cross-section	10^{-13} to 10^{-9}	m^2 cell^{-1}	Agustí (1991), Finkel (2001)
a^*	Chl *a* specific optical absorption cross-section	0.01 to 0.02	m^2 mg chl a^{-1}	Agustí (1991), Finkel (2001)
a^*_s	*In vitro* a^* (unpackaged)	0.02 to 0.04	m^2 mg chl a^{-1}	Morel & Bricaud (1981)
α	Photosynthetic efficiency		mg C cell^{-1} µE^{-1} m^2	
B	Benefit of the LHC		mg C cell^{-1} h^{-1}	
B_L	Benefit of the LHC under light limitation		mg C cell^{-1} h^{-1}	
b	Size-scaling exponent		Dimensionless	
C	Cost of the LHC		mg C cell^{-1} h^{-1}	
c_i	Intracellular chl *a* concentration	10^5 to 10^8	mg chl *a* m^{-3}	Agustí (1991)
d	Cell diameter	10^{-6} to 10^{-3}	m	
E	Growth irradiance	10^{-6} to 2×10^{-3}	mol photons m^{-2} s^{-1}	
E_k	P_{max}/α		µE m^{-1} s^{-1}	
k	Metabolic rate at reference size		h^{-1}	
$k_{P_{max}}$	Maximum photosynthetic rate per cell at reference size	$10^{-9.95}$	mg C cell^{-1} h^{-1}	Finkel (2001)
M	Metabolic rate; net photosynthetic rate, specific growth rate, etc.		h^{-1}	
N	Net benefit, net number of photons harvested resulting in carbon fixed		mg C cell^{-1} s^{-1}	
P	Photosynthetic rate per cell		mg C cell^{-1} h^{-1}	
P_{max}	Maximum photosynthetic rate per cell		mg C cell^{-1} h^{-1}	
τ	Average lifetime of the LHC over which the cost of the LHC is amortized	~24	h	Riper et al. (1979)
ϕ	Quantum yield of photosynthesis	0.1	mol C mol photons^{-1}	Kirk (1994)
V	Organism size. Can use estimates of cell volume or biomass		m^3	
ξ	Cost of the LHC (upper estimate for chl *a*)	7×10^{-4}	mol photons mg chl a^{-1}	Raven (1984)

Steady-state photosynthesis as a function of irradiance. The relationship between irradiance and photosynthetic rate (P) is commonly expressed as an exponential or hyperbolic tangent function of irradiance (E):

$$P(E) = P_{max} \times \tanh(a\,\phi\,E/P_{max}) \quad (2)$$

where a is the cellular absorption cross-section weighted to the spectral irradiance; ϕ, the quantum yield of photosynthesis, is a saturating function of the maximum quantum yield (ϕ_m) and irradiance (Welschmeyer & Lorenzen 1981); and P_{max} is the maximum photosynthetic rate (see Table 1 for a list of symbols, their units, and typical values). As E increases from zero, P increases approximately linearly with E. The slope of P versus E, as $E \to 0$, is referred to as α, or photosynthetic efficiency. When irradiances become saturating (at $E_k = P_{max}/\alpha$), photosynthesis is close to its maximum rate (P_{max}), and there is very little increase in photosynthetic rate with irradiance. Although size-dependence has been reported for P_{max} and α (Taguchi 1976, Finkel 2001), the size scaling of photosynthesis has generally not been explicitly considered in models of photosynthesis (Cullen et al. 1993).

Steady-state size scaling of photosynthesis under light-limiting conditions. Under light-limiting conditions photosynthetic rate is proportional to $\alpha\phi E$. For cells grown at irradiances below E_k, quantum yield is at its maximum, and here is assumed to be 0.1 mol C mol photons^{-1} (Kirk 1994). For simplicity, we assign ϕ a value of 0.1 mol C mol photons^{-1} for all E. Light absorption is much more variable. It is a function of pigment composition, pigment concentration and cell size. Following Morel & Bricaud (1981), light absorption for a spherical cell can be approximated as:

$$a = a^* c_i V \quad (3)$$

where c_i is the intracellular chl *a* concentration (mg chl *a* m^{-3}), and a^* is the chl *a* specific absorption cross-section (m^2 mg chl a^{-1}), which is equal to:

$$a^* = \frac{3}{2}\, a^*_s \frac{Q(\rho)}{\rho} \quad (4)$$

where a^*_s is the absorption coefficient of the cell's pigments in solution (m^2 mg chl a^{-1}) normalized to chl *a*, and:

$$Q(\rho) = 1 + 2e^{-\rho}/\rho + 2(e^{-\rho} - 1)/\rho^2 \quad (5)$$

where

$$\rho = a^*_s c_i\, d \quad (6)$$

and *d* is cell diameter. For modeling purposes we use an estimate of 0.04 m^2 mg chl a^{-1} for the spectrally averaged *in vitro* absorption coefficient of cellular pigment from Morel & Bricaud (1981).

The ratio a^*:a^*_s is known as the package effect because as the cell (or package) gets bigger, the specific optical absorption cross-section decreases. This has been established both theoretically and empirically. Internal geometry such as the packaging of pigments into chloroplasts (Berner et al. 1989) and the optical properties of vacuoles (Raven 1997) can also alter the light absorptive properties of photosynthetic cells, but for simplicity these details will not be included in this analysis.

Steady-state size scaling of photosynthesis under light-saturating conditions. We integrate allometry into our resource-based model by defining P_{max}, the maximum cellular metabolic rate by a function similar to *M* in Eq. (1), with a size-scaling exponent of ¾:

$$P_{max} = k_{P_{max}} \left(\frac{V}{V_0}\right)^{3/4} \quad (7)$$

The intercept, $k_{P_{max}}$, is specific to the taxonomic group and steady-state growth irradiance (Finkel 2001). Under light-saturating conditions, photosynthesis (*P*) will scale with cell volume with an exponent of ¾, while under light limitation the size-scaling exponent associated with photosynthesis is dictated by light absorption. This formulation is consistent with the 2 potential rate-limiting processes: (1) the metabolic rate based on the acquisition of resources under light-limiting conditions (M_R); and (2) the transport and metabolic consumption of those internal resources under light-saturating conditions (M_T) (Fig. 1).

Under steady-state conditions, the overall photosynthetic rate will be determined by the slower of these 2 processes: $M = \min(M_R, M_T)$ (Fig. 1). Resource acquisition depends on external resource supply (e.g. irradiance or nutrient flux), the fraction of internal resources allocated to the resource acquisition system (e.g. light harvesting complexes [LHCs], or enzymes and nutrient transporters), and the organism's size. In the case of light acquisition in unicellular phytoplankton, the rate of photon capture depends on total intracellular pigment concentration and cell size. The photons captured by photosynthetic pigments are used to generate reductant and, via an electrochemical H^+ gradient, ATP (Falkowski & Raven 1997). If the supply of photons is insufficient to sustain the maximum photosynthetic rate, then photosynthesis is proportional to the rate of light acquisition. If the ATP and reductant pools are large enough to sustain the maximum photosynthetic rate, then the transport network that distributes the internal resources will ultimately limit the photosynthetic rate. We determine the consequences of this scheme on the size scaling of photosynthesis under light-limiting versus light-saturating conditions, and compare our theoretical predictions with experimental data.

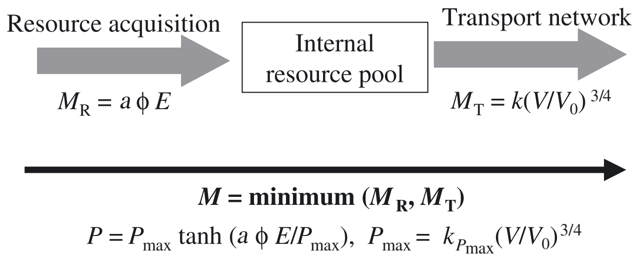

Fig. 1. Metabolic rate (*M*) is determined by the minimum of the rate of supply of resources (M_R) and the transport of the supply of resources (M_T) within the cell. When phytoplankton are limited by light, their photosynthetic rate is determined by light acquisition (M_R). Light absorption by unicellular organisms is size-dependent due to the package effect, which affects steady-state pigment concentrations and the effectiveness of the pigment at intercepting photons. When resources are not limiting and the internal resource pools are full, photosynthetic rate is determined by the transport of internal resources throughout the cell (M_T)

How much pigment is required to maximize photosynthetic rate? Phytoplankton cells regulate their pigment concentration in response to a change in incident irradiance (Richardson et al. 1983, Falkowski & LaRoche 1991, MacIntyre et al. 2002). To determine the size scaling of the resource driven photosynthetic rate, we need to know how photosynthetic rate and resource acquisition depend on cell size, and how the cell acclimates to the resource concentration in order to maximize its growth rate. It is therefore necessary to calculate the intracellular pigment concentration required to maximize photosynthesis for a given cell size at a given irradiance. This provides the basis for determining the size scaling of photosynthetic rates.

The intracellular pigment concentration required to maximize photosynthesis for a given cell size can be determined from a cost-benefit analysis of pigment. The benefit (*B*) of the pigment is the fixed carbon generated from the photons captured by the pigments that make up the LHC. For any single cell, Eqs. (2) to (6) describe the collection of metabolically useful energy by the LHCs. For simplicity, we are operationally assigning all pigment within the cell to the LHCs and assume that chl *a* is a dependable proxy for the total amount of pigment. This is a deliberately general description of the allocation of pigment; we are not distinguishing between changes in the ratio of Photosystem II to Photosystem I, the size or number of photosynthetic units, or the presence of non-photosynthetic pigments (Raven & Kubler 2002).

The cost (C) of the LHCs is the product of the quantum yield of photosynthesis (ϕ), the total pigment per cell ($c_i V$, mg chl *a* cell^{-1}), the inverse of the lifetime of the pigment within the cell (τ in hours) and its biosynthetic cost (ξ, mg carbon mg chl a^{-1}). This cost function represents the synthesis and maintenance costs of the LHC, and is intended to account for the energetic cost of light acquisition. The LHCs of phytoplankton are genetically and phenotypically variable. Changes in the composition of the LHC alter the biosynthetic cost and lifetime of the LHC. Using the data available (Riper et al. 1979, Raven 1984, Goericke & Welschmeyer 1992), we assume a constant τ of 1 d, and use an average biosynthetic cost for chl *a* as calculated by Raven (1984).

Steady-state size scaling of photosynthesis over a light gradient with explict photoacclimation. The optimal intracellular pigment concentrations were determined by maximizing the net benefit (N), which can be expressed as the difference between the carbon equivalents harvested (B) and the cost (C) of producing and maintaining the photosynthetic machinery necessary for harvesting light:

$$N = B - C = P(E) - \frac{c_i V \xi \phi}{\tau} \quad (8)$$

Numerical optimization and other computations were performed using the statistical package R (Ihaka & Gentleman 1996). We first computed optimal values of c_i as a function of d. These optimal intracellular pigment concentrations were then used to predict photosynthetic rates as a function of cell volume and irradiance.

Growth and photosynthetic rates are commonly reported after being normalized to carbon, chlorophyll content or cell number (P^C, P^* and P^{cell}, respectively). This has the potential to cause considerable confusion, especially when comparing different size-scaling exponents. Under ideal conditions, P^{cell} should have a size-scaling exponent of ¾, while P^C and P^* are normalized by a measure of cell size and thus will have smaller size-scaling exponents. We expect that this exponent will be 1 less than the exponent of P^{cell}, because C cell$^{-1} \propto V$ and $P^C \propto P^{cell} \times C$ cell^{-1}, but this is not always the case (Strathmann 1967, Montagnes et al. 1994, Montagnes & Franklin 2001). Cellular carbon content in phytoplankton is species-specific and varies with growth irradiance (Thompson et al. 1991). In the present study, we assume that carbon increases linearly with volume.

In accordance with previous experimental data (Agustí 1991, Finkel & Irwin 2000, Finkel 2001), we view c_i and P^{cell} as power-law functions of cell volume. The size-scaling exponents were estimated from linear regression. Over the size-ranges considered, model outputs are not always straight lines; thus, the range of cell volumes considered influences the estimate of the size-scaling exponent. We used the numerical model to produce data, which could have been obtained from experiments if our models had been perfectly correct, and then determine the size-scaling exponent from this simulated data in the same way we estimate exponents from laboratory data.

RESULTS

Steady-state size scaling of photosynthesis over a light gradient

The size dependence of the cellular photosynthetic rate depends on the steady-state irradiance and E_k (the irradiance where saturation occurs). At irradiances below E_k, the size-dependence of photosynthetic rate is dominated by the size-dependence of light absorp-

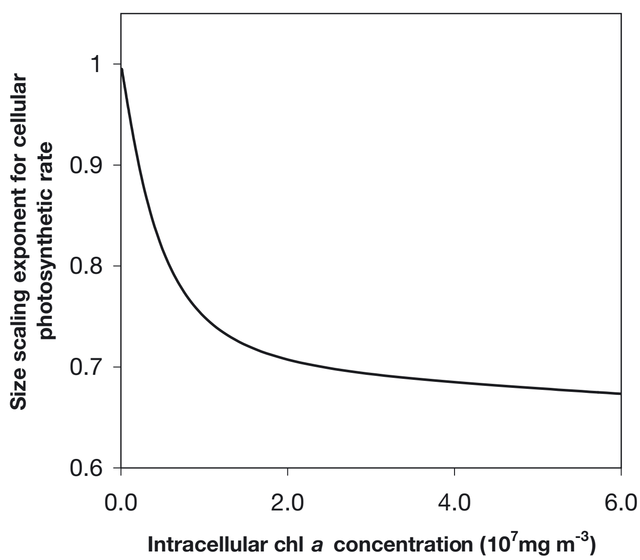

Fig. 2. Volume scaling exponent (b) associated with cellular photosynthetic rate (P, mg C cell^{-1} h^{-1}) under low irradiance as a function of intracellular chl *a* concentrations (c_i, mg chl *a* m^{-3}). Intracellular chl *a* concentrations are treated as independent of cell volume

tion and intracellular pigment concentration. At irradiances above E_k, the size-dependence of photosynthesis is dictated by the size-dependence of the maximum photosynthetic rate, and is proportional to $V^{3/4}$ (Eq. 7). When we assume that c_i does not change with cell size, the model predicts that cellular light-limited photosynthetic rates scales from $V^{2/3}$ to V^1 as a function of c_i (Fig. 2). Experimental evidence shows that c_i does change with cell size, suggesting that we must determine how c_i changes as function of cell size and irradiance to have a realistic prediction of the size scaling of light-limited photosynthetic rate.

How much pigment is needed to reap the largest photosynthetic rate?

Under sub-saturating irradiance, we can approximate the benefit of pigment as $B_L = a\phi E$. We then determine the intracellular pigment concentration required to optimize the net benefit ($N = B_L - C$) per cell by differentiating with respect to c_i and setting the derivative equal to 0:

$$\frac{dN}{dc_i} = \frac{\pi}{6} d^3 (a^* E - \xi/\tau) - \frac{\pi E a^*_s d^3}{4\rho^3} \times \left[2(3 + 3\rho + \rho^2)e^{-2} - 6 + \rho^2\right] = 0 \quad (9)$$

and after some straightforward algebra we obtain:

$$6 - 3\,(2 + 2\rho + \rho^2)e^{-\rho} - \frac{\xi}{a^*_s E\tau}\rho^3 = 0 \quad (10)$$

Solving for c_i we find:

$$c_i = \frac{f(z)}{a^*_s d} \propto \frac{1}{d} \quad (11)$$

where f is a proportionality factor evaluated numerically and depending only on z defined as:

$$z = \frac{a^*_s E\tau}{\xi} \quad (12)$$

The magnitude of c_i depends on z, but the size-scaling exponent is independent of z. Our result, $c_i \propto 1/d$ (Eqs. 11 & 12) is in excellent agreement with laboratory measurements of light-limited phytoplankton cultures (Fig. 3).

The size-dependence of the optimal intracellular chlorophyll concentrations at all irradiances can be determined using numerical optimizations to maximize photosynthetic rate based on Eqs. (2) to (8). As expected, under optimal intracellular chlorophyll concentrations, cellular photosynthetic rate, regardless of cell size, is a saturating function of irradiance. Our computations, in close agreement with measured data, show that intracellular pigment concentration increases with E under very low E, and above E_k decreases with E (Fig. 4). Different species have different intracellular pigment concentrations based on species- and class-specific differences in cell size,

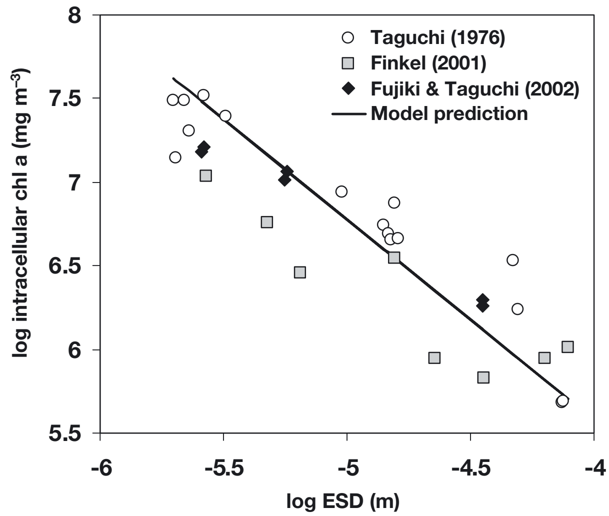

Fig. 3. Intracellular chl a concentration (c_i, mg chl a m^{-3}) as a function of equivalent spherical diameter (ESD, m) in 30 different species of light-limited, nutrient-saturated diatom cultures. Volume scaling exponent calculated from reduced major axis regression on the experimental data is -1.01 ± 0.15, in agreement with our theoretical prediction (-1)

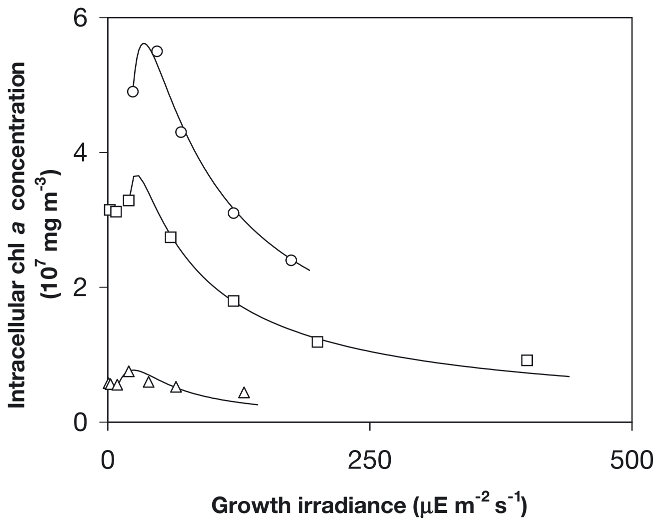

Fig. 4. Comparison of experimentally derived and modeled intracellular chl a concentration (c_i, mg chl a m^{-3}) as a function of growth irradiance (E, μE m^{-2} s^{-1}). The theoretical model (solid lines) is the optimal c_i for each species: *Skeletonema costatum* (△) and *Dunaliella tertiolecta* (□) from (Falkowski & Owens 1980), and *Emiliania huxleyi* (○) from (Muggli & Harrison 1996). The models for different species differ from one another only by having different values of a^*_s, $k_{P\max}$, τ and ξ (see Table 1 for definitions). Values of these constants were selected by minimizing the sum of squared deviations between the data points and the predictions of c_i at the corresponding irradiance

a^*_s, and the cost and turnover time of the different types of LHC. The increase in c_i with increasing irradiance at low E, despite corresponding increases in the package effect, is due to an increase in marginal benefit with irradiance. As irradiances become saturating, harvesting more photons provides no additional net benefit; therefore, intracellular pigment concentration decreases with irradiance and the package effect decreases. Given that the maximum cellular photosynthetic rate is proportional to $V^{3/4}$, our model predicts that the optimal c_i is proportional to $V^{-1/4}$ for $E \geq E_k$, and is proportional to $V^{-1/3}$ for $E < E_k$.

The theoretical predictions for the size scaling of intracellular pigment concentration compare well with Fujiti & Taguchi's (2002) experimental results on phytoplankton cultures. In this study, 6 different species, representing 3 different taxonomic groups, were grown over a range of irradiances. We calculated the size scaling of chl *a* content per cell, chl *a* cell^{-1} = K_{chl} V/V_0, for each irradiance by multiplying c_i by cell volume. The results show that under saturating irradiance, the size-scaling exponent of cellular chl *a* content with cell volume is $3/4$, in agreement with our theoretical prediction ($V^{-1/4} \times V = V^{3/4}$). As growth irradiance decreases, the size scaling of chlorophyll content decreases towards 0.71 ± 0.05 (95% confidence interval), in agreement with our theoretically predicted value under light limitation (Fig. 5).

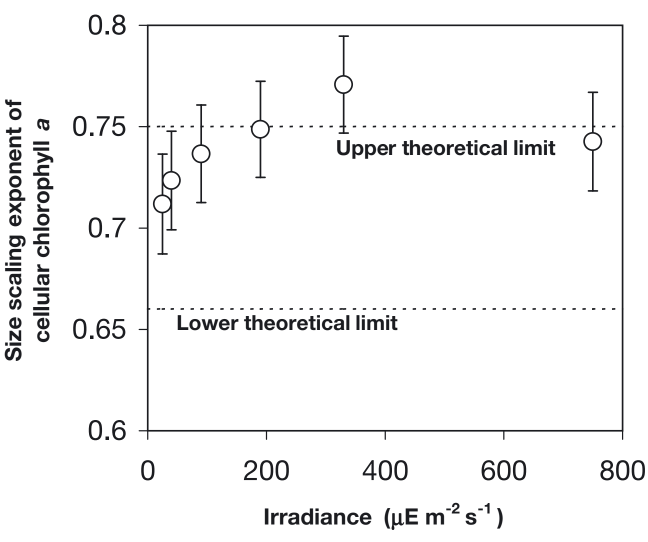

Fig. 5. Comparison between the size scaling exponent (b) associated with chl *a* per cell (mg chl *a* cell^{-1}) as a function of steady-state irradiance (E, µE m^{-2} s^{-1}) as predicted by theory (dotted lines) and observed in experimental cultures (symbols, ±1 SE). The size-scaling exponent of intracellular pigment content decreases with increasing light limitation. Open circles from (Fujiki & Taguchi 2002). As light becomes limiting, the size-scaling exponent decreases from a theoretical maximum of 0.75 to a theoretical minimum of 0.67

The parameters in z (Eq. 12) can change the intercept, but not the slope of log c_i versus log d. This is important as different taxonomic groups, under different growth conditions, can have different values of a^*_s, ξ, and τ, which will alter the value of z. Changes in z that are correlated with cell size will appear to alter the slope of log c_i versus log d. For example, many of the largest cells are not spherical, but instead resemble very long and narrow, or flat and squat, cylinders. A systematic shift in shape, from spherical cells to cylinders, with increasing cell size will reduce the effect of self-shading on the size scaling of photosynthesis and growth (Kirk 1976, 1994). Thus, a change in shape can reduce the package effect and mitigate the potential reduction in the size-scaling exponent of cellular pigment concentration and growth rates. This means that it is important to compare organisms with similar pigment composition under similar growth conditions when calculating and comparing the slope of log c_i versus log d. Species-specific changes in the parameters in z, and changes in cell shape (aspect ratio), and subtle changes in growth conditions, are likely responsible for much of the variability in the experimental data presented in Figs. 3 to 5.

Steady-state size scaling of photosynthesis over a light gradient with explicit photoacclimation

The relationship between optimal c_i and cell size can be used to determine photosynthetic rate as a function of cell size, and the resultant size-scaling exponent. Under sub-saturating irradiance, photosynthetic rate is a function of the rate of light acquisition, and therefore scales with cell volume with a $2/3$ exponent. Under saturating irradiance, growth is a function of the size-dependent transport network and therefore scales with cell volume with a $3/4$ exponent. These results are in good agreement with experimental work on phytoplankton (Table 2). These results should not be applied to organisms that are <1 µm in diameter because non-scalable components such as a minimum DNA content can result in radical changes in cellular composition (Raven 1994). At intermediate irradiances between extreme light limitation and saturation, photosynthetic rates will scale with cell volume with an exponent somewhere between $2/3$ and $3/4$. This is because E_k, the irradiance that characterizes the transition from light limitation to light saturation, is size-dependent. Commonly, E_k is defined as $P_{max}/(a\phi)$ at low E. This means that E_k is affected by both the size-dependence of the transport network ($P_{max} = kV^{3/4}$) and the size-dependence of light acquisition ($a = a^* c_i V$). Numerical calculations show that

Table 2. Size-scaling exponent as a function of cell volume of cellular photosynthetic rate (P^{cell}, mg C cell^{-1} h^{-1}) and cellular chl *a* content (mg chl *a* cell^{-1}) under light-limiting (25 µE m^{-2} s^{-1}) and -saturating conditions. Numbers in parentheses are 2 SE

	P^{cell}			Chl *a* cell^{-1}		
	Theory	Experiment	Source	Theory	Experiment	Source
Light limitation	0.67	0.60 (0.08)[a]	Taguchi (1976), Finkel (2001)	0.67	0.70 (0.03)	Taguchi (1976), Finkel (2001) Fujiki & Taguchi (2002)
Light saturation	0.75	0.79 (0.04)	Fujiki & Taguchi (2002)	0.75	0.75 (0.02)	Fujiki & Taguchi (2002)

[a] P^{cell} was calculated using the photosynthesis-irradiance parameters reported in Taguchi (1976), using an E of 25 µE m^{-2} s^{-1} to match Finkel (2001), and a reduced major axis (RMA) regression was performed on the merged dataset

the volume size scaling of $E_k \propto V^{1/12}$. This means that there are light intensities where photoacclimated small cells will be saturated for light, while larger cells are limited for light.

DISCUSSION

As organisms increase in size, their mass-specific metabolic rates decrease due to geometric constraints (West et al. 1997, Banavar et al. 2002). Specifically, larger organisms must allocate a larger proportion of their mass to their resource transportation systems or suffer a reduction in their mass-specific metabolic rates. Generally, the proportion of biomass allocated to transport systems is not strongly correlated with body size. As a consequence, under optimal growth conditions when resource supply matches demand, metabolic rate scales to the ¾ power of biomass (Banavar et al. 2002).

Under resource-limiting conditions, organisms must allocate an increasing proportion of their internal resources and total biomass towards resource acquisition. A size-dependence in resource gathering abilities can counter, or augment, the geometric constraints that cause the ¾ size scaling of metabolic rates. An increase in the ability to harvest resources with body size might lead to an increase in the size-scaling exponent of individual based metabolic rate, although constraints imposed by the demands of transportation networks will limit this effect. A decrease in the ability to harvest resources with body size will cause a decrease in the size-scaling exponent of individual based metabolic rate because there is no way for a transportation network to compensate for unavailable resources. Light acquisition by unicellular phytoplankton is just one example of the size-dependence of the ability to harvest resources due to geometric constraints.

Under light-limiting conditions, the rate of photon absorption determines the photosynthetic rate (Kiefer & Mitchell 1983, Falkowski et al. 1985). Light absorption in unicellular photoautotrophs depends on the incident irradiance, cell volume and shape, pigment concentration, composition, and distribution within the cell (Kirk 1994). Assuming optimal pigment composition and distribution, a cell can gather more photons only by increasing its pigment concentration. Under light-saturating conditions, in the absence of any package effect, pigment scales with body mass with a ¾ exponent (Fig. 5), not only for phytoplankton but also for higher plants (Niklas & Enquist 2001). As Niklas & Enquist (2001) point out, this is precisely what is expected if natural selection adjusts pigment concentration to maximize metabolic rate. In other words, an organism should not harvest more energy than it can effectively use.

Photoautotrophs generally increase their pigment concentration in response to decreasing growth irradiance. Phytoplankton cellular pigment concentrations can increase as much as 5- to 9-fold in response to decreases in irradiance, in a matter of hours to days (Falkowski & Owens 1980, Ley & Mauzerall 1982, Post et al. 1984, Prezelin et al. 1986, Cullen & Lewis 1988, Falkowski & LaRoche 1991). Pigment responses to changes in growth irradiance are less dramatic in higher plants, although increases of 2- to 3-fold are not uncommon (Evans & Poorter 2001). This is not surprising given that land plants generally experience higher photon flux densities, and spend their whole lives in one location. Phytoplankton cells are continually mixed throughout the water column, and have the ability to acclimate to a wide range of light intensities. Due to the cost of the LHC there is both a size- and irradiance-dependent limit to pigment acclimation in response to irradiance.

The maximum pigment concentration or cell size that can be maintained at a given irradiance is governed by the cost of the LHC and the diminishing returns associated with the increasing internal self-shading of pigment that leads to the decrease in the pigment-specific light absorption coefficient. The package effect depends on the product of the intracellular pigment concentration and cell diameter ($c_i d$, Eqs. 3 to 6). If c_i is constant, the package effect increases with diameter, and light-limited pigment-specific light acquisition drops rapidly with cell volume. As a result, larger phytoplankton cannot afford to maintain the same intracellular pigment concentrations as smaller cells. This accounts for the inverse relationship between c_i and d reported for phytoplankton (Agustí 1991, Finkel 2001). Consequently, the decrease in cellular photosynthesis with decreasing irradiance is size-dependent with an exponent other than ¾.

Other forms of resource limitation may also alter the ¾ size scaling of metabolic rates if the acquisition of the resource is size-dependent. For example, nutrient limitation may also cause anomalous size scaling of metabolic rates in a variety of organisms, including phytoplankton (Eppley et al. 1969, Gavis 1976, Hudson & Morel 1993, Hein et al. 1995). Consider nutrient uptake (U, nutrient cell^{-1} h^{-1}) by a phytoplankton cell, which depends on nutrient diffusion (Pasciak & Gavis 1974):

$$U \propto 4\,\pi\,d\,D\,\Delta C \tag{13}$$

where D is the diffusion coefficient of the nutrient in question, and ΔC is the concentration gradient of the nutrient from the cell surface to the concentration in the bulk media. In a Droop-type model, U is a function of growth rate (μ, h^{-1}) and the cellular quota for that nutrient (q, nutrient cell^{-1}):

$$U = \mu q \tag{14}$$

where $q \propto V^{3/4}$ (Stolte & Riegman 1995). At equilibrium, we can assume that these 2 expressions for uptake are equal. Rearranging Eqs. (13) & (14) we can solve for the size dependence of the growth rate; $\mu \propto V^{-5/12}$. Future models should also consider the dependence of uptake and cell quota on nutrient concentrations in the bulk media (nutrient acclimation). More research is needed to determine whether size-dependent resource acquisition for other limiting resources, and in other organisms, causes similar changes to the size scaling of metabolic rates.

CONCLUSIONS

The ¾ rule of metabolic rates is a key concept in macroecology (Brown 1995). It has been suggested that the ¾ rule is the key to understanding not only metabolic rates but also fundamental ecological and evolutionary patterns in abundance and diversity (Rosenweig 1995, Whitfield 2001). However, there are many reported examples where the ¾ rule does not apply. We present a model that demonstrates that resource limitation causes quantifiable, predictable deviations from the ¾ rule.

Specifically, we demonstrate that when irradiance limits photosynthetic rates in phytoplankton, light acquisition alters the size scaling of photosynthesis. In the absence of photoacclimation, the size scaling of cellular photosynthetic rate is proportional to V^b, where b ranges from ⅔ to 1 depending on the intracellular pigment concentration, irradiance and size range considered. In actuality, phytoplankton acclimate to their incident irradiance via changes in intracellular pigment concentration in order to maximize their cellular photosynthetic rate as a function of irradiance. There is a size-dependence associated with the ability of phytoplankton cells to acclimate to decreases in irradiance via their intracellular pigment concentrations due to the package effect. As a consequence, larger phytoplankton cells support lower maximum intracellular pigment concentrations, and require higher irradiances to reach their maximum cellular photosynthetic rate. This suggests that smaller phytoplankton cells are at an advantage over larger cells under steady-state light-limiting conditions.

Incorporating pigment acclimation into our model allows us to predict the irradiance and size-dependence of intracellular pigment concentration, and the resultant change in the size scaling of exponent associated with cellular photosynthetic rate. We predict that the size scaling of cellular photosynthesis is proportional to $V^{3/4}$ under light-saturating conditions and decreases towards $V^{2/3}$ as light becomes limiting, in good agreement with experimental data. This example suggests that other forms of resource limitation in other types of organisms may also alter the size scaling of metabolic rates.

Acknowledgements. We thank R. Armstrong, S. Tozzi, E. Litchman, A. Quigg, H. Stevens, J. Raven, M. Gorbunov, J. Huisman, P. Morin, and P. Falkowski for many constructive comments. This work was supported by an NSF Biocomplexity grant (OCE-0084032), ONR HyCode Program (N0014-99-0196), and an NSERC post-doctoral fellowship to A.J.I.

LITERATURE CITED

Agustí S (1991) Allometric scaling of light absorption and scattering by phytoplankton cells. Can J Fish Aquat Sci 48(5):763–767

Banavar JR, Damuth J, Maritan A, Rinaldo A (2002) Supply-demand balance and metabolic scaling. Proc Natl Acad Sci USA 99(16):10506–10509

Berner T, Dubinsky Z, Wyman K, Falkowski PG (1989) Photoadaptation and the 'package effect' in *Dunaliella tertiolecta* (Chlorophyceae). J Phycol 25:70–78

Berry J, Bjorkman O (1980) Photosynthetic response and adaptation to temperature in higher plants. Annu Rev Plant Physiol 31:491–543

Bonner JT (1988) The evolution of complexity by means of natural selection. Princeton University Press, Princeton, NJ

Brown JH (1995) Macroecology. University of Chicago Press, Chicago

Chisholm SW (1992) Phytoplankton size. In: Falkowski PG, Woodhead AD (eds) Primary productivity and biogeochemical cycles in the sea. Plenum Press, New York, p 213–237

Cullen JJ, Lewis MR (1988) The kinetics of algal photoadaptation in the context of vertical mixing. J Plankton Res 10(5):1039–1063

Cullen JJ, Reid FMH, Stewart E (1982) Phytoplankton in the surface and chlorophyll maximum off southern California in August, 1978. J Plankton Res 4(3):665–694

Cullen JJ, Geider RJ, Ishizaka J, Kiefer DA, Marra J, Sakshaug E, Raven JA (1993) Toward a general description of phytoplankton growth for biogeochemical models. In: Evans GT, Fasham MJR (eds) Towards a model of ocean biogeochemical processes, Vol 10. Springer-Verlag, Berlin, p 153–176

Eppley RW, Rogers JN, McCarthy JJ (1969) Half-saturation constants for uptake of nitrate and ammonium by marine phytoplankton. Limnol Oceanogr 14:912–920

Evans JR, Poorter H (2001) Photosynthetic acclimation of plants to growth irradiance: the relative importance of specific leaf area and nitrogen partitioning in maximizing carbon gain. Plant Cell Environ 24:755–767

Falkowski PG (1994) The role of phytoplankton photosynthesis in global biogeochemical cycles. Photosynth Res 39: 235–258

Falkowski PG, LaRoche J (1991) Acclimation to spectral irradiance in algae. J Phycol 27:8–14

Falkowski P, Owens TG (1980) Light-shade adaptation. Plant Physiol 66:592–595

Falkowski P, Raven JA (1997) Aquatic photosynthesis. Blackwell, Malden, MA

Falkowski PG, Dubinsky Z, Wyman K (1985) Growth-irradiance relationships in phytoplankton. Limnol Oceanogr 30(2): 311–321

Finkel ZV (2001) Light absorption and size scaling of light-limited metabolism in marine diatoms. Limnol Oceanogr 46(1):86–94

Finkel ZV, Irwin AJ (2000) Modeling size-dependent photosynthesis: light absorption and the allometric rule. J Theor Biol 204(3):361–369

Fujiki T, Taguchi S (2002) Variability in chlorophyll a specific absorption coefficient in marine phytoplankton as a function of cell size and irradiance. J Plankton Res 24(9):859–874

Gavis J (1976) Munk and Riley revisited: nutrient diffusion transport and rates of phytoplankton growth. J Mar Res 34:161–179

Gillooly JF, Brown JH, West GB, Savage VM, Charnov EL (2001) Effects of size and temperature on metabolic rate. Science 293(5538):2248–2251

Goericke R, Welschmeyer NA (1992) Pigment turnover in the marine diatom *Thalassiosira weissflogii*. II. The $^{14}CO_2$-labeling kinetics of carotenoids. J Phycol 28:507–517

Gould SJ (1966) Allometry and size in ontogeny and phylogeny. Biol Rev 41:587–640

Hein M, Folager Pedersen M, Sand-Jensen K (1995) Size-dependent nitrogen uptake in micro- and macroalgae. Mar Ecol Prog Ser 118:247–253

Hemmingsen AM (1960) Energy metabolism as related to body size and respiratory surfaces, and its evolution. Rep Steno Mem Hospital 9(2):15–22

Hudson RJM, Morel FMM (1993) Trace metal transport by marine microorganisms: implications of metal coordination kinetics. Deep-Sea Res 40(1):129–150

Ihaka R, Gentleman R (1996) R: a language for data analysis and graphics. J Comput Graph Stat 5:299—314

Jones RI (1978) Adaptations to fluctuating irradiance by natural phytoplankton communities. Limnol Oceanogr 23(5): 920–926

Kerr SR, Dickie LM (2001) The biomass spectrum: a predator-prey theory of aquatic production. Columbia University Press, New York

Kiefer DA, Mitchell BG (1983) A simple, steady state description of phytoplankton growth based on absorption cross section and quantum efficiency. Limnol Oceanogr 28(4): 770–776

Kirk JTO (1976) A theoretical analysis of the contribution of algal cells to the attenuation of light within natural waters. III. Cylindrical and spheroidal cells. New Phytol 77:341–358

Kirk JTO (1994) Light and photosynthesis in aquatic ecosystems. Cambridge University Press, Cambridge

Kleiber M (1947) Body size and metabolic rate. Physiol Rev 27:511–541

Kleiber M (1961) The fire of life: an introduction to animal energetics. John Wiley & Sons, New York

Ley AC, Mauzerall DC (1982) Absolute absorption cross-sections for photosystem II and the minimum quantum requirement for photosynthesis in *Chlorella vulgaris*. Biochim Biophys Acta 680:95–106

MacIntyre HL, Kana TM, Anning J, Geider R (2002) Photoacclimation of photosynthesis irradiance response curves and photosynthetic pigments in microalgae and cyanobacteria. J Phycol 38:17–38

Montagnes DJS, Franklin DJ (2001) Effect of temperature on diatom volume, growth rate, and carbon and nitrogen content: reconsidering some paradigms. Limnol Oceanogr 46(8):2008–2018

Montagnes DJS, Berges JA, Harrison PJ, Taylor FJR (1994) Estimating carbon, nitrogen, protein, and chlorophyll a from volume in marine phytoplankton. Limnol Oceanogr 39:1044–1060

Morel A, Bricaud A (1981) Theoretical results concerning light absorption in a discrete medium, and application to specific absorption of phytoplankton. Deep-Sea Res 1 28A(11):1375–1393

Morris I, Glover HE (1974) Questions on the mechanism of temperature adaptation in marine phytoplankton. Mar Biol 24:147–154

Muggli DL, Harrison PJ (1996) Effects of nitrogen source on the physiology and metal nutrition of *Emiliania huxleyi* grown under different iron and light conditions. Mar Ecol Prog Ser 130:255–267

Niklas KJ, Enquist BJ (2001) Invariant scaling relationships for interspecific plant biomass production rates and body size. Proc Natl Acad Sci USA 98(5):2922–2927

Pasciak WJ, Gavis J (1974) Transport limitation of nutrient uptake in phytoplankton. Limnol Oceanogr 19(6):881–888

Peters RH (1983) The ecological implications of body size, Cambridge University Press, Cambridge

Post AF, Dubinsky Z, Wyman K, Falkowski PG (1984) Kinetics of light-intensity adaptation in a marine planktonic diatom. Mar Biol 83:231–238

Prezelin B, Samuelsson G, Matlick HA (1986) Nutrient-dependent kinetics of photosynthesis parameters and photoinhibition of photosystem II during high light photoadaptation in *Gonyaulax polyedra*. Mar Biol 93:1–12

Raven JA (1984) A cost-benefit analysis of photon absorption by photosynthetic unicells. New Phytol 98:593—625

Raven JA (1994) Why are there no picoplanktonic O_2 evolvers with volumes less than 10^{-19} m^3 ? J Plankton Res 16:565–580

Raven JA (1997) The vacuole: a cost-benefit analysis. In: Leigh RA, Sanders D (eds) The plant vacuole, Vol 25. Academic Press, San Diego, p 59–82

Raven JA, Kubler JE (2002) New light on the scaling of meta-

bolic rate with the size of algae. J Phycol 38:11–16
Richardson K, Beardall J, Raven JA (1983) Adaptation of unicellular algae to irradiance: an analysis of strategies. New Phytol 93:157–191
Riper DM, Owens TG, Falkowski P (1979) Chlorophyll turnover in *Skeletonema costatum*, a marine plankton diatom. Plant Physiol 64:49–54
Rosenweig ML (1995) Species diversity in space and time. Cambridge University Press, Cambridge
Round FE, Crawford RM, Mann DG (1990) The diatoms: biology and morphology of the genera. Cambridge University Press, Cambridge
Schlesinger DA, Molot LA, Shuter BG (1981) Specific growth rates of freshwater algae in relation to cell size and light intensity. Can J Fish Aquat Sci 38: 1052–1058
Sommer U (1989) Maximal growth rates of Antarctic phytoplankton: only weak dependence on cell size. Limnol Oceanogr 34(6):1109–1112
Stolte W, Riegman R (1995) The effect of phytoplankton cell size on transient state nitrate and ammonium uptake kinetics. Microbiology 141:1221–1229
Strathmann RR (1967) Estimating the organic carbon content of phytoplankton from cell volume or plasma volume. Limnol Oceangr 12:411—418
Taguchi S (1976) Relationship between photosynthesis and cell size of marine diatoms. J Phycol 12(2):185–189
Thompson PA, Harrison PJ, Parslow JS (1991) Influence of irradiance on cell volume and carbon quota for ten species of marine phytoplankton. J Phycol 27:351–360
Trammer J (2002) Power formula for Cope's rule. Evol Ecol Res 4:147–153
Welschmeyer NA, Lorenzen CJ (1981) Chlorophyll-specific photosynthesis and quantum efficiency at subsaturating light intensities. J Phycol 17:283–293
West GB, Brown JH, Enquist BJ (1997) A general model for the origin of allometric scaling laws in biology. Science 276(5309):122–126
Whitfield J (2001) All creatures great and small. Nature 413: 342–344

Editorial responsibility: Andrea Belgrano, Santa Fe, New Mexico, USA

Submitted: April 16, 2003; Accepted: January 27, 2004
Proofs received from author(s): April 18, 2004

Vol. 273: 281–289, 2004

MARINE ECOLOGY PROGRESS SERIES
Mar Ecol Prog Ser

Published June 8

Non-linear dynamics in marine-phytoplankton population systems

Andrea Belgrano[1,5,*], Mauricio Lima[2], Nils C. Stenseth[3,4]

[1]Department of Biology, University of New Mexico, 167 Castetter Hall, Albuquerque, New Mexico 87131-1091, USA

[2]Center for Advanced Studies in Ecology & Biodiversity, Pontificia Universidad Católica de Chile, PO Box 114-D, Santiago 6513677, Chile

[3]Centre for Ecological and Evolutionary Synthesis (CEES), Department of Biology, University of Oslo, PO Box 1050 Blindern, 0316 Oslo, Norway

[4]Institute of Marine Research, Flødevigen Marine Research Station, 4817 His, Norway

[5]*Present address:* National Center for Genome Resources (NCGR), 2935 Rodeo Park Drive East, Santa Fe, New Mexico 87505, USA

ABSTRACT: Although non-linear density-dependence has been widely emphasized in population dynamics studies, the existence of non-linear exogenous forces have been less explored. In particular, we propose that the formulation of population dynamics models that include both non-linear endogenous (i.e. feedback structure) and exogenous (e.g. climatic) responses is relevant for understanding how climate variability affects natural systems. Here we show that single-species non-linear logistic models for marine phytoplankton in combination with non-linear exogenous forces capture observed population oscillations very well. Our results suggest that general population dynamic theory represents a useful tool for understanding the natural fluctuations of phytoplankton populations. Altogether we document what might be called a switch-on/switch-off dynamics in the phytoplankton population dynamics in relation to climate variability. We suggest the importance of, and the need for, linking population dynamics processes at local and regional scales to processes at the ecosystem level, thus reflecting a macroecological perspective of marine pelagic systems.

KEY WORDS: Phytoplankton populations · North Atlantic Oscillation · Non-linear dynamics · Density-dependence · Macroecology

INTRODUCTION

A central goal in population ecology is to understand the mechanisms underlying the numerical fluctuations of natural populations (Royama 1992, Murdoch et al. 2002) and, as part of that, to better understand how changes in population dynamics may be understood as the result of a combination of exogenous and endogenous factors (Turchin 1995, Hanski 1999). Endogenous factors represent the feedback loops created by individual interactions (within and between populations), while exogenous factors represent forcing variables which influence population changes, but they are not influenced back by the population state (Berryman 1981, 1999). In fact, nowadays most population ecologists agree that both factors are operating (Turchin 1995); however, the complex combination of exogenous and endogenous forces in ecological populations makes the study of their dynamics a conceptual and methodological challenge (Bjørnstad & Grenfell 2001). Recent studies have emphasized the implications of non-linearity in the feedback structure (Stenseth et al. 1997, Bjørnstad et al. 1998, 1999, Berryman 1999, Kristoffersen et al. 2001), while others have focused on the role of climatic forcing in ecological dynamics (Merritt et al. 2001, Mysterud et al. 2001, Stenseth et al. 2002, 2003). One interesting aspect about non-linearity is that the shape of the density-dependent function (feedback structure) may be an important clue in understanding what factors determine popula-

*Email: belgrano@unm.edu

tion growth rates (Berryman 1999, Sinclair & Krebs 2002). Moreover, determining the feedback structure is an essential step for understanding population responses to climatic variability, and how exogenous perturbations (e.g. climate) influence population processes (Royama 1992, Stenseth et al. 2002). On the other hand, the existence of non-linearity in climatic forcing has been recently explored in terrestrial (Murúa et al. 2003) and marine ecosystems (L. Ciannelli et al. unpubl.).

Although phytoplankton fluctuations have not been analyzed previously using population dynamic theory, there are a number of studies showing the role of oceanographic and climatic factors in determining algal blooms and dynamics (Reid et al. 1998, Belgrano et al. 1999). On the other hand, a recent study (Smayda 2002) showed very clearly the comparison between the ecological strategies of diatoms and dinoflagellates, describing population dynamics patterns such as growth, colonization and extinction. In a more theoretical framework, Chesson & Huntly (1997), Chesson (2000), and Anderies & Beisner (2000) described species coexistence and species interactions in fluctuating environmental conditions such as disturbance, seasonality and weather variability in order to understand some of the mechanisms regulating species diversity at a community level. Although phytoplankton fluctuations may be related to an array of limiting resources and oceanographic and climatic variables (Huisman & Weissing 1999), for planktonic systems it has generally been shown that it is important to consider non-equilibrium resource supply coupled with physical forcing and fluctuating light (Armstrong & McGehee 1976, Litchman & Klausmeier 2001).

In this study we use the classical framework of population dynamics theory (feedback structure = density-dependence and exogenous forces = density-independence) when modeling marine phytoplankton populations. We used non-parametric regression models to analyze the dynamics of 3 phytoplankton species in a Swedish fjord. Our aim was to determine the existence of non-linearity in the density-dependent structure and in the climate forcing terms in order to explain the numerical fluctuations exhibited by these marine phytoplankton populations during 11 yr of study.

MATERIALS AND METHODS

Phytoplankton and environmental data. The data used in this study consist of phytoplankton species (cell counts) and abiotic factors measured on a monthly basis using a conductivity-temperature-depth (CTD) probe (GO MARK IIIC, General Oceanics) at hydrographic standard depths and analyzed according to the Swedish standard method (SIS) as reported in Belgrano et al. (1999). The station was located at the mouth of the Gullmar fjord on the Swedish west coast (58° 15′ N, 11° 26′ E) (Fig. 1). Phytoplankton were monitored monthly from 1986 to 1996; samples collected at sea from the surface to 20 m depth at intervals of 5 m were fixed using Lugol's (acid-iodine) and concentrated through sedimentation cylinders (10 to 50 ml) of combined plate counting chambers (Belgrano et al. 1999). The counting procedure was performed according to HELCOM (1988) using an inverted microscope at 3 magnifications (×10, ×20 and ×40) with a ×10 ocular magnification. Three species were selected from a 40 species database: *Skeletonema costatum* (diatom), *Ceratium tripos* and *C. furca* (dinoflagellates) were chosen to study in more detail their dynamics in relation to the North Atlantic Oscillation (NAO) and a suite of abiotic factors (these variables were chosen based on previous work reported in Belgrano et al. 2001), and are listed in Table 1. The wind speed of the 4 quadrants (NE, SE, SW and NW) was measured every third hour at the national weather station Måseskär, which measures wind conditions along the outer archipelago and in the mouth area of the Gullmar fjord (Lindahl et al. 1998). The index of the NAO was provided online (available at www.cgd.ucar.edu/~jhurrell/nao.html) and as reported by Hurrell (1995).

It is important to note the correlation between environmental variables, e.g. salinity and density were highly positively correlated (Pearson's correlation coefficient r = 0.91), and wind intensity also showed

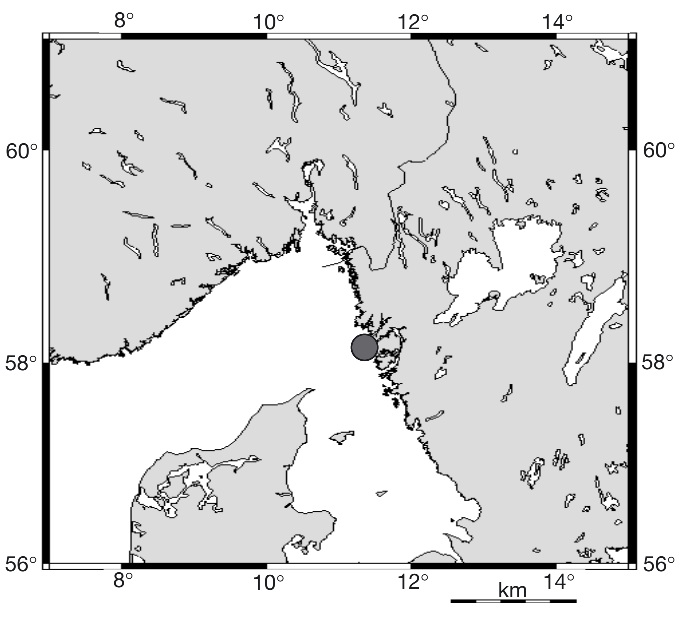

Fig. 1. Study area. The station was located at the mouth of the Gullmar Fjord on the Swedish west coast (58° 15′ N, 11° 26′ E)

Table 1. List of the abiotic variables used as input for the models. NAO: North Atlantic Oscillation

Input variable	Unit
Chl *a*	$\mu g\ l^{-1}$
PO_4^{3-}	$\mu mol\ l^{-1}$
NO_3^-	$\mu mol\ l^{-1}$
NAO	Index
Temperature	°C
Salinity	PSU
Density	σ_t
NE wind	$m\ s^{-1}$
NW wind	$m\ s^{-1}$
SW wind	$m\ s^{-1}$
SE wind	$m\ s^{-1}$

positive correlations between southwest and southeast winds (Pearson's correlation coefficient r = 0.63), southwest and northwest winds (Pearson's correlation coefficient r = 0.67), and southeast and northwest winds (Pearson's correlation coefficient r = 0.47).

The 3 species were selected in order to compare the variability of a common diatom *Skeletonema costatum* that comprised a very large bloom in the Swedish coastal waters in 1987, and 2 species of dinoflagellates, *Ceratium tripos* and *C. furca*, since an increase in their abundance may indicate a shift in the phytoplankton assemblages from larger to smaller cell sizes. Ultimately, since dinoflagellates possess different ecological adaptations to diatoms (Smayda 2002), we were interested in understanding some of the mechanisms underlying their population dynamics, in particular by comparing organisms exhibiting predictable behavior (diatoms) to those with unpredictable behaviour (dinoflagellates).

The underlying population dynamics model for these 3 species may be represented by the general model in terms of the density-dependence and density-independence in the reproduction and survival of individuals (Berryman 1999), leading to a generalized Ricker discrete-time logistic model (Ricker 1954), influenced by climate and stochastic forces:

$$N_t = N_{t-1} \times e^{\left[a_N + f_1(N_{t-1}) + \sum_{1}^{i=k} g^i(C_t^i) + \varepsilon_t\right]} \quad (1)$$

where N_t, is phytoplankton abundance at time t (in months), C is the exogenous variable, and ε_t represents normally distributed stochastic perturbations.

The function $f\,(N_{t-1})$ represents the effects of within-population ecological interactions; g^i represents the exogenous force, e.g. direct effects of oceanographic (salinity) and climatic (winds) conditions, or nutrients (nitrate) on phytoplankton population dynamics. An alternative way to express Eq. (1) is in terms of the realized per-capita population growth rates or the R-function, which represents the processes of individual survival and reproduction driving population dynamics and can be defined as $R_t = \log_e(N_t) - \log_e(N_{t-1})$; thus, Eq. (1) may be expressed as the following R-function (Berryman 1999):

$$R_t = a_N + f_1(N_{t-1}) + \sum_{1}^{i=k} g^i(C_t^i) + \varepsilon_t \quad (2)$$

This model represents the basic feedback structure and integrates the exogenous and stochastic forces that drive population dynamics in nature. In order to represent the functions we may choose a family of functional form. Hence, our model is an additive non-linear model (see Bjørnstad et al. 1998 for an ecological example), or a generalized additive model (GAM) (Hastie & Tibshirani 1990). The choice of the functional form of the non-linear functions may be approached using natural cubic splines (Green & Silvermann 1994, Stenseth et al. 1997, Bjørnstad et al. 1998). The complexity of the function (i.e. the number of degrees of freedom) and the number of terms was estimated using penalized regression splines and generalized cross validation (GCV) (Wood 2001). Smoothing terms are estimated using penalized regression splines with smoothing parameters selected by GCV. In general, the most logically consistent method to use for deciding which terms to include in the model is to compare GCV scores for models with and without the term. More generally, the score for the model with a smooth term can be compared to the score for the model with the smooth term replaced by appropriate parametric terms. Candidates for replacement by parametric terms are smooth terms with estimated degrees of freedom close to their minimum possible (1 degree of freedom). This statistical modeling approach may then be used in order to determine the climatic influences and the density-dependence structure. The models were implemented using S-Plus (2000).

RESULTS

The 3 phytoplankton species showed large fluctuations in cell density during the study period (Fig. 2). In the case of marine phytoplankton populations, there are strong seasonal dynamics characterized by the fact that, in winter, phytoplankton species are often not present in the water column. To avoid the problem caused by presence/absence data, we eliminated the zero values from the series: only data with positive values were analyzed. After eliminating the zero values, the realized per capita population growth rates in the 3 species showed a negative relationship with population density (Fig. 3), suggesting that these phytoplankton populations may be characterized by first order negative feedback (i.e. direct density-dependence).

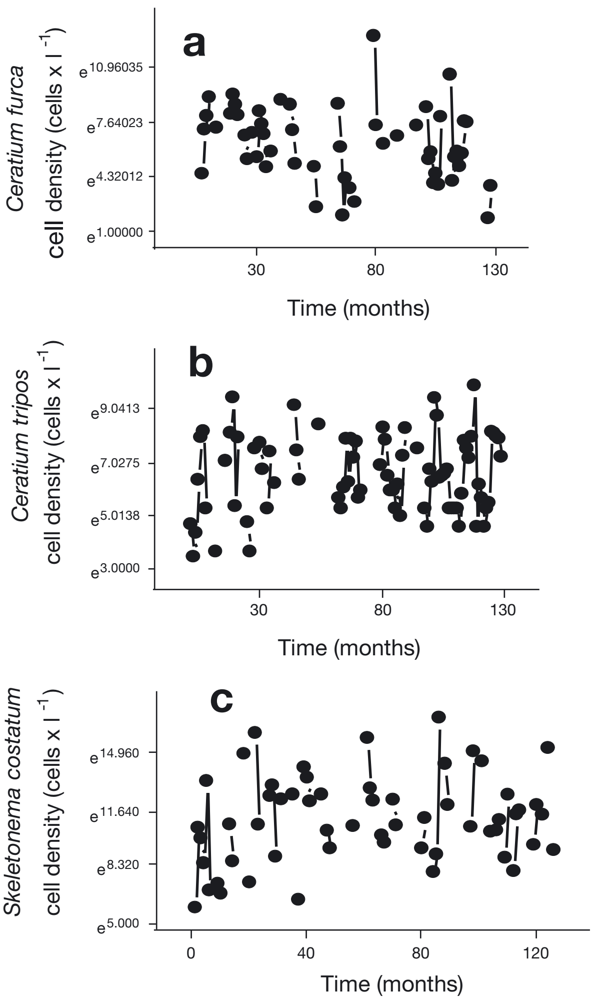

Fig. 2. Temporal dynamics of (a) *Ceratium furca*, (b) *C. tripos*, and (c) *Skeletonema costatum*. Phytoplankton population density is expressed as number of cells l^{-1}, missing points correspond to those months with no phytoplankton cells in the column of seawater

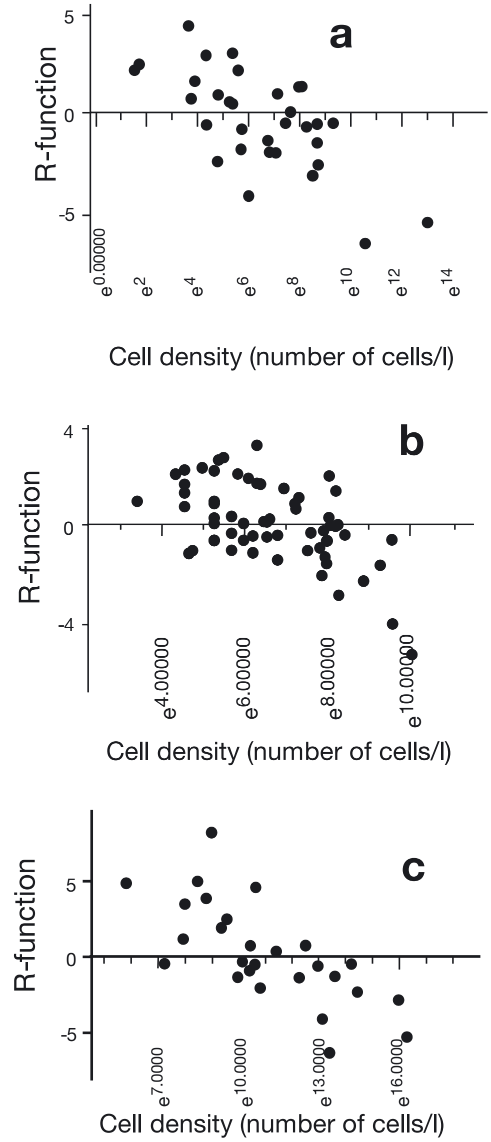

Fig. 3. R-functions (per capita growth rates estimated as ln N_t – ln N_{t-1}) against population density for (a) *C. furca*, (b) *C. tripos* and (c) *S. costatum*

The model obtained for the dinoflagellate *Ceratium furca* (Fig. 4) showed a weak non-linear negative first-order feedback structure, non-linear positive effects of the NAO, negative non-linear effects of the seawater density and negative non-linear effects of northeast wind intensity (Fig. 4, Tables 2 & 3). This model accounts for 89% of the variance (Table 2). The model obtained for *C. tripos* (Fig. 5) clearly suggests a log-linear negative first-order feedback, a positive non-linear effect on temperature, non-monotonic effects of northeast wind intensity, a positive non-linear effect of NAO and nitrates, and negative non-linear effect of southeast wind intensity and salinity (Fig. 5, Tables 2 & 3). The model accounts for 90% of the variance.

The diatom *Skeletonema costatum* (Fig. 6) exhibits log-linear first-order feedback, a non-monotonic effect of southwest wind intensity, non-linear positive effect of temperature and non-linear positive effect of northeast wind intensity; in addition we determined a linear positive effect of nitrates and a negative effect of salinity (Fig. 6, Tables 2 & 3). The model for *S. costatum* including the covariates accounts for 97% of the observed variance.

DISCUSSION

Population dynamics of these phytoplankton species are governed by endogenous and exogenous factors

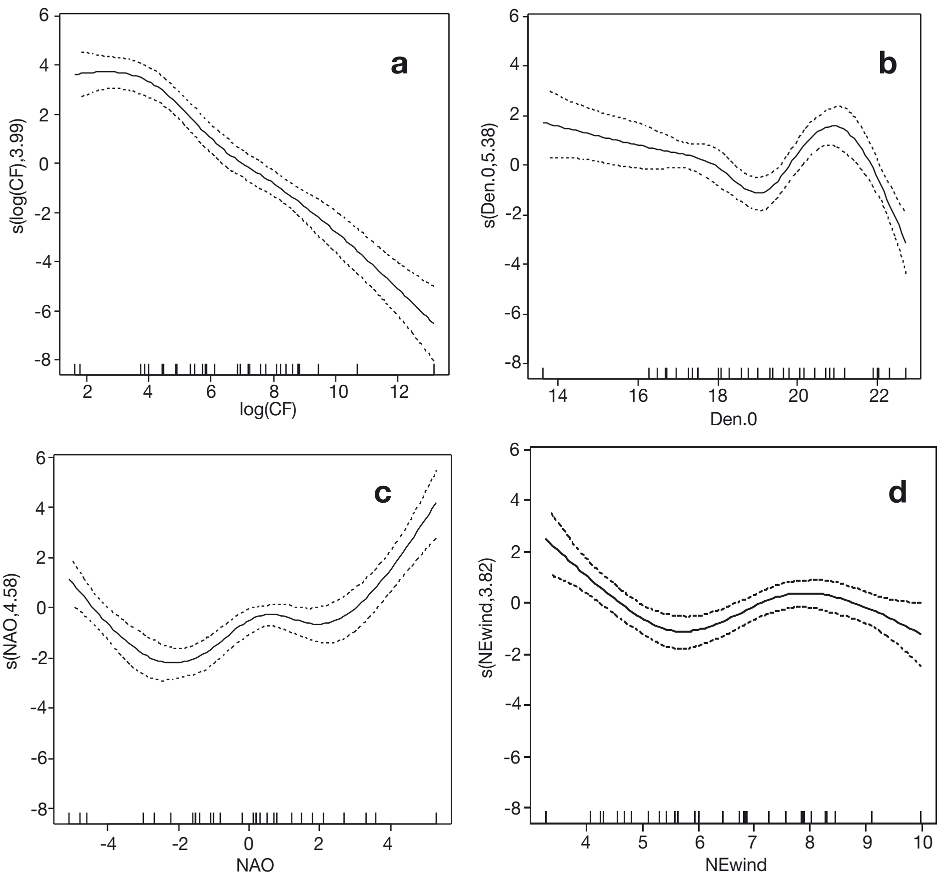

Fig. 4. Partial residuals of the non-linear terms estimated by means of generalized additive models (GAM) with smoothing splines. The appropriate smoothness for each applicable model term was selected using generalized cross validation (GCV). We used a GAM model for determining non-linear effects on population growth rates of *Ceratium furca*, the independent variables showing non-linearity were: *C. furca* density (CF); density of seawater (Den.0); North Atlantic Oscillation index (NAO); and northeast wind intensity (NEwind). Tick marks on *x*-axis show the locations of the observations on each variable

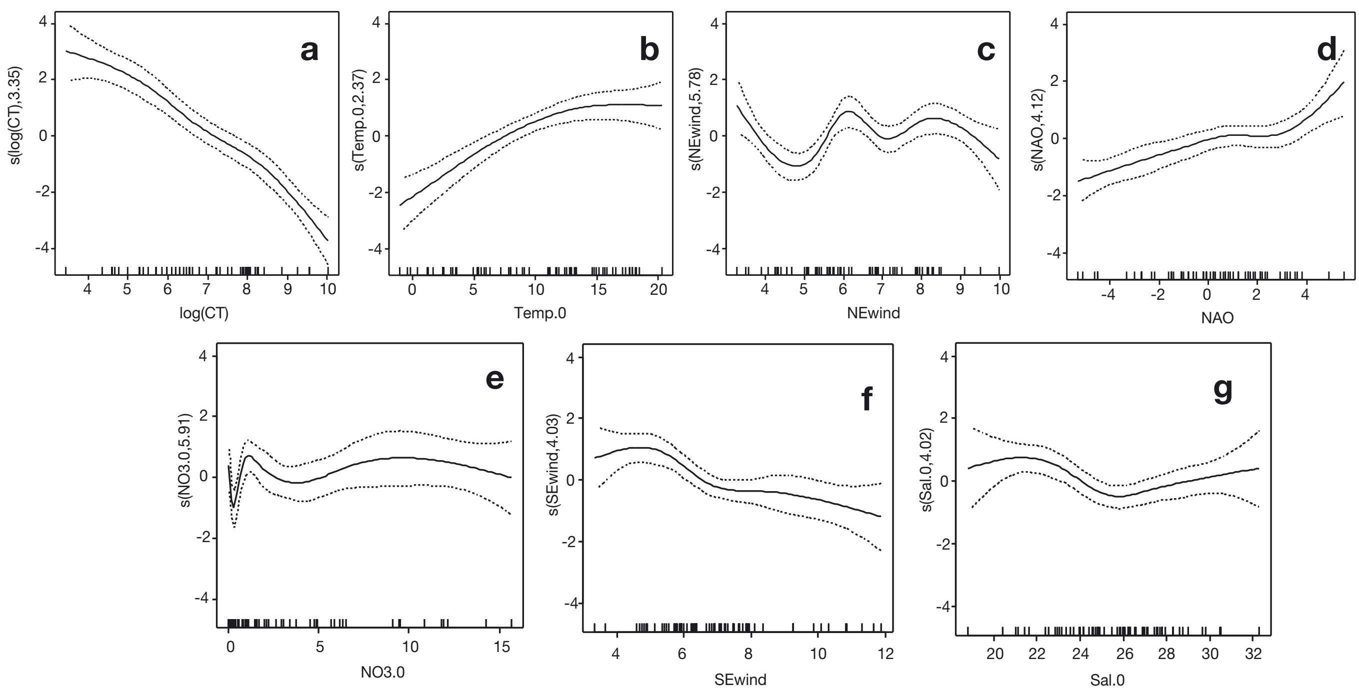

Fig. 5. *Ceratium tripos.* See legend to Fig. 4 for details. *C. tripos* density (CT); temperature (Temp.0); northeast wind (NEwind); north Atlantic Oscillation (NAO); nitrate (NO_3.0); southeastern wind intensity (SEwind); and salinity (Sal.0) are shown

Table 2. Best population dynamic models for each phytoplankton species. Incorporation of all variables produces a large number of possible models. We present only the statistically optimal models, chosen by Schwarz's Bayesian criterion (SBC) (S-Plus 2000). SBC is obtained as –2 × log-likelihood + npar × log (nobs), where npar and nobs represent number of parameters and observations in the fitted model, respectively. Model parameters were estimated by regression analysis in R-project software. Most parsimonious models according to Bayesian Information Criterion (ΔBIC > 2 is considered significant) are chosen and denoted in **bold**. p = probability value, R^2 = coefficient of determination, BIC = BIC criterion value, ΔBIC is the difference in Schwarz's Bayesian criterion (SBC) from the most parsimonious model. Model notations are: N_{t-1} = phytoplankton density or abundance, NAO = North Atlantic Oscillation index, NO_3 = nitrate, PO_4 = phosphate, Temp = temperature, Sal = salinity, Den = density of seawater, SEwind = southeast wind, NEwind = northeast wind, SWwind = southwest wind and NWwind = northwest wind

	F_{df}	p	R^2	BIC	ΔBIC
***Ceratium furca* models**					
$R_t = f_1\ (N_{t-1}) + f_2$ (NAO) + f_3 (Den)	**10.03 (13,16)**	**0.00002**	**0.89**	**117.90**	**0.00**
$R_t = f_1\ (N_{t-1}) + f_2$ (NAO) + f_3 (Den) + f_4 (SWwind)	8.95 (12,17)	0.00004	0.90	121.22	40.83
$R_t = f_1\ (N_{t-1}) + f_2$ (NAO) + f_3 (Den) + f_4 (PO_4) + f_5 (SWwind)	7.54 (15,14)	0.0003	0.89	124.96	44.55
$R_t = f_1\ (N_{t-1}) + f_2$ (NAO) + f_3 (Den) + f_4 (NO_3) + f_5 (SWwind)	7.08 (15,14)	0.0004	0.88	126.61	49.96
$R_t = f_1\ (N_{t-1}) + f_2$ (NAO) + f_3 (Sal) + f_4 (SWwind)	6.68 (12,17)	0.0003	0.83	128.62	57.36
$R_t = f_1\ (N_{t-1}) + f_2$ (NAO) + f_3 (Den) + f_4 (NEwind)	5.38 (12,17)	0.0009	0.79	133.88	70.02
$R_t = f_1\ (N_{t-1}) + f_2$ (NAO) + f_3 (Temp) + f_4 (SWwind)	5.15 (12,17)	0.0012	0.78	134.93	83.73
$R_t = f_1\ (N_{t-1}) + f_2$ (NAO) + f_3 (Den) + f_4 (SEwind)	5.13 (12,17)	0.0012	0.78	135.00	97.51
$R_t = f_1\ (N_{t-1}) + f_2$ (NAO) + f_3 (Den) + f_4 (NWwind)	5.09 (12,17)	0.0013	0.78	135.19	115.48
***Ceratium tripos* models**					
$R_t = f_1\ (N_{t-1}) + f_2$ (Temp) + f_3 (NO_3) + f_4 (NWwind) + f_5 (NEwind) + f_6 (SEwind) + f_7 (NAO)	**12.92 (25,37)**	**<0.00001**	**0.90**	**205.44**	**0.00**
$R_t = f_1\ (N_{t-1}) + f_2$ (Temp) + f_3 (NWwind) + f_4 (SEwind)	10.33 (12,50)	<0.00001	0.71	216.36	10.92
$R_t = f_1\ (N_{t-1}) + f_2$ (Temp) + f_3 (NWwind) + f_4 (SEwind) + f_5 (NO_3)	9.78 (15,47)	<0.00001	0.75	218.12	12.66
$R_t = f_1\ (N_{t-1}) + f_2$ (NAO) + f_3 (Temp) + f_4 (NWwind)	9.22 (12,50)	<0.00001	0.70	218.15	14.45
$R_t = f_1\ (N_{t-1}) + f_2$ (NAO) + f_3 (Temp) + f_4 (SEwind)	9.69 (12,50)	<0.00001	0.69	219.20	17.29
$R_t = f_1\ (N_{t-1}) + f_2$ (NAO) + f_3 (Temp) + f_4 (NEwind)	8.22 (12,50)	<0.00001	0.66	226.25	27.18
$R_t = f_1\ (N_{t-1}) + f_2$ (Temp) + f_3 (NWwind) + f_4 (SEwind) + f_5 (PO_4)	8.01 (15,47)	<0.00001	0.72	227.00	37.82
$R_t = f_1\ (N_{t-1}) + f_2$ (NAO) + f_3 (Temp) + f_4 (SWwind)	7.80 (12,50)	<0.00001	0.65	228.42	49.88
***Skeletonema costatum* models**					
$R_t = f_1\ (N_{t-1}) + f_2$ (NO_3) + f_3 (Sal) + f_4 (Temp) + f_5 (SWwind) + f_6 (NEwind)	**11.11 (16,6)**	**0.0035**	**0.97**	**99.73**	**0.00**
$R_t = f_1\ (N_{t-1}) + f_2$ (NO_3) + f_3 (Sal) + f_4 (Den) + f_5 (SWwind)	9.36 (15,7)	0.0031	0.95	105.21	5.48
$R_t = f_1\ (N_{t-1}) + f_2$ (NO_3) + f_3 (Sal) + f_4 (SWwind)	8.65 (12,10)	0.0009	0.91	109.97	10.24
$R_t = f_1\ (N_{t-1}) + f_2$ (NO_3) + f_3 (Den) + f_4 (SWwind)	8.51 (12,10)	0.00096	0.91	110.31	15.39
$R_t = f_1\ (N_{t-1}) + f_2$ (NO_3) + f_3 (Sal) + f_4 (NWwind)	4.54 (12,10)	0.011	0.84	123.05	33.23
$R_t = f_1\ (N_{t-1}) + f_2$ (NO_3) + f_3 (Sal) + f_4 (NEwind)	4.10 (12,10)	0.016	0.83	124.98	53.00
$R_t = f_1\ (N_{t-1}) + f_2$ (NO_3) + f_3 (Sal) + f_4 (SEwind)	3.08 (12,10)	0.040	0.79	130.32	78.11
$R_t = f_1\ (N_{t-1}) + f_2$ (NO_3) + f_3 (Temp) + f_4 (SWwind)	2.95 (12,10)	0.048	0.78	131.09	103.99

that may be captured using simple and general population dynamics models. In particular, phytoplankton fluctuations appear to be represented by a sort of switch-on/switch-off dynamic related to the within-year seasonal forcing. When we analyzed the non-zero data in the phytoplankton fluctuations, the 3 phytoplankton populations showed a negative first-order feedback (direct density-dependence), suggesting that a biological process such as intra-specific competition represents a basic principle underlying the fluctuations of abundance in these species. In particular, the 3 species showed almost log-linear density-dependencies (Gompertz model), and intra-specific competition could be an important ecological force in these systems. However, as pointed out by Chesson & Huntly (1997), fluctuations in environmental and weather conditions can create spatial and temporal ecological niche opportunities that can favor species coexistence. Looking at the results, it seems that nitrate could be regarded as a limiting nutrient in combination with fluctuations in temperature, NAO and associated wind conditions. The models also suggest that the species coexistence and fluctuating environmental conditions deviate from the common assumption that the association between species and abiotic conditions are always linear and additive (Chesson & Huntly 1997), and also that since phytoplankton compete for a handful of resources, their dynamics may be complex and difficult to predict (Huisman & Weissing 1999). The 2 dinoflagellate species showed some interesting differences; while *Ceratium furca* showed less influence of exogenous variables, *C. tripos* appeared to

Table 3. Coefficients of the GAM models selected for each species. Smooth terms are represented using penalized regression splines with smoothing parameters selected by GCV (generalized cross validation) or by regression splines with fixed degrees of freedom (mixtures of the 2 are permitted). Parametric coefficients represent the linear terms in each model, edf are the estimated degrees of freedom of the smooth terms using cubic splines. Model notations are: CF = *Ceratium furca* density; CT = *Ceratium tripos* density; SC = *Skeletonema costatum* density; NAO = North Atlantic Oscillation index; NO_3 = nitrate; PO_4 = phosphate; Chl = chl *a*; Temp = temperature; Sal = salinity; Den = density of seawater; SEwind = southeast wind; NEwind = northeast wind; SWwind = southwest wind and NWwind = northwest wind. The appropriate smoothness for each applicable model term was selected using GCV. We initialized the analyses using splines with 7 df. s: splines

Ceratium furca

Parametric coefficients

	Estimate	SE	*t* ratio	Pr(>|*t*|)
Constant	–0.300	0.21	–1.41	0.18

Approximate significance of smooth terms

	edf	χ^2	p-value
s(log[CF])	3.99	183.58	<0.00001
s(Den)	5.38	52.48	<0.00001
s(NAO)	4.58	74.69	<0.00001
s(NEwind)	3.82	19.64	0.0006

Ceratium tripos

Parametric coefficients

	Estimate	SE	*t* ratio	Pr(>|*t*|)
Intercept	–0.55	0.24	–2.33	0.026

Approximate significance of smooth terms

	edf	χ^2	p-value
s(log[CT])	3.35	121.85	<0.00001
s(Temp)	2.37	29.44	<0.00001
s(NEwind)	5.78	34.09	<0.00001
s(NAO)	4.12	27.47	<0.00001
s(NO_3)	5.92	25.53	0.0002
s(SEwind)	4.03	29.85	<0.00001
s(Sal)	4.02	18.01	0.0011

Skeletonema costatum

Parametric coefficients

	Estimate	SE	*t* ratio	Pr(>|*t*|)
Intercept	18.75	3.62	5.75	0.00043
NO_3	0.98	0.13	7.66	<0.00001
Sal	–0.93	0.14	–6.82	0.0001

Approximate significance of smooth terms

	edf	χ^2	p-value
s(log[SC])	3.10	94.52	<0.00001
s(SWwind)	3.22	29.86	<0.00001
s(Temp)	3.51	27.92	<0.00001
s(NEwind)	2.25	8.89	0.015

be largely influenced by exogenous forces. However, the latter species is more persistent at our study site.

On the other hand, our results are consistent with the role that physical and environmental processes play in determining phytoplankton fluctuations (Smayda 2002). All species showed effects of different exogenous variables. In particular, our results may suggest that the NAO and nitrates positively affect these dinoflagellate species, whereas salinity/density, northeast and southeast wind intensity have negative effects, suggesting that algal blooms of *Ceratium furca* and *C. tripos* are related to these particular environmental conditions. For example, Margalef et al. (1979) and Smayda & Reynolds (2001) showed that favorable conditions for dinoflagellate growth include high irradiance, low turbulence and high nutrient concentration. However, regarding turbulence, Sullivan & Swift (2003) showed that contrary to the paradigm in phytoplankton ecology, stating that dinoflagellates are always affected negatively by turbulence, when considering different small-scale turbulence regimes the response is species specific and in some cases can be contradictory. Interestingly, *C. furca* and *C. tripos* both showed positive responses to the NAO in the study area, as previously reported by Belgrano et al. (1999) for 3 species of *Dynophysis* dinoflagellates, showing strong correlations with NAO (R^2 = 0.9) and temperature (R^2 = 0.66). This reflects the increase in sea surface temperature associated with a positive NAO phase at the study site (Belgrano et al. 1999) and in the North Sea and adjacent areas (Reid et al. 1998, Ottersen et al. 2001).

In contrast, the exogenous forces influencing the dynamics of the diatom species *Skeletonema costatum* showed some interesting differences and similarities with the population dynamics of dinoflagellates. For example, in the same vein as the 2 *Ceratium* species, the diatom showed positive effects of nutrient (NO_3) concentration and temperature, and negative effects of high salinity. In particular temperature plays an important role in the aggregations of *S. costatum* cells, resulting in higher sinking rates, thus reflecting changes in the flux rate of carbon from the euphotic zone to deeper waters (Thorton & Thake 1998). However, in contrast with dinoflagellates, *S. costatum* appears to benefit from high northeast wind intensity and intermediate southwest wind intensity. The role of nutrients and temperature suggest the importance of resource limitation as well as a direct link to metabolic rate, and this in turn may be related to higher production and faster turnover or generation times. The negative effects of wind intensity on *C. furca* and *C. tripos* reveal that dinoflagellate growth rate increases during a period of low mixing (low wind intensity); in contrast, the diatom appears to benefit from high or intermedi-

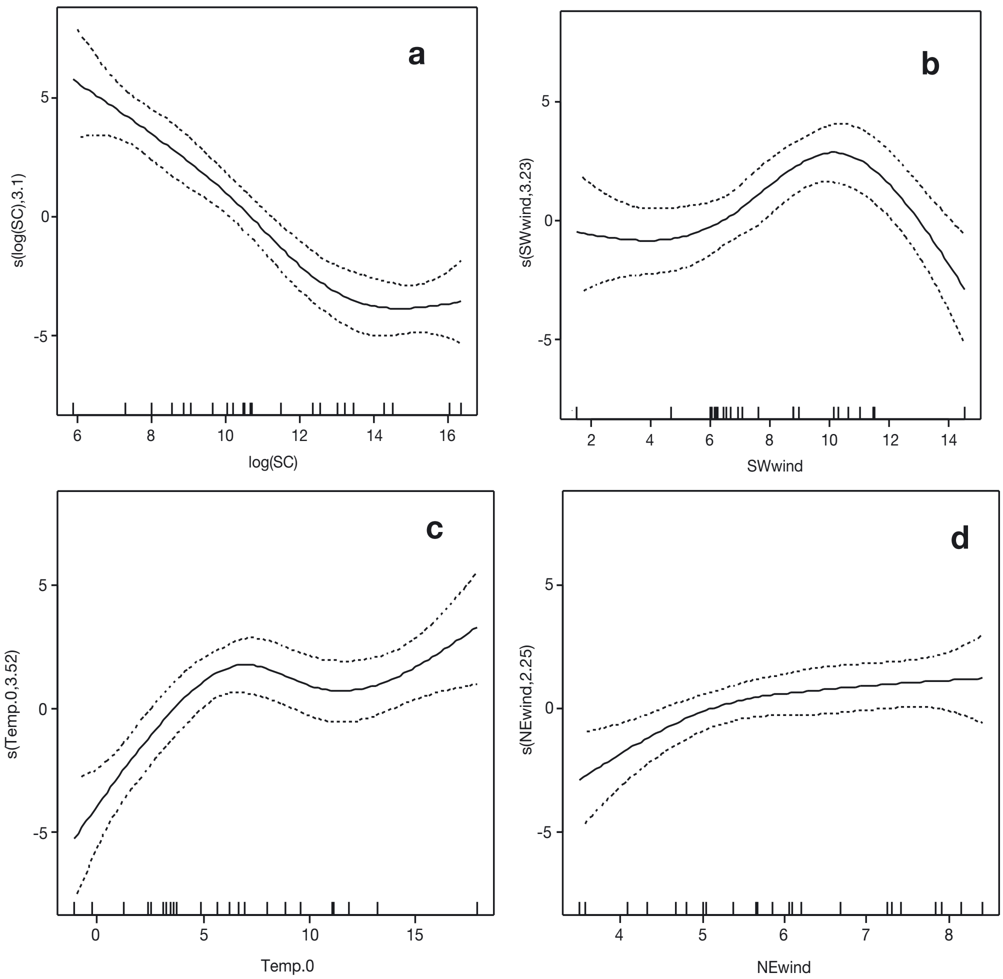

Fig. 6. *Skeletonema costatum.* See legend to Fig. 4 for details. *S. costatum* density (SC); southwest wind (SWwind); temperature (Temp.0); and northeast wind (NEwind) are shown

ate wind intensity, which represents periods of high mixing in the column of water. These changes in the abiotic condition along the Swedish west coast have been observed before (Lindahl et al. 1998), and suggest that transport of nutrients associated with stronger southwest winds from the Kattegat area, which are directly linked to a positive NAO scenario, may be related to large phytoplankton blooms, as was observed for *S. costatum* in 1987.

As suggested by Andereis & Beisner (2000), it is the interaction of abiotic and biotic factors and stochasticity that determines fluctuations at the species level, but this also allows species coexistence on common exploitable and fluctuating resources. The amplitude of this transfer function relating species to environmental fluctuations can increase at longer time scales, providing an indication of the integrative properties of cellular physiology. A reduction in vertical mixing from a few days to a period of ca. 2 wk may reduce the vertical mixing, leading to increased biomass (Harris 1986) in relation to the variance in the physical structure. The resulting dynamics may be reflected in the nonlinear relations found between species abundance and exogenous factors.

Single-species logistic models represent an appropriate general theoretical framework for understanding natural fluctuations in population dynamics studies. Moreover, conceptual elements, such as feedback structure and exogenous forces (climate), provide the basis for understanding the factors that may trigger phytoplankton bloom events (Huppert et al. 2002), including potentially toxic species (Belgrano et al. 1999). Phytoplankton population dynamics need to be considered to obtain a macroecological perspective of marine ecosystem dynamics (Brown 1999, Belgrano & Brown 2002). Ultimately, the goal is to link long-term and large-scale climatic fluctuations to species dynamics, thus resulting in the role of 'emergence' from pelagic organisms to pelagic organization, as proposed by Reynolds (2001).

Acknowledgements. A.B. acknowledges the support of an NSF Biocomplexity Grant (DEB-0083422). M.L. acknowledges financial support from FONDAP-FONDECYT Grant 1501-0001 (Program 2). N.C.S. acknowledges the Norwegian science council support through the EcoClim-project.

LITERATURE CITED

Anderies JM, Beisner B (2000) Fluctuating environments and phytoplankton community structure: a stochastic model. Am Nat 155:556–569

Armstrong RA, McGehee R (1976) Coexistence of two competitors on one resource. J Theor Biol 56:499–502

Belgrano A, Brown JH (2002) Oceans under the macroscope. Nature 419:128–129

Belgrano A, Lindahl O, Hernroth B (1999) North Atlantic Oscillation (NAO) primary productivity and toxic phytoplankton in the Gullmar Fjord, Sweden (1985–1996). Proc R Soc Lond B 266:425–430

Belgrano A, Malmgren B, Lindahl O (2001) The use of artificial neural network for predicting primary productivity. J Plankton Res 23:651–658

Berryman AA (1981) Population systems: a general introduction. Plenum Press, New York

Berryman AA (1999) Principles of population dynamics and their applications. Stanley Thornes Publishers, Cheltenham

Bjørnstad ON, Grenfell BT (2001) Noisy clockwork: time series analyses of population fluctuations of animals. Science 293:638–643

Bjørnstad ON, Stenseth, NC, Falck W (1998) A geographical gradient in small rodent density fluctuations: a statistical modeling approach. Proc R Soc Lond B 262:127–133

Bjørnstad ON, Fromentin JM, Stenseth, NC, Gjøsæter J (1999) A new test for density-dependent survival: the case of coastal cod populations. Ecology 80:1278–1288

Brown JH (1999) Macroecology: progress and prospect. Oikos 87:3–14

Chesson P (2000) Mechanisms of maintenance of species diversity. Annu Rev Ecol Syst 31:343–366

Chesson P, Huntly N (1997) The roles of harsh and fluctuating conditions in the dynamics of ecological communities. Am Nat 150:519–533

Green PJ, Silvermann BW (1994) Nonparametric regression and generalized linear models — a roughness penalty approach. Chapman & Hall, London

Hanski I (1999) Metapopulation ecology. Oxford University Press, Oxford

Harris GP (1986) Phytoplankton ecology. Chapman & Hall, London

Hastie T, Tibshirani R (1990) Generalized additive model. Chapman & Hall, London

HELCOM (1998) Guidelines for the Baltic Monitoring Programme for the third stage. Balt Sea Environ Proc 27:1–49

Huisman J, Weissing FJ (1999) Biodiversity of plankton by species oscillations and chaos. Nature 402:407–410

Huppert A, Blasius B, Stone L (2002) A model of phytoplankton blooms. Am Nat 159:156–171

Hurrell JW (1995) Decadal trends in the North Atlantic Oscillation: regional temperatures and precipitation. Science 269:676–679

Kristoffersen AB, Lingjærde, OC, Stenseth NC, Shimada M (2001) Non-parametric modelling of non-linear density dependence: a three-species host-parasitoid system. J Anim Ecol 70:808–819

Lindahl O, Belgrano A, Davidsson L, Hernroth B (1998) Primary production, climatic oscillations, and physicochemical processes: the Gullmar Fjord time-series data set (1985–1996). ICES J Mar Sci 55:723–729

Litchman E, Klausmeier CA (2001) Competition of phytoplankton under fluctuating light. Am Nat 157:170–187

Margalef R, Estrada M, Blasco D (1979) Functional morphology of organisms involved in red tides, as adapted to decay turbulence. In: Taylor DL, Seliger HH (eds) Toxic dinoflagellate blooms. Elsevier, New York, p 505

Merritt JF, Lima M, Bozinovic F (2001) Seasonal regulation in fluctuating small mammal populations: feedback structure and climate. Oikos 94:505–514

Murdoch WW, Kendall BE, Nisbet RM, Briggs CJ, McCauley E, Bosler R (2002) Single-species models for many-species food webs. Nature 417:542–543

Murúa R, González L, Lima M (2003) Population dynamics of rice rats (a Hantavirus reservoir) in southern Chile: feedback structure and non-linear effects of climatic Oscillations. Oikos 102:137–145

Mysterud A, Stenseth NC, Yoccoz NG, Laangvatn R, Steinheim G (2001) Nonlinear effects of large-scale climatic variability on wild and domestic herbivores. Nature 410: 1096–1099

Ottersen G, Planque B, Belgrano A, Post E, Reid PC, Stenseth NC (2001) Ecological effects of the North Atlantic Oscillation. Oecologia 128:1–14

Reid PC, Edwards M, Hunt HG, Werner J (1998) Phytoplankton change in the North Atlantic. Nature 391:546

Reynolds CS (2001) Emergence in pelagic communities. Sci Mar 65:5–30

Ricker WE (1954) Stock and recruitment. J Fish Res Board Can 11:559–623

Royama T (1992) Analytical population dynamics. Chapman & Hall, London

Sinclair AER, Krebs CJ (2002) Complex numerical responses to top-down and bottom-up processes in vertebrate populations. Proc R Soc Lond B 357:1221–1231

Smayda TJ (2002) Adaptive ecology, growth strategies, and the global bloom expansion of dinoflagellates. J Oceanogr 58:281–294

Smayda TJ, Reynolds CS (2001) Community assembly in marine phytoplankton: application of recent models to harmful dinoflagellate blooms. J Plankton Res 23:447–461

S-Plus (2000) Guide to statistics, Vol 1. MathSoft, Seattle

Stenseth NC, Falck W, Bjørnstad ON, Krebs CJ (1997) Population regulation in snowshoe hare and Canadian lynx: asymmetric food web configuration between hare and lynx. Proc Natl Acad Sci USA 94:5147–5152

Stenseth NC, Mysterud A, Ottersen G, Hurrell JW, Chan KS, Lima M (2002) Ecological effects of climate fluctuations. Science 297:1292–1296

Stenseth NC, Ottersen G, Hurrell JW, Mysterud A, Lima M, Chan, KS, Yoccoz, NG, Adlandsvik B (2003) Studying climate effects on ecology through the use of climate indices: the North Atlantic Oscillation, El Niño Southern Oscillation and beyond. Proc R Soc Lond Ser B 270:2087–2096

Sullivan JM, Swift E (2003) Effects of small-scale turbulence on net growth rate and size of ten species of marine dinoflagellates. J Phycol 39:83–94

Thorton DCO, Thake B (1998) Effect of temperature on the aggregation of *Skeletonema costatum* (Bacillariophyceae) and the implication for carbon flux in coastal waters. Mar Ecol Prog Ser 174:223–231

Turchin P (1995) Population regulation: old arguments and a new synthesis. In: Capuccino N, Price PW (eds) Population dynamics: new approaches and synthesis. Academic Press, San Diego, p 19–37

Wood SN (2001) MGCV, GAMs and generalized ridge regression for R. R News 1:20–25

Editorial responsibility: Otto Kinne (Editor), Oldendorf/Luhe, Germany

Submitted: April 16, 2003; Accepted: February 5, 2004
Proofs received from author(s): April 22, 2004

Vol. 273: 291–302, 2004 | MARINE ECOLOGY PROGRESS SERIES Mar Ecol Prog Ser | Published June 8

Network structure and robustness of marine food webs

Jennifer A. Dunne[1,4,*], Richard J. Williams[2,4], Neo D. Martinez[3,4]

[1]Santa Fe Institute, 1399 Hyde Park Road, Santa Fe, New Mexico 87501, USA

[2]National Center for Ecological Analysis and Synthesis, University of California Santa Barbara, 735 State St., Suite 300, Santa Barbara, California 93101-3351, USA

[3]Center for Applied Mathematics, 657 Frank HT Rhodes Hall, Cornell University, Ithaca, New York 14853, USA

[4]Pacific Ecoinformatics and Computational Ecology Lab, Rocky Mountain Biological Laboratory, PO Box 519, Crested Butte, Colorado 81224, USA

ABSTRACT: Previous studies suggest that food-web theory has yet to account for major differences in food-web properties of marine versus other types of ecosystems. We examined this issue by analyzing the network structure of food webs for the Northeast US Shelf, a Caribbean reef, and Benguela, off South Africa. The values of connectance (links per species^2), link density (links per species), mean chain length, and fractions of intermediate, omnivorous, and cannibalistic taxa of these marine webs are somewhat high but still within the ranges observed in other webs. We further compared the marine webs by using the empirically corroborated 'niche model' that accounts for observed variation in diversity (taxon number) and complexity (connectance). Our results substantiate previously reported results for estuarine, fresh-water, and terrestrial datasets, which suggests that food webs from different types of ecosystems with variable diversity and complexity share fundamental structural and ordering characteristics. Analyses of potential secondary extinctions resulting from species loss show that the structural robustness of marine food webs is also consistent with trends from other food webs. As expected, given their relatively high connectance, marine food webs appear fairly robust to loss of most-connected taxa as well as random taxa. Still, the short average path length between marine taxa (1.6 links) suggests that effects from perturbations, such as overfishing, can be transmitted more widely throughout marine ecosystems than previously appreciated.

KEY WORDS: Food webs · Network structure · Marine ecosystems · Robustness · Connectance · Niche model · Biodiversity loss

INTRODUCTION

Recent studies have described general properties of complex food-web structure as well as simple rules that accurately predict such structure in a wide variety of terrestrial and aquatic ecosystems (e.g. Williams & Martinez 2000, Camacho et al. 2002a,b, Dunne et al. 2002a,b, Williams et al. 2002, Krause et al. 2003). The data used in these studies generally have substantially higher diversity and more comprehensive and even resolution of taxa at different trophic levels than the earlier 'ECOWeB' food-web data used to initiate topological food-web research (Briand & Cohen 1984, Cohen et al. 1990), which are still occasionally used today (Neutel et al. 2002). Analyses of improved data have modified earlier food-web theory and contributed new insights into the trophic network structure and robustness of ecosystems (Martinez 1991, Williams & Martinez 2000, Dunne et al. 2002a,b). However, food webs from marine ecosystems have been conspicuously absent from recent synthetic work. An earlier analysis of ECOWeB data, including 11 marine food webs with low average diversity (18 trophic species), reported strong contrasts between marine and other ecosystems, with marine food webs having greater average links per species (*L*/*S*) and chain lengths than

*Email: jdunne@santafe.edu

other food webs (Cohen 1994). Similarly, a recent analysis of a more diverse, highly resolved marine food web (81 taxa) for the Northeast US Shelf found that L/S and connectivity are either an order of magnitude higher than non-marine webs or are disproportionate to the diversity of the system (Link 2002). The study concluded, 'it is clear that the emergent properties of this marine food web are very different than their terrestrial and freshwater counterparts.'

Previous studies of marine food-web structure rely on making direct comparisons of food-web properties among marine systems and between marine and non-marine systems. However, it is now well documented that most food-web properties are scale-dependent, meaning that they change as diversity and complexity change (e.g. Martinez 1993, 1994). This scale-dependence makes direct comparison of properties among food webs with different levels of species richness and trophic interaction richness (which we use to refer collectively to measures such as links per species, connectivity, and connectance) potentially misleading. Comparing observed food webs against food webs generated by a simple model that accounts for different levels of ecological diversity and complexity provides one solution to this problem. This type of modeling approach is useful for at least 5 reasons. First, if a model successfully characterizes the overall network structure of a range of food webs, those food webs can be considered to have a similar topology. Second, a model can act as a benchmark for comparing observed food webs. The ways in which the structure of observed food webs varies from structure predicted by a model that incorporates scale-dependence provides a way to compare food webs with different diversity and complexity. Third, a model can help to identify problems with particular datasets and to quantify how methodological biases ramify through analysis. Fourth, a model that successfully characterizes the network structure of observed food webs can be used to extend our understanding of what food webs with even greater diversity or complexity than currently available might look like, and also how food-web properties may be expected to vary with those factors (e.g. Williams et al. 2002). Fifth, if a model is phenomenologically successful (i.e. fits current datasets well, and successfully predicts new datasets), its underlying assumptions can point us towards potential mechanisms that generate general patterns of food-web structure.

We focus on the first 3 issues using 2 food-web structure models: the cascade model (Cohen et al. 1990) and the niche model (Williams & Martinez 2000). These simple models use only 2 input parameters: S (species richness) and C (connectance — links per species^2, L/S^2). These parameters are set equal to the S and C of each empirical food web, and then multiple stochastic models of each food web are produced using simple ordering rules. The use of those 2 parameters embodies the notion that the network structure of food webs will vary in predictable ways in accordance with their diversity (i.e. number of taxa) and complexity (i.e. connectance).

We analyzed 4 recently published marine food webs with 29 to 249 taxa, representing 3 marine ecosystems. In particular, we considered the questions: (1) Do marine food webs show similarities to each other? (2) Do marine food webs look like other types of food webs? (3) Do food-web theory and models apply to marine ecosystems? (4) What are the empirical limitations of recent marine food-web data? We also used the marine datasets to simulate the potential effects of different types and magnitudes of species loss in triggering cascading secondary extinctions. This allows a comparison of the potential robustness to biodiversity loss associated with the network structure of marine versus other types of food webs (Dunne et al. 2002a). This type of research on food-web structure and robustness is just one example of the statistical mechanics of technology, information, social, and biotic networks (see Strogatz 2001, Albert & Barabási 2002 for reviews). Even in the absence of dynamical modeling, which is challenging even for relatively low diversity systems, analysis of network structure can have important implications for network function (Strogatz 2001). For marine ecosystems, historically subject to intense fisheries pressure and subsequent collapse (Jackson et al. 2001, Pauly et al. 1998, 2002), more detailed knowledge of the complex network of trophic relationships that encompass species of economic interest will be important for guiding more sustainable policy.

METHODS

We analyzed the network structure of food webs with relatively detailed species and trophic interaction data from 3 marine ecosystems. The first, the Benguela ecosystem off the southwest coast of South Africa (Yodzis 1998, 2000), is represented by a 29-taxa food web. The second, the Northeast US Shelf ecosystem, is represented by an 81-taxa food web (Link 2002). The third, a Caribbean coral reef ecosystem from the Puerto Rico-Virgin Islands shelf complex (Opitz 1996), is represented by 2 versions of the same food web, with 249 and 50 taxa. The original investigator generated the smaller food web from the larger dataset in order to analyze the smaller web with the ECOPATH II box model, which allows for a maximum of 50 compartments (Christensen & Pauly 1992). For the smaller food web, 243 fish species were aggregated into 25 fish groups based on size, activity level, and food type, while 41 non-fish taxa, many of which were already aggregated, were reduced further into 25 groups based on mortality, food consumption, size, diet composition, lifestyle, and taxonomic closeness (Opitz 1996). We refer to these ecosystems and their food webs as Benguela, NE US Shelf, and small and large Caribbean Reef.

We use the term 'taxa' to refer to the groups of organisms identified by the original investigators as the core units of analysis in their food webs. These range from species (e.g. spotted hake, humans), to species grouped by trophic habit, taxonomy, or other criteria (e.g. benthic filter feeders, macrozooplankton, whales and dolphins), to mixed pools (e.g. detritus — a combination of live organisms, organic matter, and inorganic matter). All 3 ecosystems are subject to intense human fishing, and the marine food-web data reflect a strong fish bias, which represent ≥50 % of the taxa in each web (Table 1). The large version of the Caribbean Reef food web is particularly biased, with fish representing 84 % of taxa. In all 4 webs, invertebrates (14 to 41 % of taxa) are under-represented and poorly resolved relative to the fishes (as also noted by Link 2002) and basal taxa are very highly aggregated into groups such as 'phytoplankton' and 'detritus' (2 to 7 % of taxa).

How does the quality of these datasets compare to earlier marine food webs used for structural studies, in particular the marine food webs from the ECOWeB database (Cohen et al. 1990, Cohen 1994) A 1993 article on 'Improving food webs' (Cohen et al. 1993) called for 'more explicitness and more exhaustiveness' in the compilation of food webs, and suggested the admittedly ideal goal that *all* species and *all* links between them for a particular ecological time and volume should be reported. However, this type of exhaustiveness is difficult or impossible (particularly when considering microorganisms and other cryptic organisms), may be unnecessary for certain kinds of investigations (Martinez et al. 1999), and may impede useful analytical and theoretical development focused on fundamental patterns and mechanisms. Instead, we suggest that, in addition to methodological explicitness (Cohen et al. 1993), food web compilation should continually strive for higher degrees of consistency and comprehensiveness. The food webs in ECOWeB are generally plagued by low diversity, reflecting in many (but not all) cases a lack of comprehensiveness, as well as inconsistent resolution of different types of taxa, with lower, non-vertebrate trophic levels often highly aggregated. An example of one of the more diverse marine food webs in ECOWeB is web 29, a food web of the Arctic seas (Dunbar 1954). This web has 22 taxa, with 2 basal taxa, 4 invertebrate taxa, and 16 vertebrate taxa (primarily whales, seals, and fishes). While the Benguela, small Caribbean Reef, and NE US Shelf food webs similarly fail to distinguish among basal taxa, they are improved over the Arctic seas and other earlier marine food webs given their more comprehensive inclusion, higher resolution, and more even resolution of taxa at other trophic levels. The large Caribbean Reef web is particularly interesting: while it is an order of magnitude more diverse than earlier ECOWeB marine food webs, we do not consider it necessarily higher quality than many of the early food webs. The Arctic seas food web, despite its lack of diversity, is more consistently and evenly resolved than the large 249-taxa Caribbean Reef web with its 84 % fish species and <2 % basal taxa. Because of the flaws of the large Caribbean Reef web, we limit most of our discussion of marine food-web characteristics to the Benguela, small Caribbean Reef, and NE US Shelf food webs.

We studied trophic species versions of the food webs. Trophic species are groups of taxa whose members share the same set of predators and prey (Briand & Cohen 1984). The use of trophic species, hereafter referred to as species (S), is a convention in structural food-web studies that can reduce methodological biases of uneven resolution of taxa within and among food webs (Briand & Cohen 1984, Williams & Martinez 2000). Trophic species aggregation alters the marine food webs very little, with no changes to the Benguela and small Caribbean Reef webs, and reductions of the NE US Shelf and large Caribbean food webs from 81 to 79 taxa and 249 to 245 taxa, respectively (see Table 2). The use of trophic species is not a panacea, as demonstrated by the large Caribbean Reef web. Although this food web is excessively biased towards fishes, the use of the trophic species aggregation does almost nothing to alleviate its extremely uneven resolution. The ecologically more sophisticated criteria used to aggregate the large food web into a smaller 50-taxa web (Opitz 1996) are much more effective than 'trophic species' in rendering a higher quality, more evenly resolved, albeit lower diversity, food web.

Table 1. Number (percentage) of different types of taxa in 4 marine food webs

	Benguela	Caribbean Reef (small)	Caribbean Reef (large)	NE US Shelf
All taxa	29	50	249	81
Fishes	18 (62)	25 (50)	208 (84)	41 (51)
Other vertebrates	3 (10)	2 (4)	2 (1)	5 (6)
Invertebrates	6 (22)	18 (36)	35 (14)	33 (41)
Basal groups	2 (7)	3 (6)	4 (2)	2 (2)

For each food web, we calculated 18 network structure properties (see Tables 2 & 3). Two standard measures of food-web trophic interaction richness are reported: links per species (L/S), which equals the mean number of species' predators plus prey, also referred to as link density; and connectance (C), where $C = L/S^2$, the proportion of all possible trophic links (S^2) that are actually realized (L), also referred to as 'directed connectance.' Seven properties give percentages of types of species in a food web: top (T) (taxa that lack any predators or parasites), intermediate (I), and basal species (B) (taxa that lack any prey items); cannibals (*Can*); omnivores (*Omn*) (taxa with food chains of different lengths, where a food chain is a linked path from a non-basal to a basal species); herbivores plus detritivores (*Herb*); and species involved in looping (*Loop*) by appearing in a food chain twice. Most of these are commonly calculated properties that have been reviewed elsewhere (e.g. Williams & Martinez 2000), although *Herb* has not been previously reported.

The remaining 10 properties quantify overall properties of food-web network structure. We calculated a trophic level measure called the mean 'short-weighted trophic level' (*TL*) (Williams & Martinez 2004). For a particular taxon, short-weighted trophic level is the average of 'prey-averaged trophic level' (1 plus the mean trophic level of all the taxon's trophic resources) and 'shortest trophic level' (1 plus the shortest chain length from the consumer taxon to a basal taxon). An examination of 6 ways of estimating trophic level based on network structure, compared to trophic level calculations based on more information-rich flow-weighted trophic data, shows that short-weighted trophic level gives the most accurate estimate of trophic level based on binary link information (Williams & Martinez 2004). Short-weighted trophic level estimates, like estimates based on flow-weighted link information, produce lower trophic levels than those reported by studies using the more common 'chain-averaged trophic level' algorithm (Martinez 1991, Polis 1991, Fussman & Heber 2002).

We report 3 food-chain-length related measures, the mean (*ChLen*) and standard deviation (*ChSD*) of chain lengths and the log of the number of chains (*ChNum*). We report the standard deviation of mean generality (*GenSD*), how many prey items a species has, and vulnerability (*VulSD*), how many predators a species has. These 2 measures quantify the variabilities of species' normalized predator and prey counts (Schoener 1989). The number of predators and prey shared in common by a pair of species divided by the pair's total number of predators and prey is referred to as trophic similarity. We averaged across each species' highest trophic similarity index to another species to report the mean maximum trophic similarity (*MaxSim*). The previous 6 properties follow Williams & Martinez (2000). We also report 2 measures of 'small-world' network structure (Watts & Strogatz 1998): characteristic path length (*Path*), the mean shortest path length between species pairs; and clustering coefficient (*Clust*), the mean fraction of species pairs connected to the same species that are connected to each other (Camacho et al. 2002b, Dunne et al. 2002b, Montoya & Solé 2002, Williams et al. 2002).

For each marine food web, we compare the ability of 2 simple stochastic food-web structure models, the cascade model (Cohen et al. 1990) and the niche model (Williams & Martinez 2000), to predict 16 food-web properties. The models have 2 input parameters: the number of trophic species (S) and connectance (C) of the food web being modeled. We do not report random network models (e.g. Erdös & Rényi 1960) because food-web structure, as well as the structure of most, if not all, real-world networks is clearly not random (Watts & Strogatz 1998, Williams & Martinez 2000). The cascade model (Cohen et al. 1990) assigns each species a random value drawn uniformly from the interval (0,1) and each species has a probability p = $2CS$ / (S – 1) of consuming species with values lower than its own. The niche model (Williams & Martinez 2000) builds on the cascade model, with each species similarly assigned a randomly drawn 'niche value' (n_i) from the interval (1,0) (Fig. 1). Each species is then constrained to consume all prey species within a range of values (r_i) whose randomly chosen center (c_i) is less than the consumer's niche value. In the niche model, the placement of the feeding range relaxes the cascade model's strict feeding

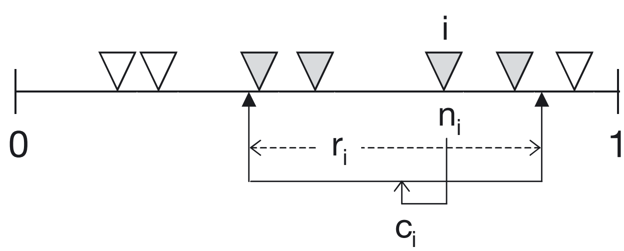

Fig. 1. Diagram of the niche model. S (trophic species richness) and C (connectance) are set at the observed values for the empirical web being modeled. Each of S species (here S = 7, shown by inverted triangles) is assigned a 'niche value' (n_i) drawn uniformly from the interval (0,1). Species i consumes all species falling in a range (r_i) that is placed by uniformly by drawing the center of the range (c_i) from the interval ($r_i/2$, n_i). Thus, in this diagram, species i consumes 4 species (shaded triangles) including itself. The size of r_i is assigned by using a beta function to randomly draw values from the interval (0,1) whose expected value is $2C$ and then multiplying that value by n_i to obtain a C that matches the C of the empirical web being modeled

hierarchy by allowing up to half a consumer's range to include species with higher niche values than the consumer, thus allowing looping and cannibalism. Also, the consumer must feed on all species that fall within its feeding range, a contiguity that is absent from the cascade model. For each marine food web, we used Monte Carlo simulations to generate 1000 cascade and niche model webs with the same *S* and *C* as the empirical web, allowing calculation of a model mean and standard deviation for each of the 18 network properties. If the normalized error (raw error divided by model SD) between the empirical property and the mean model value for that property falls with ±2 model SD, the model is considered to be a good fit to the empirical data (Williams & Martinez 2000). Due to the relatively high diversity and connectance of the NE US Shelf web, and the high diversity of the large Caribbean Reef web, the computational time required to run the models for the 3 food-chain-length related measures was prohibitive. For those webs, model results for the other 13 properties are reported.

In an extinction analysis, we simulated species loss in the Benguela, small Caribbean Reef, and NE US Shelf food webs by sequentially removing species selected by 1 of 3 criteria: (1) the most-connected species; (2) randomly chosen species (1000 random removal sequences initiated for each web); and (3) the least-connected species (Dunne et al. 2002a). We did not analyze the large version of the Caribbean Reef web due to its extreme bias discussed above. A species' connectedness is the sum of both its predator and prey links. When the most- and least-connected species are targeted for 'primary extinctions,' we protect basal species because removing such highly aggregated species (e.g. 'phytoplankton') in marine food webs has obviously large and not particularly informative consequences. 'Secondary extinctions' result when a consumer species loses all of its prey items or when a cannibalistic species loses all of its prey items except its own species. The most- or least-connected species in a web was determined at each step of the simulation, i.e. after the web had reconfigured after the previous removal and any resulting secondary extinctions. The structural 'robustness' of each food web to the 3 types of species loss was calculated as the fraction of species that had to be removed in order to result in total species loss (i.e. primary species removals plus secondary extinctions) of ≥50 % of the species in the original web. Maximum robustness (0.50) occurs when no secondary extinctions follow primary extinction of 50 % of the species and minimum robustness (1/*S*) occurs when the first primary extinction leads to 50 % total loss of species (Dunne et al. 2002a).

RESULTS AND DISCUSSION

Direct comparisons of food webs

Direct comparison of some common food-web properties suggests that the 3 marine ecosystems, as represented by the Benguela, small Caribbean Reef, and NE US Shelf food webs, have strong structural similarities (Tables 1 & 2). The trophic species version of these 3 webs have similar numbers of top (*T*, 0 to 4 %), intermediate (*I*, 93 to 94 %), and basal taxa (*B*, 3 to 7 %), as well as omnivores (*Omn*, 76 to 86 %). Mean shortest path length among all pairs of taxa is nearly identical (~1.6 links) and *C* ranges from 0.22 to 0.24. Consistent with current food-web theory (e.g. Martinez 1992), *L*/*S* and chain length vary strongly among the marine webs, increasing with *S*. Thus, Benguela, with 29 taxa, has the smallest values (*L*/*S* = 7.0, mean chain length = 6.4) and NE US Shelf, with 79 taxa, has the largest values (*L*/*S* = 17.8, mean chain length = 15.3).

How do marine food webs compare with food webs from other types of ecosystems? Direct comparisons of food-web properties across and often within ecosystem types reveal a wide range of values (Table 2). Since many food-web properties are scale-dependent, in that they depend on the diversity and complexity of a system (e.g. Martinez 1994, Williams & Martinez 2000, Dunne et al. 2002b), this variation is neither surprising nor strongly suggestive of fundamental differences among food webs. However, given that caveat, marine food webs have levels of *I* (93 to 94 %), *Omn* (76 to 86 %), and *Can* (24 to 42 %) taxa that are on the high end of the range of values across all of the food webs, as suggested by previous studies (Cohen 1994, Link 2002). Levels of *I*, *Omn*, and *Can* in the marine webs are comparable to 2 small webs (Coachella Valley and Skipwith Pond) also noted by Link (2002) for the NE US Shelf web. The high levels of *I*, *Omn*, and *Can* in these 2 non-marine webs appear due to high aggregation of taxa in the Coachella Valley web and the predominance of generalist (wide-diet) insect species in the Skipwith Pond web. While marine food webs define the high end of the range of *Omn*, there are a number of food webs besides Coachella Valley and Skipwith Pond that show levels of omnivory greater than 55 % (St. Martin Island, El Verde Rainforest, Mirror Lake, Lake Tahoe, St. Mark's Estuary, and Ythan Estuary with parasites).

Whether high *I*, *Omn*, and *Can* in marine webs result from methodological problems with marine data (e.g. uneven resolution with a bias towards omnivorous fishes), from methodological problems with non-marine data (e.g. the tendency to overlook cannibalistic interactions), or from fundamental differences of marine versus non-marine ecosystems (e.g.

Table 2. Some commonly reported structural food-web properties for 19 food webs from a variety of ecosystem types. Taxa = number of taxa from original food web, S = number of trophic species, C = connectance (L/S^2), L/S = links per species, ChLen = mean food chain length, TL = mean trophic level, Path = characteristic path length, T = % top species, I = % intermediate species, B = % basal species, Can = % cannibalistic species, Omn = % omnivorous species. See Dunne et al. (2002a) for more detailed descriptions of the non-marine datasets. Food webs are arranged from least to most trophic species (S) within a given ecosystem type

	Taxa	*S*	*C*	*L/S*	ChLen	TL	Path	*T*	*I*	*B*	Can	Omn	Source
Terrestrial													
Coachella Valley[a]	30	29	0.31	9.0	6.7	3.0	1.4	0	90	10	66	76	Polis (1991)
St. Martin Island[a]	44	42	0.12	4.9	5.2	2.4	1.9	17	69	14	0	60	Goldwasser & Reagan (1996)
UK Grassland	75	61	0.03	1.6	3.2	2.6	3.7	31	56	13	0	21	Memmott et al. (2000)
El Verde	156	155	0.06	9.7	8.4	2.5	2.3	13	69	18	1	57	Waide & Reagan (1996)
Lake/Pond													
Skipwith Pond[a]	35	25	0.32	7.9	6.2	2.7	1.3	4	92	4	32	60	Warren (1998)
Bridge Brook Lake[a]	75	25	0.17	4.3	4.0	2.0	1.9	0	68	32	12	40	Havens (1992)
Little Rock Lake[a]	182	92	0.12	10.8	7.3	2.4	1.9	1	86	13	14	38	Martinez (1991)
Mirror Lake	586	172	0.15	25.1	9.1	2.1	1.8	1	74	25	17	59	Martinez (unpubl. data)
Lake Tahoe	800	172	0.13	22.6	10.7	2.1	1.9	9	66	28	17	58	Martinez (unpubl. data)
Stream													
Canton Creek	108	102	0.07	6.8	3.2	1.5	2.3	25	22	53	1	8	Townsend et al. (1998)
Stony Stream	112	109	0.07	7.6	3.1	1.5	2.3	17	27	56	2	10	Townsend et al. (1998)
Estuary													
Chesapeake Bay[a]	33	31	0.07	2.2	4.0	2.4	2.7	32	52	16	3	52	Baird & Ulanowicz (1989)
St. Mark's Estuary	48	48	0.10	4.6	6.6	2.5	2.0	17	69	12	6	71	Christian & Luczkovich (1999)
Ythan Estuary[a]	92	83	0.06	4.8	5.9	2.6	2.2	37	54	9	4	54	Hall & Raffaelli (1991)
Ythan Estuary with parasites	134	124	0.04	4.7	6.3	2.9	2.4	40	56	4	3	62	Huxham et al. (1996)
Marine													
Benguela	29	29	0.24	7.0	6.4	3.2	1.6	0	93	7	24	76	Yodzis (1998)
Caribbean Reef, small	50	50	0.22	11.1	9.8	2.9	1.6	0	94	6	42	86	Opitz (1996)
NE US Shelf	81	79	0.22	17.8	15.3	3.1	1.6	4	94	3	32	78	Link (2002)
Caribbean Reef, large	249	245	0.05	13.8	10.5	3.1	1.9	0	98	2	4	87	Opitz (1996)

[a]Food webs analyzed in Williams & Martinez (2000)

unusually widespread generality in marine systems related to gape size and filter feeding), continues to be an open question that requires more detailed and evenly resolved data to settle (Cohen et al. 1993). The excessively low percentage of basal taxa in these marine food webs compared to other systems is clearly an artifact of poor resolution of primary producers and consumer links to them. Better resolution at the basal level would tend to mitigate, but probably not erase, current high levels of *I*, *Omn*, and *Can* in marine food webs.

As also discussed by Link (2002) for the NE US Shelf web, and Cohen (1994) for a set of 11 highly aggregated low-diversity marine food webs, the 3 marine webs examined here have high L/S and mean chain lengths compared to most other food webs from other ecosystems, particularly the small Caribbean Reef and NE US Shelf webs (Table 2). However, Lake Tahoe and Mirror Lake have greater L/S, and there are a number of other food webs (Coachella Valley, El Verde Rainforest, Skipwith Pond, and Little Rock Lake) with comparable L/S. The NE US Shelf displays the longest mean chain length (15.3), but the small Caribbean Reef, Lake Tahoe, and Mirror Lake food webs display comparable mean chain lengths of ~9 to 11. Six other webs fall close to (Coachella Valley, Skipwith Pond, St. Mark's Estuary, Ythan Estuary with parasites) or greater than (El Verde Rainforest, Little Rock Lake) Benguela's mean chain length of 6.4. In addition to the known diversity dependence of these measures, Cohen (1994) extensively discusses a variety of other biological and methodological reasons that marine webs might display high L/S and chain lengths relative to non-marine webs.

The 3 marine food webs have relatively high C of 0.22 to 0.24, which is within the previously observed

Table 3. Comparison of 16 empirically observed structural food-web properties with niche model means in parentheses for 3 marine food webs. Empirical values whose normalized error falls within ±2 model SD, demonstrating a good fit between the model and empirical data, are shown in **bold**. Niche model food-chain properties were not calculated for the NE US Shelf and the large Caribbean Reef food webs due to the excessive computing time required. *Herb* = % herbivores plus detritivores, *Loop* = % species in loops, *GenSD* = generality standard deviation, *VulSD* = vulnerability standard deviation, *MaxSim* = mean maximum similarity, *ChSD* = food chain length standard deviation, *ChNum* = log food chain number, *Clust* = clustering coefficient. See Table 2 for other definitions

	Benguela	Caribbean Reef, small	Caribbean Reef, large	NE US Shelf
T	**0** (5)	**0** (3)	**0** (4)	**4** (2)
I	**93** (83)	**94** (88)	98 (86)	**94** (92)
B	**7** (12)	**6** (9)	2 (10)	**3** (6)
Herb[a]	**7** (5)	**6** (4)	**4** (4)	19 (2)
Can	**24** (31)	42 (29)	**4** (6)	**32** (30)
Omn	**76** (78)	**86** (83)	**87** (48)	78 (88)
Loop	**41** (56)	**68** (68)	**73** (35)	**67** (78)
GenSD	**0.88** (0.91)	**0.90** (0.93)	1.92 (1.20)	**0.90** (0.92)
VulSD	**0.73** (0.55)	**0.61** (0.55)	1.18 (0.59)	0.73 (0.53)
MaxSim	**0.66** (0.70)	0.58 (0.74)	0.61 (0.68)	0.70 (0.77)
TL[a]	**3.2** (3.2)	**2.9** (3.5)	**3.1** (3.0)	**3.1** (3.8)
ChLen	**6.4** (7.5)	**9.8** (10.3)	–	–
ChSD	**1.5** (1.6)	**2.1** (1.9)	–	–
ChNum	**3.8** (4.4)	**6.3** (6.5)	–	–
Path[a]	**1.6** (1.6)	**1.6** (1.6)	1.9 (2.2)	**1.6** (1.6)
Clust[a]	**0.30** (0.36)	**0.36** (0.34)	0.16 (0.10)	**0.31** (0.34)

[a]Properties not previously evaluated by Williams & Martinez (2000)

range of 0.03 to 0.3 (Table 2, Dunne et al. 2002a). We do not follow Link's (2002) use of 'connectivity,' also known as 'interactive connectance' ($L/[S(S-1)/2]$). The denominator represents less than ½ of the full predation matrix and renders cannibalism and mutual predation links impossible, while the numerator includes such links, leading to double counting of links and exaggerated connectance (Martinez 1991). Instead, we use 'directed connectance' ($C = L/S^2$) (Martinez 1991, 1992) because it avoids these problems by forcing the numerator to account for mutual predation and cannibalism links (Polis 1991), and allowing for the possibility for any species to feed on any species in a web (including the potential for plants to parasitize other plants). Thus, the assertion that an order-of-magnitude higher connectivity in the NE US Shelf food web indicates dramatic differences between marine and other types of ecosystems (Link 2002) appears incorrect. Instead, the marine food webs examined here display connectance above the mean but within the range seen in non-marine food webs.

Comparisons using the food-web models

As discussed in the 'Introduction', the dependence of many food-web properties on diversity and complexity confounds direct assessment of the similarity, or dissimilarity, of food-web structure. Using direct comparisons makes it difficult to gauge the significance of differences, especially when the available datasets are few and highly variable both ecologically and methodologically. Instead, an approach that uses simple models that incorporate variable diversity and connectance, such as the niche model (Williams & Martinez 2000) and certain implementations (Williams & Martinez 2000) of the cascade model (Cohen et al. 1990), provides a more robust way to evaluate empirical food-web structure.

The cascade model fails to accurately predict marine food-web structure. Across all 3 higher-quality marine webs, the cascade model provides a good fit for only 33% of the properties examined: 5 of 16 properties for Benguela, 6 of 16 for the small Caribbean Reef, and 4 of 13 for the NE US Shelf (results not shown). The cascade model disallows looping and cannibalism, which occurs in all 3 food webs. The cascade model also systematically underestimates 4 other properties across all 3 webs: *GenSD*, *MaxSim*, *Path*, and *Clust*. For Benguela and the small Caribbean Reef, the 2 food webs for which computationally intensive chain length metrics could be modeled, the cascade model overestimated all 3 chain length properties. These results are very similar to an analysis of network structure of 2 lake, 1 pond, 2 estuary, and 2 terrestrial food webs (Williams & Martinez 2000, Table 2), where the overall success rate of the cascade model was 27%.

In contrast, the niche model more closely predicts the structure of the 3 marine food webs. Of 16 niche model means, all 16 are within 2 model SD of the empirical values for Benguela, with a good fit for 14 of 16 (88%) properties for the small Caribbean Reef web (Table 3). The niche model underestimates *Can* and overestimates *MaxSim* in the small Caribbean Reef web. The niche model predicts the structure of the NE US Shelf web less well than the other 2 marine food webs, but still much better than the cascade model. Nine of 13 (69%) properties are well predicted, with *VulSD* and *Herb* underestimated and *Omn* and *MaxSim* overestimated by the niche model. The drastic underestimation of *Herb* may be connected to the hyper-aggregation of basal groups, which represent only 3% of taxa in the NE US Shelf web; very low compared to most other food webs

(Table 2). However, it may also reflect a limitation of the niche model, which tends to underestimate *Herb* for most food webs (data not shown).

While the niche model appears able to identify fundamental food-web structure that is fairly robust to some bias, variability, and aggregation in the data, it is sensitive to systematic bias. For example, in all 3 marine webs the niche model underestimates *VulSD*. This underestimation may occur due to methodological bias in these marine food webs towards inclusion of high trophic level taxa (i.e. fishes) without identifying their full complements of predators or parasites (Williams & Martinez 2000). The niche model is also sensitive to extreme bias in particular webs. Consider the large Caribbean Reef food web, with 84% fish taxa and only 0.05 connectance. The niche model does a poor job of predicting its network structure as illustrated by a good fit to only 6 of 13 properties (46%) (Table 3). This is better than the cascade model, which successfully predicts only 3 of 13 properties (23%), but far worse than the success of the niche model for the other 3 marine webs. The niche model's failure to fit the structure of the large Caribbean Reef food web echoes the relatively poor fit of the niche model (7 of 12 properties) to the data for the Ythan Estuary food web (Hall & Raffaelli 1991), which appears related to over-representation of top bird species (Williams & Martinez 2000).

For the 3 more evenly resolved marine food webs, the average 87% predictive success rate of the niche model is similar to its 79% success rate across 7 non-marine food webs (Williams & Martinez 2000). While the 16 properties currently examined are not completely independent, and the degree to which they co-vary has yet to be assessed, there is clearly a strong difference in how accurately the cascade and niche models characterize the topology of food webs. The similarly high level of the niche model's predictive success for marine, estuary, freshwater, and terrestrial food webs suggests that marine and non-marine food webs have remarkably similar network structure, once diversity and connectance levels are incorporated. However, because the niche model assumes a particular level of connectance, it does not explain why marine food webs appear to have relatively high trophic interaction richness compared to other webs. Both of these aspects of marine food-web structure, i.e. its niche-model similarity to the structure of other food webs, as well as its differences in connectance from other webs, must be considered provisional until more highly and evenly resolved data for lower-trophic-level taxa and interactions are incorporated into marine food-web datasets, and until a greater variety and higher quality of all types of food webs are compiled and analyzed.

Structural robustness of marine food webs to species loss

We systematically removed species from the 3 higher-quality marine food webs in biodiversity-loss simulations. The secondary extinctions resulting from the loss of all prey items varied both among webs and among types of species removed (Fig. 2). Very few secondary extinctions occurred as a result of removing taxa with very few connections, whereas removing

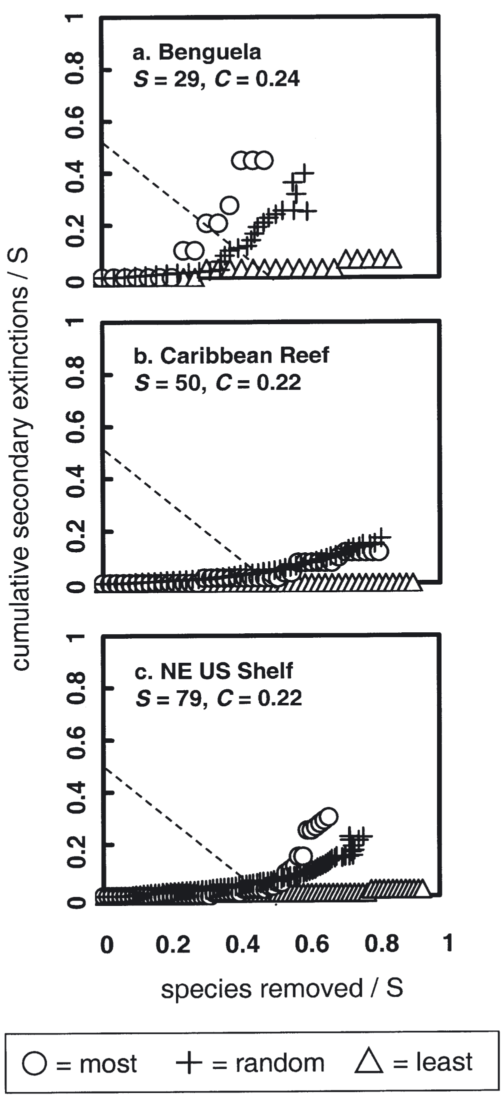

Fig. 2. Secondary extinctions resulting from 3 types of primary species removal in 3 marine food webs. 95% error bars for random species removals fall within the size of the symbols and are not shown. Dashed line shows the points at which there is ≥50% total species loss (primary species removals plus secondary extinctions) in a food web for each type of species removal. Proportion of species that must be removed to reach that point is referred to as 'structural robustness'. *S*: species richness; *C*: connectance (links per species^2, L/S^2)

random taxa and the most-connected taxa did result in additional species loss after 25% of the species in the original webs were removed. Benguela showed the most dramatic effects and differences among the 3 targeting strategies, where removal of ~30% of most-connected, random, and least-connected taxa resulted in ~20, 11, and 3% of the taxa undergoing secondary extinctions, respectively. In general, the small Caribbean Reef and NE US Shelf web displayed very high robustness to species removals, with >50% primary removals required to induce >5% secondary extinctions.

Marine food webs generally show high structural robustness to species loss compared to other food webs analyzed previously (Solé & Montoya 2001, Dunne et al. 2002a), which appears related to their relatively high connectance (Fig. 3, Dunne et al. 2002a). When most-connected or random species are targeted, structural robustness increases significantly with increasing connectance, and saturates at 0.50, which is the point at which there are no secondary extinctions as a result of 50% primary removals (Fig. 3). Targeting least-connected species was not significantly related to *C*, partially because of the low level of secondary extinctions that resulted (results not shown). Benguela is an outlier compared to the other 2 marine and 16 non-marine webs represented, with lower robustness than expected for both random and most-connected species

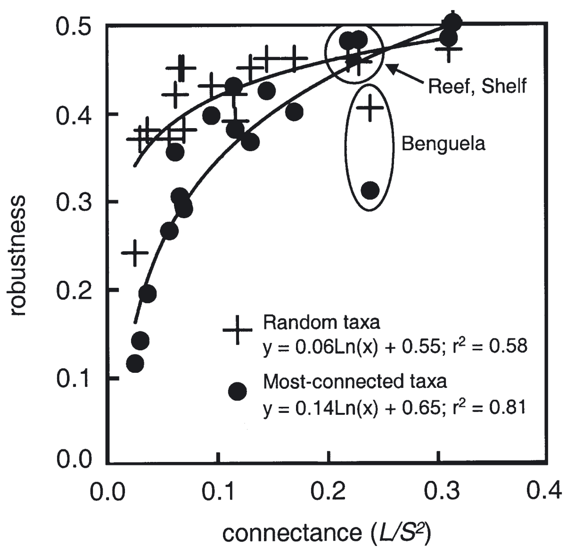

Fig. 3. Structural robustness (the proportion of primary species removals required to induce a total loss of ≥50% of species) as a function of connectance (L/S^2) in 16 food webs from Dunne et al. (2002a) plus 3 recent marine food webs (circled data points). Data shown for loss of most-connected taxa are for deletion sequences where basal taxa are protected from removal. Maximum robustness value = 0.50 (i.e. no secondary extinctions)

removals. Structural robustness did not vary significantly with *S*, regardless of type of species loss (linear regression data not shown, see Dunne et al. 2002a).

Why is Benguela an outlier? The first 10 most- and least-connected taxa removed in the simulations are shown for each food web in Table 4. In the Benguela food web, there are highly connected taxa such as macro- and mesozooplankton that are at fairly low trophic levels in the food web, unlike in the small Caribbean Reef and NE US Shelf webs. This may suggest that from a structural perspective, removing highly connected lower trophic level taxa is even more destabilizing than removing highly connected upper trophic level taxa.

CONCLUSIONS

Previous examinations of marine food-web structure concluded that marine food webs are fundamentally different from other kinds of food webs, based on their high *L/S*, connectivity, and chain lengths; differences which may relate in part to high levels of omnivorous, generalist organisms in marine habitats (Cohen 1994, Link 2002). The current study corroborates aspects of the previous studies. Direct comparisons of measures such as *L/S*, connectance, omnivory, and cannibalism suggest that marine food webs: (1) tend to look similar to each other; and (2) have high values for those properties compared to estuary, freshwater, and terrestrial food webs. Marine webs thus appear to have relatively high trophic interaction richness. However, in most cases marine food webs do fall within previously reported ranges of observed food-web properties from non-marine systems, and the least diverse marine web (Benguela) has values that are often quite similar to those of many non-marine food webs. More evenly and highly resolved data from marine and non-marine systems will help to decide whether current patterns are artifacts or whether they reflect more significant similarities or differences among and within different types of ecosystems.

Even given possible differences in food-web properties between marine and other ecosystems, it does not appear that 'food web theory needs to be modified to accommodate observations from marine ecosystems' (Link 2002). Instead, our study shows that when species richness and connectance are taken into account, observations from marine food webs corroborate current theory concerning the topology of food webs. In particular, the niche model very accurately predicts the structure of marine food webs, particularly the Benguela and small Caribbean Reef webs, as it does for other types of food webs (Williams & Martinez 2000,

Table 4. First 10 taxa eliminated from 3 marine food webs when targeting the most and least connected taxa, with basal taxa protected from removal. Qualifiers in parentheses refer to body size classes (int. = intermediate). Names are drawn from the original studies

	Benguela	Caribbean Reef, small	NE US Shelf
Most connected taxa			
1	Sharks	Sharks/rays (large)	Cod
2	Hakes	Carnivorous reef fish #3 (int.)	Red hake
3	Squid	Shrimps/hermit crabs/ stomatopods	Spotted hake
4	Birds	Carnivorous reef fish #2 (int.)	White hake
5	Macrozoo-plankton	Carnivorous reef fish #1 (small)	Silver hake
6	Other groundfish	Omnivorous reef fish #1 (small)	Little skate
7	Mesozoo-plankton	Crabs	Spiny dogfish
8	Anchovy	Gastropods	Goosefish
9	Benthic carnivores	Carnivorous reef fish (large)	Winter skate
10	Goby	Omnivorous reef fish #2 (small)	Other decapods
Least connected taxa			
1	Bacteria	Kyphosidae	Snails
2	Zooplankton, gelatinous	Gobiidae (small)	Tunicates
3	Microzoo-plankton	Groupers (large)	Billfish
4	Lightfish	Hemiramphidae	Birds
5	Other pelagics	Scaridae (large)	Seals
6	Yellowtail	Scaridae (int.)	Pteropods
7	Geelbek	Scaridae (int.)	Sponges
8	Whales and dolphins	Sea turtles	Sea cucumbers
9	Benthic carnivores	Lobsters	Baleen whales
10	Tunas	Jacks (large)	*Calanus* sp.

Williams et al. 2002). This suggests that the network structure of food webs is a general property of ecosystems. It also suggests that the simple rules of the niche model, which specify a relaxed feeding hierarchy that allows cannibalism and looping as well as a contiguity of feeding within a niche, may point to common ecological, evolutionary, and thermodynamic mechanisms shaping the complex network structure of food webs from all types of ecosystems examined thus far (Williams & Martinez 2000).

Such aspects of marine food webs are particularly interesting because of the intense economic fishing pressure, overexploitation, and collapse of many coastal and shelf marine fisheries (e.g. Boreman et al. 1997, Jackson et al. 2001). What can network structure tell us about the potential robustness of food webs to biodiversity loss? Current and previous results (Dunne et al. 2002a) suggest that high connectance communities will tend to be more robust to species loss than low connectance communities, and that the loss of highly connected taxa will tend to induce higher levels of secondary extinctions than loss of random taxa (Albert et al. 2000, Solé & Montoya 2001, Dunne et al. 2002a). This suggests that marine systems, if their relatively high connectance is not an artifact of methodology, will have greater inherent structural robustness than other ecosystems. However, other structural effects can come into play. First, extinctions in marine systems do not appear random, particularly with regard to anthropogenic effects over the last several centuries. Humans tend to selectively and intensively take marine taxa at high trophic levels (Pauly et al. 1998, Jackson et al. 2001), which are often the taxa that are highly connected (Table 4). Also, the mean shortest path length between pairs of taxa within marine webs is low (1.6 links) compared to other types of food webs, which have values ranging from 1.3 to 3.7 (Table 2, Dunne et al. 2002b). This suggests that most species in marine food webs are potentially very close 'neighbors,' and that negative effects can spread rapidly and widely throughout the food web (Williams et al. 2002). However, the rich network of interactions quantified by high connectance and low path length may also suggest that strong effects can rapidly disperse throughout marine food webs, thus decreasing the overall impact of any particular fluctuation (Link 2002).

This analysis, like other structural food-web studies, does not incorporate the dynamics of interacting taxa. Useful predictions of ecosystem response to perturbations such as population or biomass fluctuations, changes in size and age class distributions, and species losses or introductions require models that integrate ecologically plausible diversity and network structure with non-linear population dynamics of species (Yodzis 1998, 2000, Williams & Martinez in press). Studies that ignore or drastically simplify structure (e.g. approaches focused on 2 species, food chains, or small modules) or dynamics (e.g. mass-balance, Lotka-Volterra, and topological approaches) may provide unreliable approximations of the structurally complex, nonequilibrium, nonlinear, diffuse dynamics that likely characterize most ecosystems (Yodzis 2000). Marine food webs, particularly those strongly impacted by humans, may be the ideal test case for developing and applying integrated structure and dynamics models, as explored in the Benguela food web (Yodzis 1998, 2000). The desperate need for more sophisticated interdisciplinary ecological and economic models to assist fisheries and marine reserve policy formulation is clear (Micheli et al. 2001). An improved understanding of marine food-web structure, which explicitly focuses on the complex network of interactions in which exploited taxa are embedded, should be an important part of future marine ecosystem research and policy.

Acknowledgements. This work was supported by NSF grants DEB/DBI-0074521 (J.A.D), DEB-0083929 (N.D.M), DBI-0234980 (N.D.M., J.A.D., R.J.W.), and DBI-9904777 (R.J.W.). We thank J. Link for sharing the NE US Shelf data, and C. Melian for providing the large Caribbean Reef dataset. We are grateful to D. Stouffer for pointing out errors in the data. Please contact J.A.D. for data referred to in this paper.

LITERATURE CITED

Albert R, Barabási AL (2002) Statistical mechanics of complex networks. Rev Mod Phys 74:47–97

Albert R, Jeong H, Barabási AL (2000) Error and attack tolerance of complex networks. Nature 406:378–382

Baird D, Ulanowicz RE (1989) The seasonal dynamics of the Chesapeake Bay ecosystem. Ecol Monogr 59:329–364

Boreman J, Nakashima BS, Wilson HA, Kendall RL (1997) Northwest Atlantic groundfish: perspectives on a fishery collapse. American Fisheries Society, Bethesda, MD

Briand F, Cohen JE (1984) Community food webs have scale-invariant structure. Nature 398:330–334

Camacho J, Guimerà R, Amaral LAN (2002a) Analytical solution of a model for complex food webs. Phys Rev Lett E 65: 030901

Camacho J, Guimerà R, Amaral LAN (2002b) Robust patterns in food web structure. Phys Rev Lett 88:228102

Christensen V, Pauly D (1992) ECOPATH II: a software for balancing steady-state ecosystem models and calculating network characteristics. Ecol Model 61:169–185

Christian RR, Luczkovich JJ (1999) Organizing and understanding a winter's seagrass foodweb network through effective trophic levels. Ecol Model 117:99–124

Cohen JE (1994) Marine and continental food webs: three paradoxes? Phil Trans R Soc Lond B 343:57–69

Cohen JE, Briand F, Newman CM (1990) Community food webs: data and theory. Springer-Verlag, New York

Cohen JE, Beaver RA, Cousins SH, De Angelis DL and 20 others (1993) Improving food webs. Ecology 74:252–258

Dunbar MJ (1954) Arctic and subarctic marine ecology: immediate problems. Arctic 7:213–228

Dunne JA, Williams RJ, Martinez ND (2002a) Network structure and biodiversity loss in food webs: robustness increases with connectance. Ecol Lett 5:558–567

Dunne JA, Williams RJ, Martinez ND (2002b) Food-web structure and network theory: the role of connectance and size. Proc Natl Acad Sci USA 99:12917–12922

Erdös P, Rényi A (1960) On the evolution of random graphs. Publ Math Inst Hung Acad Sci 5:17–61

Fussman GF, Heber G (2002) Food web complexity and chaotic population dynamics. Ecol Lett 5:394–401

Goldwasser L, Roughgarden JA (1993) Construction of a large Caribbean food web. Ecology 74:1216–1233

Hall SJ, Raffaelli D (1991) Food-web patterns: lessons from a species-rich web. J Anim Ecol 60:823–842

Havens K (1992) Scale and structure in natural food webs. Science 257:1107–1109

Huxham M, Beany S, Raffaelli D (1996) Do parasites reduce the chances of triangulation in a real food web? Oikos 76: 284–300

Jackson JB, Kirby MX, Berger WH, Bjorndal KA and 15 others (2001) Historical overfishing and the recent collapse of coastal ecosystems. Science 293:629–638

Krause AE, Frank KA, Mason DM, Ulanowicz RE, Taylor WW (2003) Compartments revealed in food-web structure. Nature 426:282–285

Link J (2002) Does food web theory work for marine ecosystems? Mar Ecol Prog Ser 230:1–9

Martinez ND (1991) Artifacts or attributes? Effects of resolution on the Little Rock Lake food web. Ecol Monogr 61: 367–392

Martinez ND (1992) Constant connectance in community food webs. Am Nat 139:1208–1218

Martinez ND (1993) Effect of scale on food web structure. Science 260:242–243

Martinez ND (1994) Scale-dependent constraints on food-web structure. Am Nat 144:935–953

Martinez ND, Hawkins BA, Dawah HA, Feifarek BP (1999) Effects of sampling effort on characterization of food-web structure. Ecology 80:1044–1055

Memmott J, Martinez ND, Cohen JE (2000) Predators, parasitoids and pathogens: species richness, trophic generality and body sizes in a natural food web. J Anim Ecol 69:1–15

Micheli F, Polis GA, Boersma PD, Hixon MA, Norse EA, Snelgrove PVR, Soulé ME (2001) Human alteration of food webs: research priorities for conservation and management. In: Soulé ME, Orians GH (eds) Conservation biology: research priorities for the next decade, 2nd edn. Island Press, Washington, DC, p 31, 58

Montoya JM, Solé RV (2002) Small world patterns in food webs. J Theor Biol 214:405–412

Neutel AM, Heesterbeek JAP, de Ruiter PC (2002) Stability in real food webs: weak links in long loops. Science 296: 1120–1123

Opitz S (1996) Trophic interactions in Caribbean coral reefs. ICLARM Tech Rep 43, Manila, Philippines

Pauly D, Christensen V, Dalsgaard J, Froese R, Torres F (1998) Fishing down marine food webs. Science 279: 860–863

Pauly D, Christensen V, Guënette S, Pitcher TJ, Sumaila UR, Walters CJ, Watson R, Zeller D (2002) Toward sustainability in world fisheries. Nature 418:689–695

Polis GA (1991) Complex desert food webs: an empirical critique of food web theory. Am Nat 138:123–155

Schoener TW (1989) Food webs from the small to the large. Ecology 70:1559–1589

Solé RV, Montoya JM (2001) Complexity and fragility in ecological networks. Proc R Soc Lond B 268:2039–2045

Strogatz SH (2001) Exploring complex networks. Nature 410: 268–275

Townsend CR, Thompson RM, McIntosh AR, Kilroy C, Edwards E, Scarsbrook MR (1998) Disturbance, resource supply, and food-web architecture in streams. Ecol Lett 1: 200–209

Waide RB, Reagan WB (eds) (1996) The food web of a tropical rainforest. University of Chicago Press, Chicago

Warren PH (1989) Spatial and temporal variation in the structure of a freshwater food web. Oikos 55:299–311

Watts DJ, Strogatz SH (1998) Collective dynamics of 'small-world' networks. Nature 393:440–442

Williams RJ, Martinez ND (2000) Simple rules yield complex food web. Nature 404:180–183

Williams RJ, Martinez ND (in press) Stabilization of chaotic and non-permanent food web dynamics. Eur J Phys B

Williams RJ, Martinez ND (2004) Trophic levels in complex food webs: theory and data. Am Nat 163:458–468

Williams RJ, Berlow EL, Dunne JA, Barabási AL, Martinez ND (2002) Two degrees of separation in complex food webs. Proc Natl Acad Sci USA 99:12913–12916

Yodzis P (1998) Local trophodynamics and the interaction of marine mammals and fisheries in the Benguela ecosystem. J Anim Ecol 67:635–658

Yodzis P (2000) Diffuse effects in food webs. Ecology 81: 261–266

Editorial responsibility: Andrea Belgrano, Santa Fe, New Mexico, USA

Submitted: April 16, 2003; Accepted: January 27, 2004
Proofs received from author(s): April 20, 2004